André Filipe Rainho Pereira

Licenciatura em Ciências de Engenharia Electrotécnica e de Computadores

Rail Corrugation: A Software Tool for Detection and Analysis Using Wavelets

Dissertação para obtenção do Grau de Mestre em
Engenharia Electrotécnica e de Computadores

Supervisor: Arnaldo Guimarães Batista, FCT-UNL

FACULDADE DE CIÊNCIAS E TECNOLOGIA
UNIVERSIDADE NOVA DE LISBOA

Março 2018

Copyright

Acknowledgments

To Professor Arnaldo Batista, for all the support given and his dedication to this project and all the knowledge he shared with me.

To Professor Manuel Ortigueira for all his advice in signal processing.

To Professor José Varandas for helping with corrugation data.

To my parents, a special thanks for all the support in this stage of my life and especially my mother for always pushing me to work and study.

To my friends for being a part of my life and without them it would have been more difficult to accomplish this stage of my life.

To Mafalda, for always being there for me.

Abstract

Corrugation is an oscillatory wear of the rail and it is a consequence of the interaction between wheel and rail [1].

Rail corrugation usually appears in curves, but it may also arise in linear tracks. It usually appears in curves because of the friction between the rail and wheel due to curving [2].

The main objective of this master thesis is to develop new methods that can detect if there is corrugation in the rail and quantify it according to the frequency and amplitude of the signal.

A program has been already developed at FCT-UNL enabling the detection of rail corrugation, RailScan V2.1. However, this application is outdated, so the aim is to update it and make it more efficient, building a brand-new RailScan V3.0.

The implementation of the function Corrugram, a patent developed in FCT-UNL, was a huge evolution in RailScan. Corrugram is a new way to represent where and if corrugation is present in the rail.

Another implementation was the norm EN 13231-3:2012, another method to analyze if rail corrugation is present. This norm was incorporated within RailScan V3.0, and it ensured compliance against the best international practice among rail corporations [3].

The remaining part of this thesis was to create a database with robust data, allowing the validation of both RailScan and Corrugram as powerful tools to quantify rail corrugation.

The results proved that RailScan is a powerful tool to detect and locate rail corrugation and that the Corrugram is very simple, effective and useful in signal analysis.

Keywords: Corrugation, Wavelet Transform, Corrugram, One Third Octave Spectrum, EN 13231-3:2012

Resumo

O desgaste ondulatório aparece nas linhas férreas e é uma consequência da interação entre a roda e o carril [1].

O desgaste ondulatório nas linhas férreas aparece geralmente nas curvas, mas é possível aparecer em linhas retas. Aparece geralmente em curvas devido à fricção entre o carril e a roda devido ao estar a curvar [2].

O principal objetivo desta tese de mestrado é desenvolver um método que seja capaz de detetar se existe desgaste ondulatório na linha férrea e qualificar de acordo com a frequência e amplitude do sinal.

Já foi desenvolvido um programa na FCT-UNL, que era capaz de detetar, o RailScan V2.1, mas este programa já estava desatualizado e o meu objetivo era de o atualizar e tornar mais eficiente, criando assim o RailScan V3.0.

A implementação da função Corrugrama, uma patente desenvolvida na FCT-UNL foi também uma evolução no RailScan. O Corrugrama é uma nova maneira de representar e localizar desgaste ondulatório.

Outra implementação foi a norma EN 13231-3:2012, uma norma que também deteta se existe desgaste ondulatório. Esta norma é uma inovação do RailScan V3.0 e fez todo o sentido ser implementada porque é a norma geralmente utilizada pelas empresas ferroviárias [3].

A outra parte desta tese era criar uma base de dados com dados suficientes para ser possível validar o RailScan, como uma poderosa ferramenta na análise de desgaste ondulatório nas linhas férreas.

Os resultados provaram que o RailScan é uma ferramenta útil na deteção e localização do desgaste ondulatório e que o Corrugrama é um programa simples, eficaz e benéfico na análise de sinais.

Palavras-Chave: Desgaste ondulatório, Transformada de ondulas, Corrugrama, Espectro de um terço de oitava, EN 13231-3:2012

Contents

List of figures

List of Tables

Acronyms

mm	Millimeter
cm	Centimeter
m	Meter
µm	Micrometer
FT	Fourier Transform
FFT	Fast Fourier Transform
STFT	Short Time Fourier Transform
CWT	Continuous Wavelet Transform
DWT	Discrete Wavelet Transform
WPT	Wavelet Packet Transform
λ	Wavelength
ν	Speed
EN	European Norm
σ	Standard Deviation

Introduction

1.1 Introduction

Rail corrugation is one of the most common types of wear in the railroad industry. It is generally considered that there are six types of rail corrugation, according to damage and wavelength. Once present, corrugation can affect the wheel-rail and vehicle-track interaction, leading to an unpleasant ride and a deterioration of the system [4], [5].

Rail corrugation (figure 1.1) displays wavelengths between 3cm and 100cm and it is divided in two groups: short wavelength rail corrugation (3cm to 10cm) and long wavelength rail corrugation (10cm to 100cm) [6].

About 40% of all tracks are prone to develop corrugation, so this is a very considerable problem in the railroad industry [2].

Figure 1.1 – Example of a corrugated rail [2]

Rail corrugation is one of the most serious and expensive problems that railways suffer.

This phenomenon results in reduced rail and wheel lifetime and it can lead the transport company to prematurely replace the rail, meaning higher costs.

The noise emitted can be painful to the passengers and the community that lives nearby the rails. Most of the European cities are adopting environmental noise policies, making public transportation networks reduce their noise emission even on existing lines, a process that is very expensive [2], [7].

There are various ways to detect rail corrugation. These methods can be divided into two classes, direct and indirect measurement.

In the direct measurement, the rail is directly examined. The advantage of using this method is that the irregularities of the wheel do not interfere with the measurement. The disadvantage of

this method is that for long-distance rails it becomes ineffective as it can only measure the rail at low speeds [4].

In the indirect measurement, the rail is examined through the vibrations and sounds the train emits. With this method, long-distance rails are no longer a problem because the measurement can be done in two ways. The first one is to use sensors on the rail and measure its vibration. The second way is to put sensors on the train and measure its acceleration [4].

The indirect measurement also has disadvantages, as irregularities of the wheel affect the data, so a rail without corrugation could be still erroneously considered damaged, leading to inconclusive results and an incorrect analysis.

In this master thesis, the data analyzed was acquired with the "RMF" model of Vogel & Plotscher, a direct measurement method. This equipment can measure corrugation from wavelengths of 10 mm to 3000 mm and is an approved measuring device for EN 13231:2012 [8],[34].

The data analyzed was also acquired using an indirect method, using a sensor to measure the acceleration of the train. The equipment used was not disclosed.

Having data acquired from two different methods leads a more robust analysis.

The main objective of this master thesis is to develop a method that can detect if there is corrugation in a rail and quantify it according to the frequency and amplitude of the signal.

The software used to detect corrugation has been developed in Matlab.

This work aims to develop a program that can detect and analyze corrugation using wavelets because they are the most powerful form to scrutinize non stationary signals and to implement new ways to detect if there is corrugation in the rail, such as the European Norm 13231-3:2012 and the Corrugram.

A previous program (RailScanV2.1) was developed at FCT-UNL [15]. Using this software, it was possible to detect and quantify rail corrugation using wavelet packets. RailScanV2.1 can also analyze the one-third-octave bands to verify if the wavelengths are compliant with DIN ISO 3095 requirements, which specify the noise emission level [9].

RailScanV2.1 was initially developed in 2009/2010. Since then, no further updates were implemented, leaving existing functions outdated after ISO 3095 revision in 2013, such as the wavelet filter and the one third-octave spectrum. The new version of the program named RailScanV3.0, will include all the previous version features and add some major changes in the layout in order to become more user friendly. The parameters of the data are no longer requested to the user. To analyze signals with RailScan, file selection is sufficient. In addition, it can now evaluate both rails simultaneously, making differences clearly comparable.

One of the biggest changes in RailScan will be the addiction of a function called Corrugram. The patent for this function was recently approved and it is a new way to represent if and where corrugation is present in the rail [26].

Another development is the inclusion of EN 13231-3, because it is the norm most commonly used by railway transportations [3]. This norm aims to tighten allowed limits in the irregularities of the rail.

1.2 Methods to Detect Rail Corrugation

There are companies that develop some instruments to detect if there is corrugation on the rail. A brief explanation of this instruments will be given in the next chapter.

1.2.1 CAT (Corrugation Analysis Trolley)

CAT (RailMeasurement Ltd) is an instrument that can be operated and carried by one person. It can only analyze one rail. While is analyzing the longitudinal profile of the surface of the rail it can also measure its acoustic roughness. For high speed rails this is not a very good method because it analyzes the rail at the speed of the person walking (approximately 1 m/s) [9], [10].

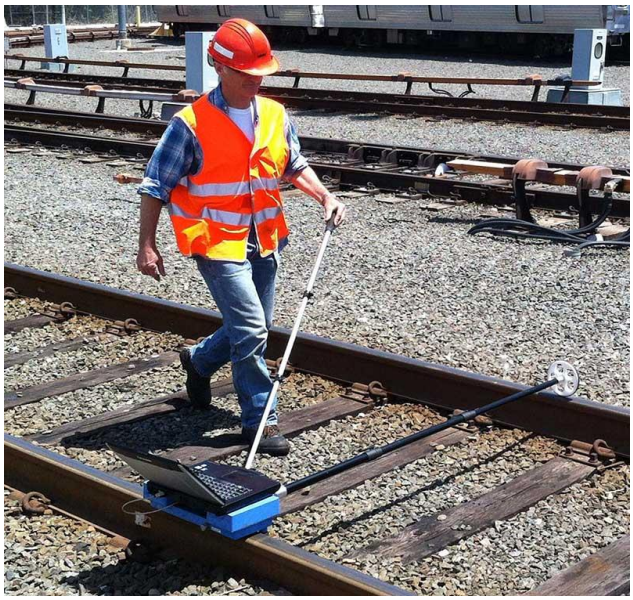

Figure 1.2 – CAT being used to detect any signs of corrugation on the track [10]

1.2.2 BI-CAT

BI-CAT (RailMeasurement Ltd) can measure both rails simultaneously with the same precision of the CAT.

The BI-CAT uses the same technology as the CAT and the same software to analyze the rail longitudinal profile and measure acoustic roughness on both rails at the speed of the person walking (approximately 1 m/s) [11],[27].

Figure 1.3 – BI-CAT being used to detect any signs of corrugation on the track [11]

1.2.3 RCA (Rail Corrugation Analyzer)

The RCA (RailMeasurement Ltd) measures irregularities, in particular rail corrugation.Using this analyzer brings the advantage that it can measure irregularities from a vehicle and can analyze both rails at the same time. The RCA works at a speed range of 0.5 km/h to 50 km/h, but the precision of the data collected is better if the speed is closer to the minimum range [12].

Figure 1.4 – RCA being used to detect any signs of corrugation on the track [12]

1.2.4 HSRCA (High Speed Rail Corrugation Analyzer)

The HSRCA (RailMeasurement Ltd) is designed to measure the longitudinal irregularities in rails at line speeds (approximately 120 km/h). The main irregularities measured are corrugation and acoustic roughness. The hardware of the HSRCA is accelerometers on both axle boxes. This instrument can measure both rails at the same time [13].

Figure 1.5 – HSRCA being used to detect any signs of corrugation on the track [13]

1.2.5 TriTops

TriTops is an instrument designed to measure irregularities on a railway wheel. It can measure displacement, corrugation and acoustic roughness present on the rail.

The Tritops can be carried by one person and it can measure 4 wheels at the same time [14].

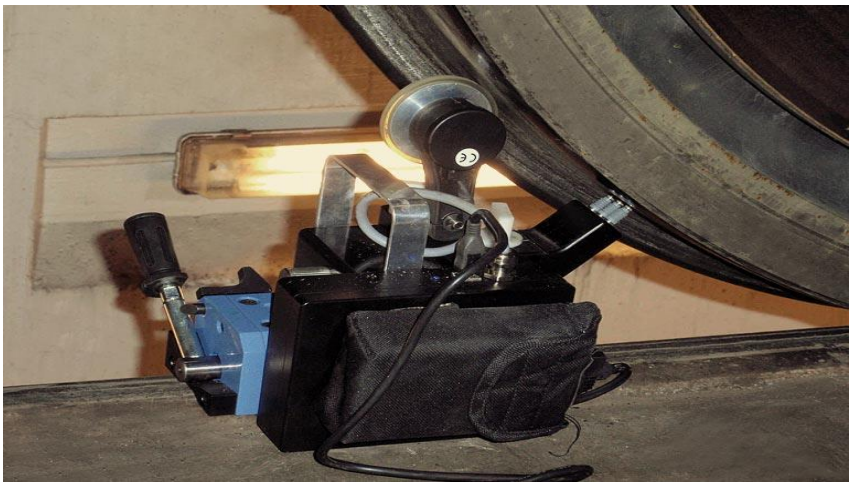

Figure 1.6 – TriTops being used to detect any signs of corrugation on the track [14]

1.3 Thesis organization

The thesis will be organized the following way:

- **Chapter 1** – Introduction of rail corrugation, methods to detect it and the thesis structure.
- **Chapter 2** – Describes the theoretical aspects of the time-frequency analysis used in RailScan.
- **Chapter 3** – A detailed description of the functions used to detect rail corrugation.
- **Chapter 4** – RailScan and methodology.
- **Chapter 5** – Results.
- **Chapter 6** – Conclusions and guidelines for future work.

Description of the time frequency analysis used in RailScan

2.1 Short-Time Fourier Transform (STFT)

Fourier transform (FT) reveals the frequency composition of a signal by transforming the signal from time domain into the frequency domain. [17]

FT presents a problem, it cannot represent time and frequency localization and if the signal being analyzed is non-stationary the analysis will be limited. The data obtained to analyze rail corrugation is generally non-stationary, so it is necessary to use a different technique. [17]

To overcome this limitation of the FT, it was created the short-time Fourier transform (STFT).

The STFT has a sliding window function that is centered at a specific time τ. For each τ, a time-localized FT is performed on the signal. After that, the window is moved by τ and another FT is performed on the signal. This process is done until there is no more signal to analyze. This is the method used to analyze non-stationary signals using FT, because if the signal is divided by time-windows, in each window the signal is considered stationary. This method reduces the number of computations made [17], [28].

As it is show in figure 2.1, The STFT decomposes the signal into a time-frequency representation.

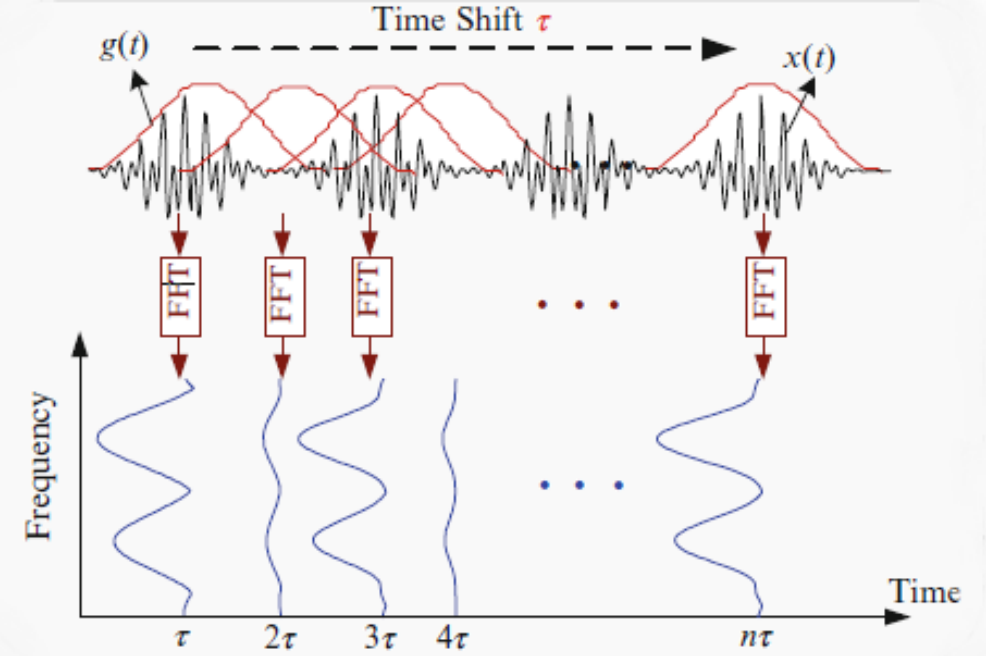

Figure 2.1 – Apllication of a STFT on a signal [17]

The STFT can be expressed as Equation 3.1:

$$\text{STFT}(\tau, f) = \int x(t)\, g^*_{t,f}(t)\, dt = \int x(t) g(t-\tau) e^{-j2\pi f t}\, dt \quad (2.1)$$

In equation 3.1,$x(t)$ is the signal being analyzed, g (t- τ) the sliding window function, f the frequency of the signal and τ the time of the signal.

Basically, the STFT provides information about when and what frequencies a signal has in certain events.

Having a sliding window means that a longer window produces a different result than having a smaller window. In this case, a shorter window gives a good time resolution and a longer window gives a good frequency resolution. It is impossible to have both [29].

Once the window length is defined, that length will be the same for all frequencies but for almost all vibrating signals, higher frequencies do not need to have the same resolution as the lower frequencies. To overcome this window length problem, it is necessary to use a different method.

2.2 Wavelet analysis

The FT is a powerful tool in data analysis, however it does not represent abrupt changes efficiently.

FT represents data decomposed in sine waves, which oscillate theoretically forever. Therefore, to analyze data with abrupt changes, we need to use functions that are localized in time and frequency. [18]

A Wavelet is a waveform of limited duration that has an average value of zero. They differ from sine waves because they are asymmetric and irregular. The wavelet transform can modify the resolution for different frequency ranges unlike the FFT [19].

Wavelets come in different sizes and shapes, known as mother wavelets. Figure 2.2 shows various examples of mother wavelets.

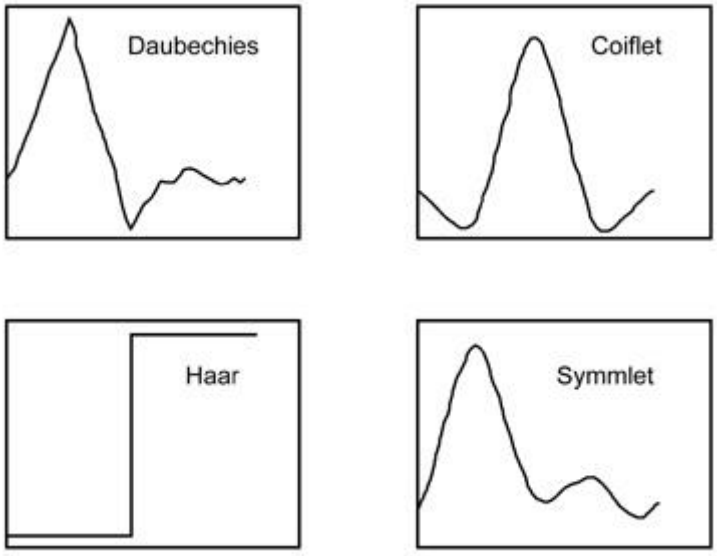

Figure 2.2 – Examples of mother wavelets [19]

The choice of which wavelets to use depends only on what features of the signal are trying to be detected, for instance to detect abrupt changes in a signal we can choose one wavelet but if we are trying to detect oscillations we can choose another. [19]

The two major transforms in wavelet analysis are Continuous Wavelet Transform (CWT) and Discrete Wavelet Transform (DWT).

The CWT and DWT differ in how they discretize the scale and shifting parameters. [19]

2.2.1 CWT (Continuous Wavelet Transform)

The CWT is used in RailScan because it allows a time-scale analysis of the signals, it decomposes them considering their frequency components [30].

The CWT is defined as the sum over the time of the signal, multiplied by the scale and shifted versions of the mother wavelet $\Psi(\tau)$.

$$\mathrm{CWT}^{\Psi}{}_{x}(\tau, s) = \frac{1}{\sqrt{|s|}} \int x(t)\, \Psi * \frac{t-\tau}{s}\, \mathrm{dt} \qquad (2.2)$$

CWT is a function defined by two variables, s is the scale and τ is the location of the wavelet as it passes through the signal. [20]

In figure 2.3, it will be shown how the CWT is calculated.

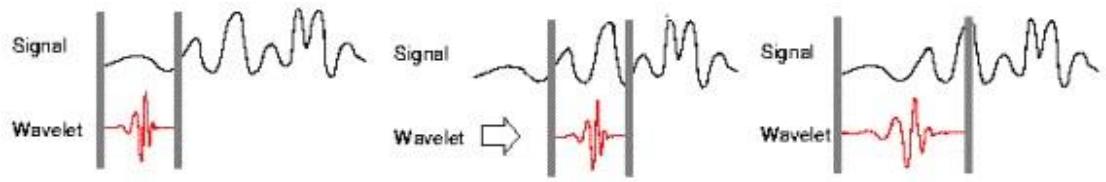

Figure 2.3 – Wavelet changing in scale and position [20]

In figure 2.3 it is possible to see how the CWT affects the signal. The figure must be divided in 3 parts for a better understanding. The first part is the definition of which wavelet to use, following the calculation of the first coefficient. In the second part, the scale is the same, but the position of the wavelet changed to be able to calculate all coefficients. All windows are versions of the mother-wavelet. After calculating all coefficients, the signal returns to the initial position but the scale is different and the process to determine the coefficients initiates again [32].

After all the coefficients of the wavelet are calculated they must be multiplied by the appropriately scaled and shifted wavelet [18]. The scale parameter is somewhat equal to the scale of a map, if the scale is larger it is possible to observe more information, but with no detail and if the scale is smaller it shows the detailed information. [15]

Scaling is the process of stretching and shrinking the signal in time and it is inversely proportional with the frequency. Table 3.1 shows how the wavelet scale influences the frequency, the higher the scale the smaller the frequency.

Table 2.1 – Comparing the wavelet scale with frequency [18]

Wavelet Scale	2	4	8	16
Frequency (F)	$\frac{F}{2}$	$\frac{F}{4}$	$\frac{F}{8}$	$\frac{F}{16}$

Figure 2.4 – Relation between scale and frequency. [20]

The relation between scale and frequency is represented in figure 2.4. With a small scale factor, we obtain a compressed wavelet to help capture the abrupt changes in the signal and the wavelet has high frequency. With a high scale factor, we obtain a stretched wavelet that helps capture slow changes in a signal and the wavelet has low frequency.

Shifting the wavelet means delaying its onset (figure 2.5).

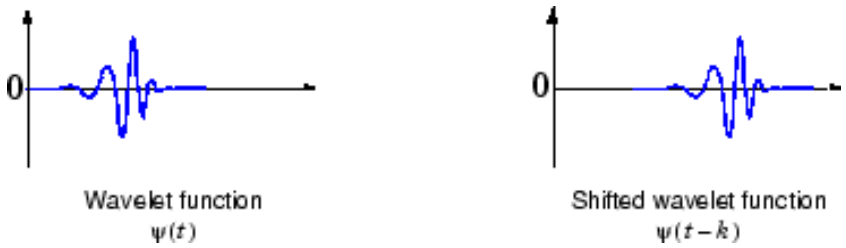

Figure 2.5 – Shifting a wavelet [20].

The CWT is a representation with a high degree of redundancy, because there is an overlap between wavelets at each scale and between scales. It can operate at every scale, but that requires a high level of computation. [21]

In the CWT, we can analyze the signal in intermediary scales, known as scales per octave. The larger the number of scales per octave, the finer the scale discretization.

Calculating the wavelet coefficients at every scale brings redundancy when trying to reconstruct a signal, a different form of wavelet transform is used, the DWT.

The scales of the DWT are based on power of two. [21]

2.2.2 DWT (Discrete Wavelet transform)

The DWT is the equivalent of comparing the signal with discrete multirate filter banks.

The filtering process is explained in the next figure (figure 2.6)

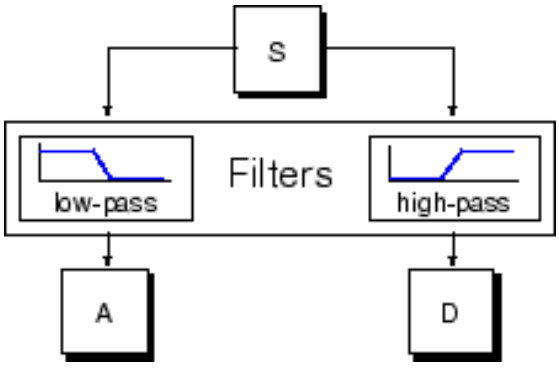

Figure 2.6 – Filtering process for the DWT [22]

The signal S passes through a low-pass and high-pass filter, dividing the signal into two coefficients, coefficient A and coefficient D. The coefficients are approximation (A) and detail (D). The approximation coefficient A is the high scale, low-frequency part of the signal [33].

The detail coefficient D is the low scale, high-frequency part of the signal.

If the process of figure 2.6 happened, the number of coefficients will double. To correct this, a down sample must occur. The filter output is down sampled by two, throwing away every second coefficient and with that now the number of coefficients is half the original signal [22].

In figure 2.7 it is explained how this process works.

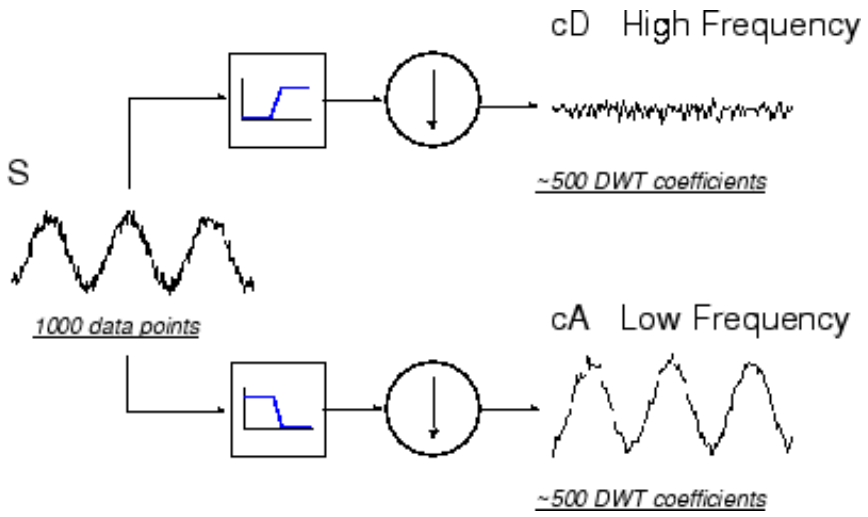

Figure 2.7 – Down sampling a signal [22]

The decomposition process can be iterated, decomposing the generated approximation into many lower resolution components. This process is called the wavelet decomposition tree.

Theoretically this process can be done until on sample is left.

In practice, the number of decomposition levels depends on the signal we are trying to analyze.

In figure 2.8 is represented an example of a 3-level decomposition tree.

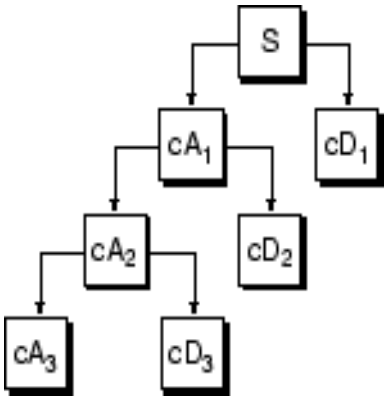

Figure 2.8 – 3 level decomposition tree [15]

2.2.3 Wavelet Reconstruction

The DWT can be used to decompose signals, but the process of decomposition can be reversed without loss of information. The wavelet reconstruction process consists in up sampling and filtering. Up sampling is the process of lengthening a signal by inserting zeros between samples [20].

The decomposition and reconstruction filters form a system that is called quadrature mirror filters (figure 2.9) [20].

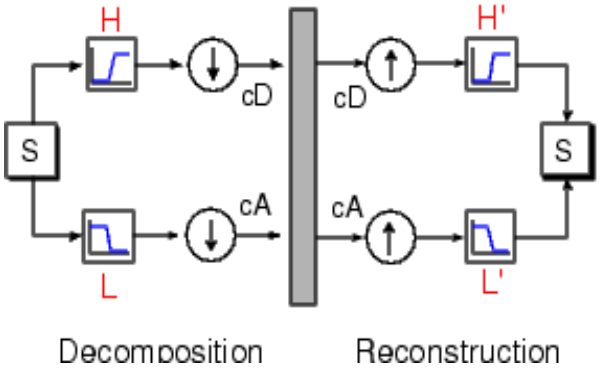

Figure 2.9 –Wavelet reconstruction example [20]

Figure 2.10 is an example of how a signal is reconstructed using wavelets. The signal is decomposed into a 3-level tree and coefficient A is being decomposed as it was shown in figure 2.8. To reconstruct the filtered signal into the original, different equations can be used, as it is explained in figure 2.10. To reconstruct the filtered signal into the original signal, there are 3 different ways in this case. If the decomposition tree was bigger, the number of cases that could be used to reconstruct the signal would be higher [33].

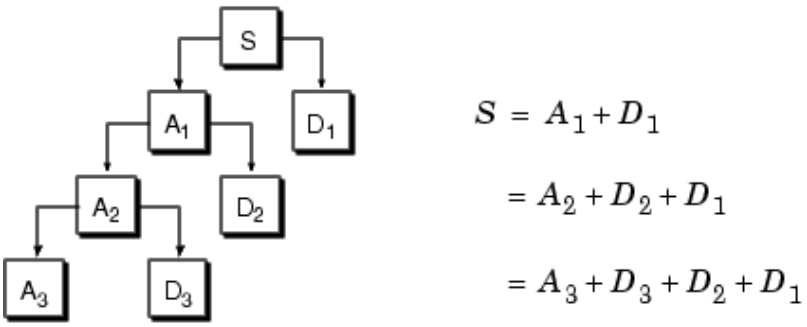

Figure 2.10 – 3-level decomposition tree [20]

It is possible to reconstruct the approximation and detail coefficients. That can be done by passing the approximation and detail coefficient vectors with a vector of zeroes.

2.2.4 Wavelet Packet Decomposition

In the DWT, the signal is split into an approximation and a detail. The approximation is split again generating a sub level approximation and detail.

In the wavelet packet both details and approximation can be split, generating more ways to reconstruct the signal. Figure 2.11 represents the wavelet packet decomposition tree.

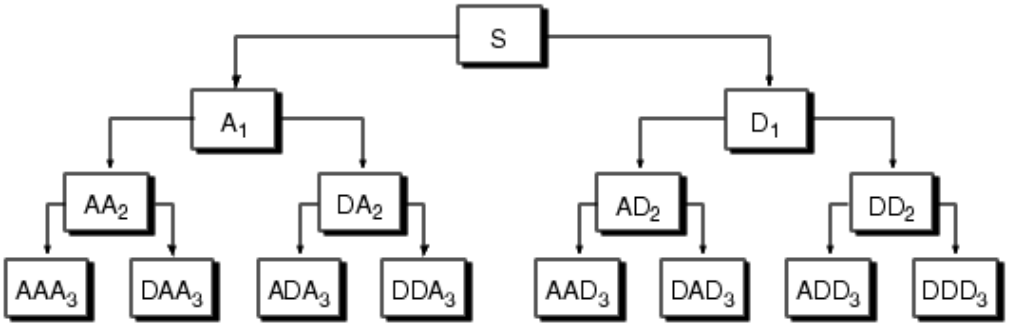

Figure 2.11 – Wavelet Packet 3-level decomposition tree [16]

Wavelet packet analysis allows the signal S to be represented for example as A1+AAD3+DAD3+DD2, which is not possible in ordinary wavelet reconstruction.

Norms used to analyze Rail Corrugation

3.1 DIN ISO 3095:2013 and EN 13231-3:2012

To monitor if there is corrugation, two different methods can be used. One method measures the acoustic roughness of the rail and the other if rail irregularities surpassed a certain limit.

The first method considers the acoustic roughness criteria of DIN ISO 3095:2013 related to corrugation and the second method the wavelength limit criteria EN 13231-3:2013.

Basically, these two methods could work together to achieve the best result of a rail without corrugation. Using DIN ISO 3095 to monitor the roughness level is a very effective method and when the roughness level passes the upper limit accepted, a process called rail grinding is used to re-profile the rail. After re-profiling the rail, EN 13231-3 criteria is used because DIN IS0 3095 does not specify how much irregularities a rail can have.

In this thesis, both norms will be implemented even though ISO 3095 is more complete, EN 13231-3 is the most used by all railway companies. [3]

3.2 DIN ISO 3095:2013

DIN ISO 3095, shows a spectrum (figure 3.1) where for each wavelength there is a limit for the acoustic roughness it can have, meaning that if the roughness level is above the wavelength limit, there is corrugation on the rail.

The one-third octave spectrum is originally used to analyze acoustic signals. This spectrum can be used to measure the acoustic roughness of the signal because it can measure the power in each frequency band. [23]

If the one-third spectrum can measure acoustic roughness it can be used to measure corrugation.

Figure 3.1 will show the one third octave spectrum used to detect corrugation.

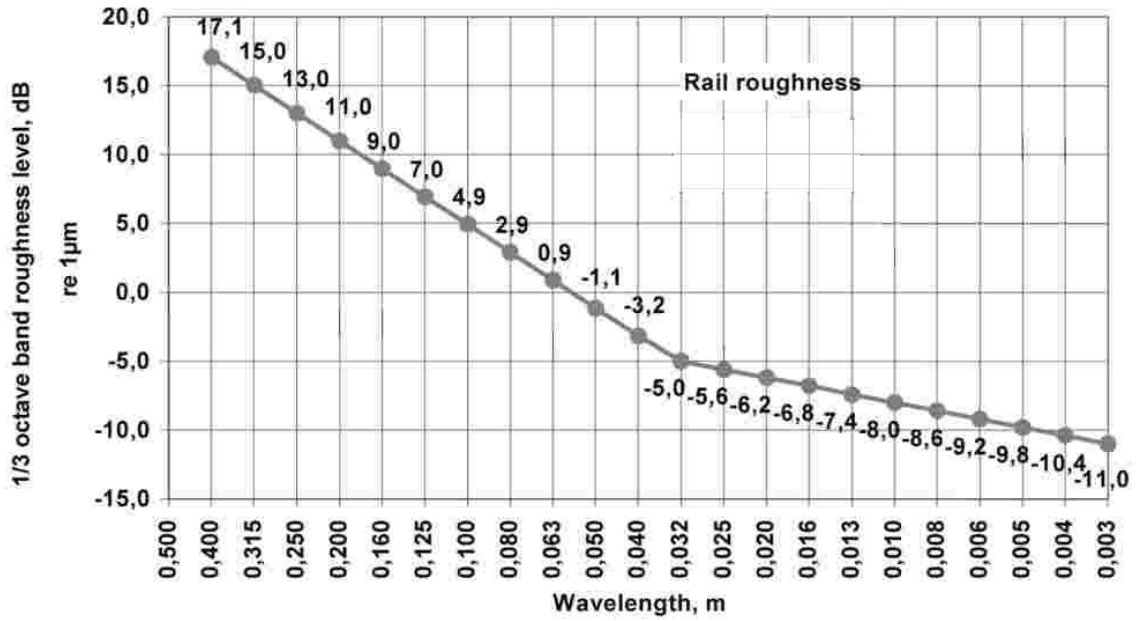

Figure 3.1 – One-third octave spectrum used to measure rail roughness [23]

Using equation (3.1) the pre-defined ISO wavelengths (v = 1m/s) were converted to frequencies and the following table (table 3.1) was obtained. [16]

$$f = \frac{v}{\lambda} \tag{3.1}$$

Table 3.1– One third octave band frequencies [16]

Wavelength (m) λ	Central frequency (Hz) f_c	One third octave band (Hz) $f_{lcut} - f_{hcut}$
0.4	2.5	2.2281 - 2.8050
0.315	3.1746	2.8294 - 3.5620
0.25	4.0	3.5650 - 4.4881
0.2	5.0	4.4563 - 5.6101
0.16	6.25	5.5703 - 7.0126
0.125	8.0	7.1300 - 8.9761
0.1	10.0	8.9125 - 11.2202
0.08	12.5	11.1406 - 14.0252
0.063	15.8730	14.1468 - 17.8098
0.05	20.0	17.8250 - 22.4404
0.04	25.0	22.2813 - 28.0505
0.0315	31.7460	28.2937 - 35.6196
0.025	40.0	35.6500 - 44.8807
0.02	50.0	44.5625 - 56.1009
0.016	62.5	55.7032 - 70.1262
0.00125	80.0	71.3001 - 89.7615
0.001	100.0	89.1251 - 112.2018
0.008	125.0	111.4064 - 140.2523
0.0063	158.7302	141.4684 - 178.0982
0.005	200.0	178.2502 - 224.4037
0.004	250.0	222.8127 - 280.5046
0.00315	317.4603	282.9368 - 356.1963

The f_{lcut} and f_{hcut} frequencies are calculated by the following expressions:

$$f_{lcut} = \frac{f_c}{10^{\frac{1}{20}}} \tag{3.2}$$

$$f_{hcut} = f_c * 10^{\frac{1}{20}} \tag{3.3}$$

Equations 3.2 and 3.3 are used to calculate the superior and inferior limit of the central frequency.

For frequencies close to the Nyquist value or zero an interpolation factor is applied to the data to improve the stability of the filter. [16]

3.2.1 Implementation of the norm ISO 3095:2013

To implement this norm, a Matlab function was implemented, a function that considers the signal we want to analyze, the distance travelled and the average speed of the measuring equipment.

In this function, the wavelength limits defined by the norm were considered, as it is referred in table 3.1.

Using a Butterworth filter of order 8, the signal is filtered using the superior and inferior limits of the central frequency (equations 3.2 and 3.3).

After filtering the signal, it is necessary to calculate its roughness level in db. To calculate the roughness level for each wavelength, the following expression must be used.

$$L_r = 10 \log(\frac{r}{r_0})^2 \tag{3.4}$$

Where,

L_r is the roughness level in dB

r is the RMS roughness in µm

r_0 the reference roughness; r_0 = 1 µm

After calculating L_r, a comparison between the roughness level calculated and the maximum roughness level allowed must be done, and if it passes the maximum allowed, the rail is considered corrugated in that specific wavelength.

In figure 3.2 it is a flow chart explaining how the implementation was done.

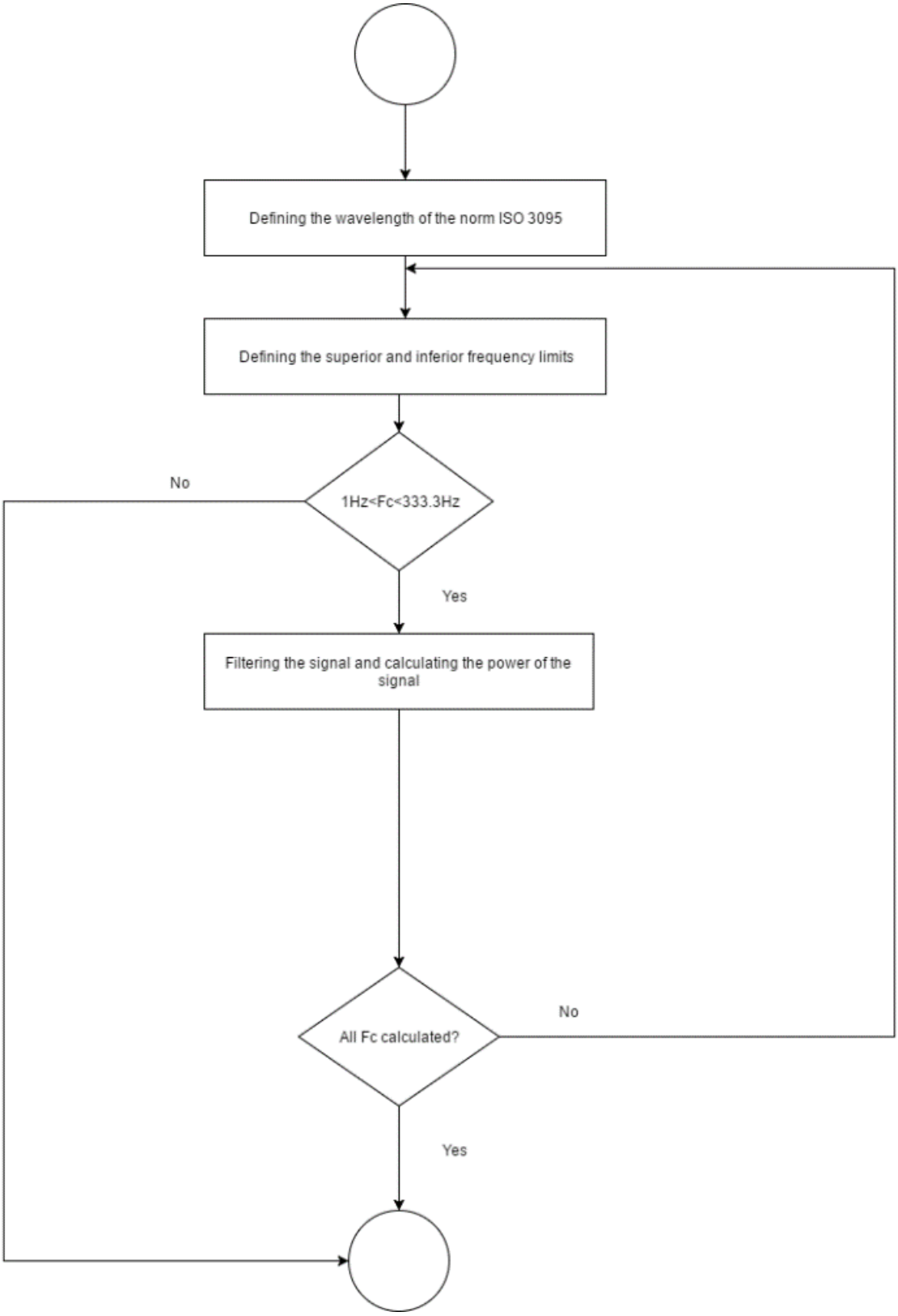

Figure 3.2 – Flow chart of the implementation of the one third spectrum function

Figure 3.2 explains how the process of implementing the EN ISO 3095 was done. First, the wavelength to filter the signal must be defined (table 4.1). After that, equations 3.2 and 3.3 are

used to calculate the upper and lower limits of the filter. After filtering the signal, equation 3.4 is used to calculate the roughness level of the signal for that specific wavelength and that value is compared to the maximum value defined in ISO 3095. This process is done until there are not more wavelengths to use.

3.3 EN 13231-3:2012

The European norm EN 13231-3 presents two tables in its published document. Table 3.2, shows the acceptance criteria in terms of allowable percentage of exceeding and table 3.3 shows the acceptance criteria to peak to peak limits.

Table 3.2 – Acceptance criteria of allowable percentage of exceeding [24]

Wavelength range (mm)	10 to 30	30 to 100	100 to 300	300 to 1 000
Class 1	5 %	5 %	5 %	5 %
Class 2	No requirement	10 %	10 %	No requirement

In table 3.2 it is possible to notice that wavelengths are divided into four groups, implicating that the implementation of this norm will have to ensure that these wavelengths are considered. In all wavelength ranges, the percentage of exceeding is 5%, meaning that all signal being measured cannot surpass more that 5% of the established limit.

Class 2 will not be used in this program, it is a very specific class and does not represent what it is trying to be proved by using this norm. Class 2 only contemplates two groups of wavelengths and using it will not bring any added value to RailScan.

Table 3.3 – Acceptance criteria of peak to peak limits [24]

Wavelength range (mm)	10 to 30	30 to 100	100 to 300	300 to 1 000
Limit of peak-to-peak values (mm)	± 0,010	± 0,010	± 0,015	± 0,075

Table 3.3 is where the wavelength maximum peak to peak value is defined. Table 3.2 shows the percentage of exceeding. However, does not mention the limit and table 3.3 demonstrates it. For each wavelength group there is a different restriction and that restriction is specified in peak-to-peak values.

If the peak-to-peak values of a signal exceed the established limit and it represents more than 5% of all signal than it is possible to infer that there is corrugation in the rail for those wavelengths.

Using equation (3.5) the pre-defined wavelengths (v = 1m/s) were converted to frequencies and the following table was obtained.

$$f = \frac{v}{\lambda} \tag{3.5}$$

Table 3.4 – One third octave band [16]

Wavelength (mm)	**Frequency (Hz)** f_{lcut} - f_{hcut}
10-30	33.33-100
30-100	10-33.33
100-300	3.33-10
300-1000	1-3.33

For frequencies close to the Nyquist value or zero an interpolation factor is applied to the data to improve the stability of the filter. [16]

3.3.1 Implementation EN 13231-3:2012

To apply this norm, a Matlab function was implemented, a function that considers the signal we want to analyze, the distance travelled by the signal and the average speed.

In this function the wavelength limits defined by the norm were considered, as it is referred in table 3.4.

Using a Butterworth filter of order 8, the signal is filtered using the superior and inferior limits of the wavelengths (table 3.4).

EN 13231 maximum is in peak to peak value, meaning that after filtering the signal, the peak to peak value must be calculated.

After this calculation, we must compare the peak to peak values to the max peak to peak allowed and if it passes the 5% criteria, the rail is considered corrugated.

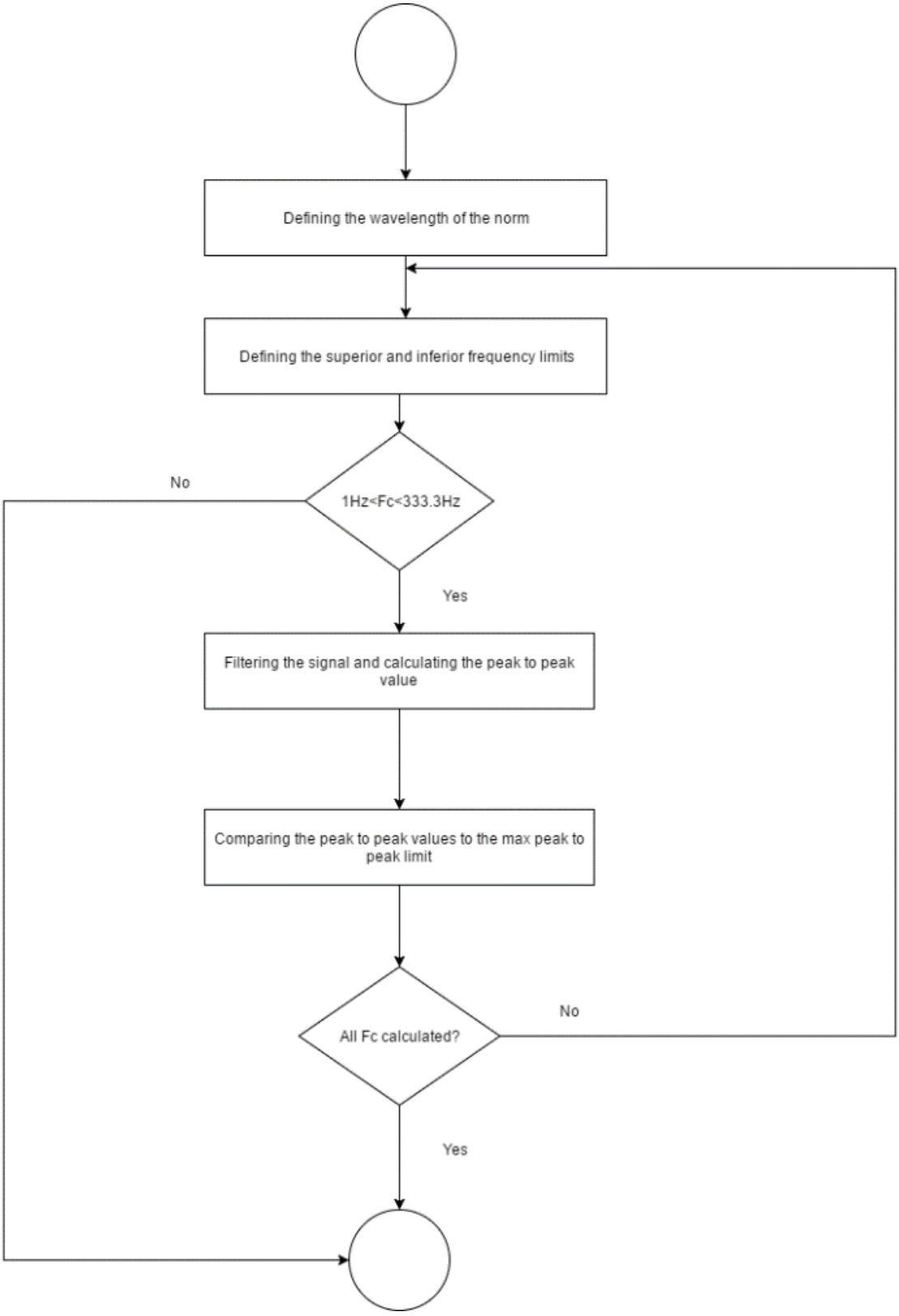

Figure 3.3 – Flow chart of the EN13231 function

Figure 3.3 explains how the norm EN 13231 was implemented. This implementation is not very different from the EN ISO 3095 because both implementations select a range of wavelengths to filter the signal. After filtering, the peak to peak value must be calculated and compared to the

maximum peak to peak value allowed. This process is done until there are not more wavelengths to use.

Even thought, EN 13231-3 is a different norm than ISO 3095 it can also be applied to the one third octave spectrum (figure 3.4).

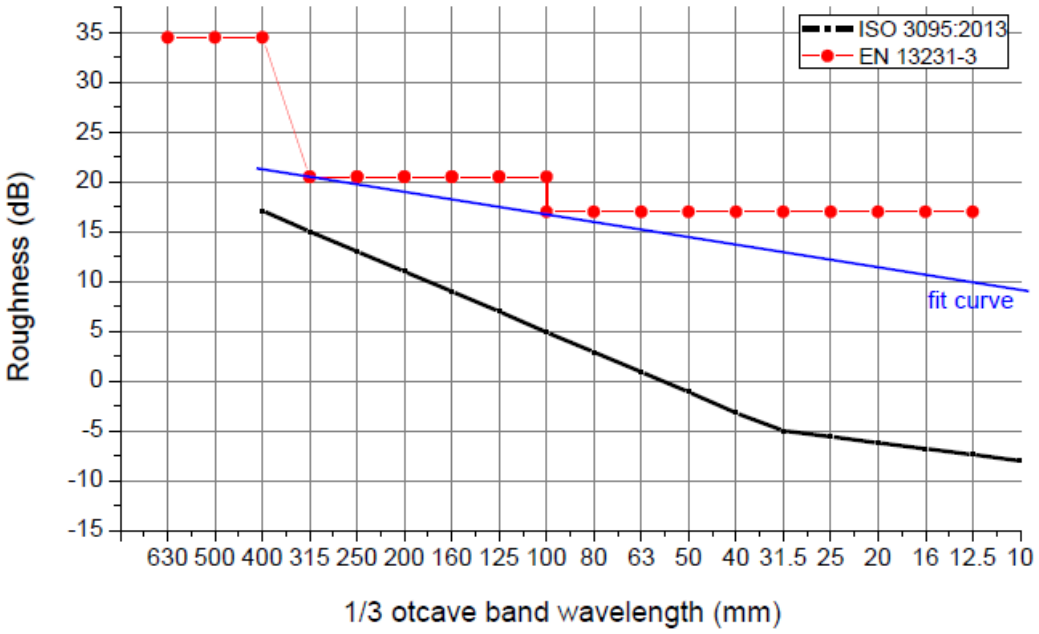

Figure 3.4 – Roughness level comparison between the ISO 3095:2012 and EN 13231-3 [3]

Although the representation of figure 3.4 is not according to the norms, because EN 13231-3 does not use the one third octave spectrum, figure 3.4 represents how exigent both norms are, the roughness level is much higher in EN 13231-3. Figure 3.4 displays that two different results will be achieved if both norms are used simultaneously.

3.4 Corrugram

Corrugram is a program developed by Arnaldo Batista Nuno Barrento, Manuel Ortigueira and Fernando Coito, in FCT-UNL. The main objective of this program is to find a new representation of rail corrugation. Corrugram will help to visually detect if there is any corrugation exceeding the norms.

It is very useful to identify sections of the rail that have corrugation and to provide a differential indicator of rail corrugation amplitude for each wavelength and for each rail section. Corrugram can be applied to have smarter and simple preventive action and to learn which section of the rail needs intervention. It contemplates the power spectrum associated with the vibrations in each section of the rail. This innovation also presents a differential analysis of the power spectrum for all wavelengths and that analysis will be compared to values that are considered

adequate for the safety of the rail. Additionally it presents the sections of the rail that need maintenance.

Corrugram works directly with the norm DIN ISO 3095, it depends on roughness level values, as it is demonstrated in the one third octave spectrum (figure 3.1). Basically, if a 2 cm wavelength has a greater value than 0 dB, the Corrugram will show a yellow color and the greater the value of rail roughness the color will become red.

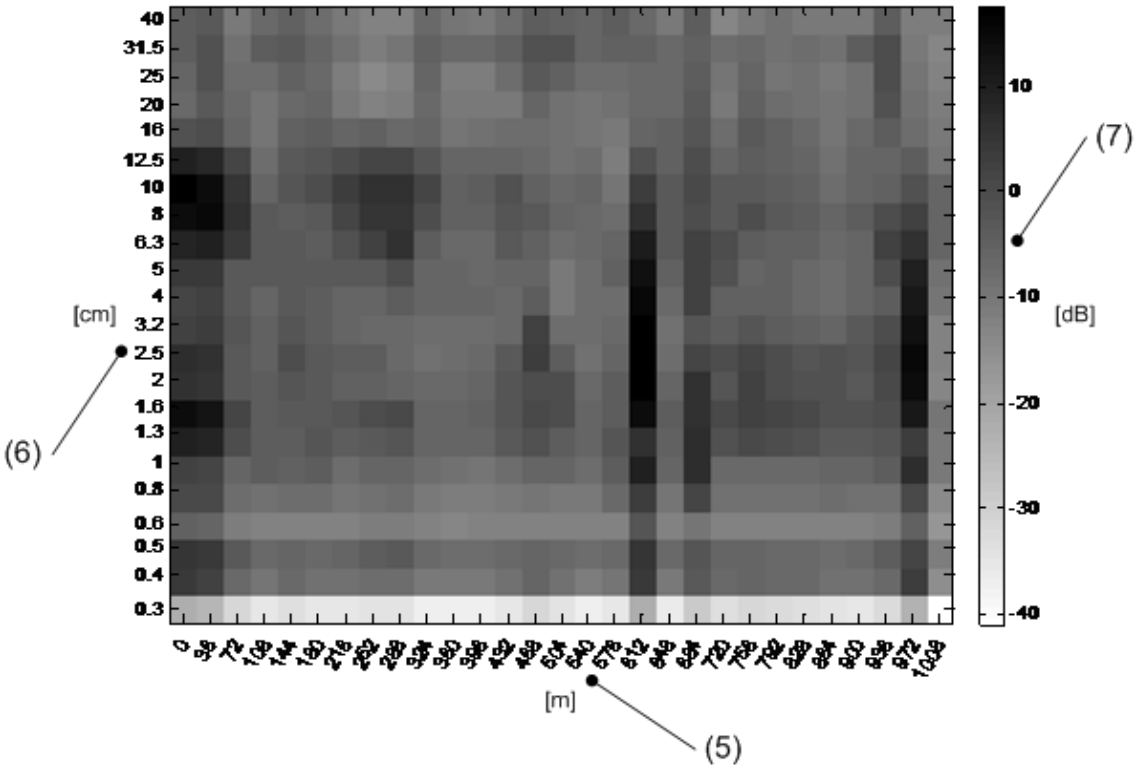

Figure 3.5 – Ilustration of the Corrugram patent document [26]

Figure 3.5 is an example presented in the patent [26]. In the x axis, represented by number 5, it shows the distance traveled by the train. The x axis is divided by parts of 36 m, though that value can be altered. The x axis can be divided by any distance, if that distance is inferior to the distance travelled by the train. The y axis, represented by number 6, represents all the wavelengths of the one third octave spectrum. Number 7 is a colorbar, that if Corrugram has values above 0 dB it will show yellow and if the value increases it will become red. The same equivalent is applied to values below 0 dB, it begins with a grey color, but if the value decreases a green color will appear. Figures 4.6 and 4.7, show an example of Corrugram being applied to a signal using RailScan v3.0 where norms ISO 3095 and EN 13231 were added to the Corrugram algorithm.

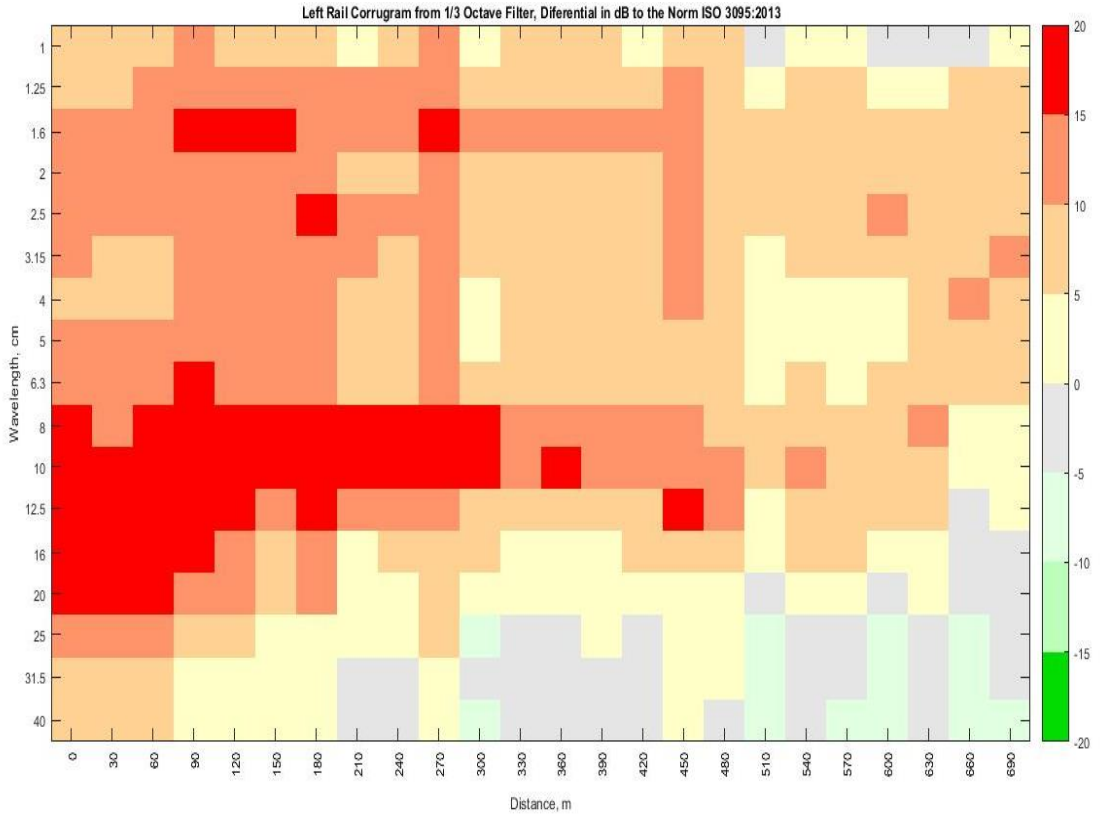

Figure 3.6 – Corrugram example of a random signal using the norm DIN ISO 3095:2013

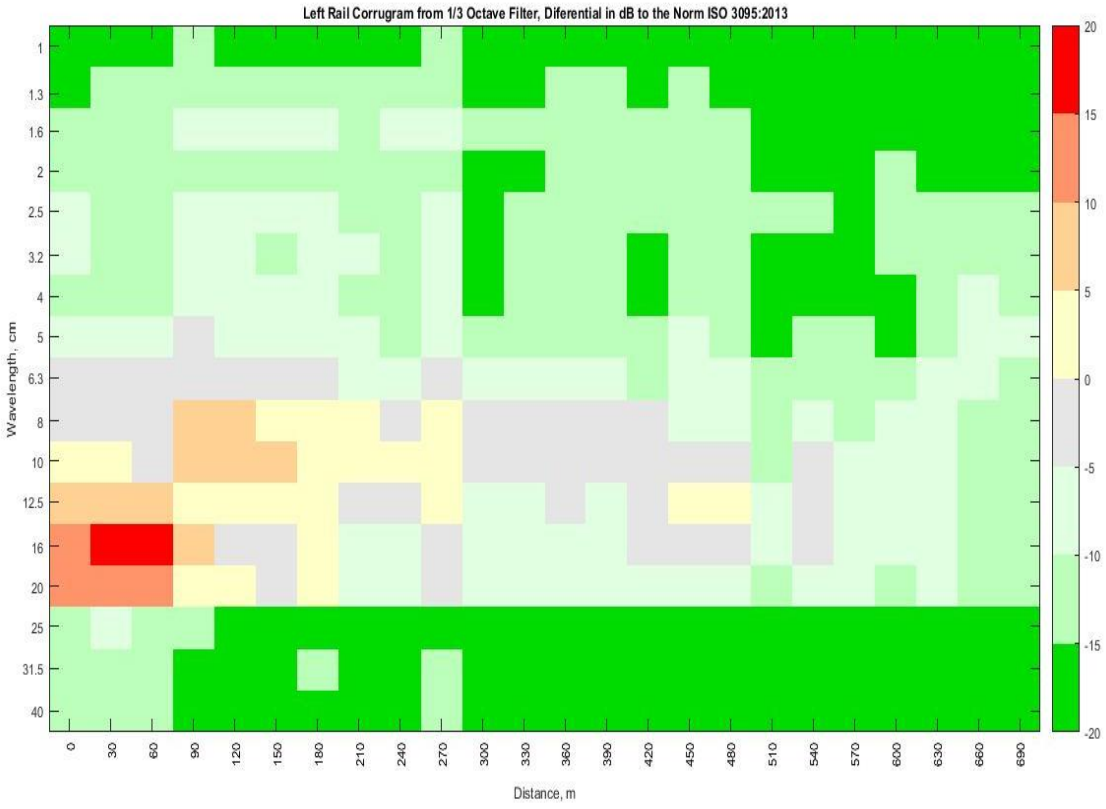

Figure 3.7 – Corrugram example of a random signal using the norm EN 13231-3:2012

One of the biggest changes made was to implement the Corrugram to work with EN 13231-3:2012. The implementation of this new norm in the Corrugram, made all sense because the Corrugram is a very flexible program, it can always adapt to different situations. EN 13231-3:2012, uses different wavelengths and has different rail roughness levels when compared to DIN ISO 3095.

Comparing figures 3.6 and 3.7 it is possible to see that even though the signal is the same, the results are very different. Figures 3.6 and 3.7 are in agreement with the one third octave spectrum that displayed both norms (figure 3.4), ISO 3095 is more exigent than EN 13231.

RailScan

4.1 Data organization and RailScan V3.0

Wavelet analysis has been used for vibration signals analysis and proved to be the most efficient tool for non-stationary signal analysis. [16]

Other methods can be used to analyze non-stationary signals, like the classic Fourier Transform analysis, but this analysis proved to be incomplete. Later in this thesis it will be explained why the Fourier analysis has proven to be incomplete.

RailScan uses the Continuous Wavelet Transform (CWT) and the Wavelet Packet Transform (WPT) to analyze data and also compares the signal (using the norm ISO 3095 parameters) with the one third octave spectrum [15].

An older version of RailScan was already implemented, so the following table represents the main differences between RailScan then and now.

Table 4.1 – Comparative table between RailScan V2.1 and RailScan V3.0

Comparative table	RailScan V2.1	RailScan V3.0
Inverse CWT	×	✓
Wavelet Packet	✓	✓
DIN ISO 3095:2013	×	✓
EN 13231-3:2012	×	✓
Corrugram	×	✓
Capability of analyzing both rails	×	✓

The first column refers to the CWT implementation. In RailScan V2.1, the CWT was integrated by its developers and the representation of the signal was easier because the y axis was linear and for that reason it would not use to much graphic memory. In RailScan V3.0 the CWT used is the CWT function of Matlab, a function already implemented, but in the graphic representation of the new CWT, the y axis is represented in log2 scales. Y axis must be represented linearly or the analysis will be inconclusive and to do that a function that uses more

memory needs to be applied, which represents a problem because bigger signals take too long to be represented.

Using the CWT function of Matlab it is possible to invert the CWT representation of the signal into the original signal, in any part chosen by the user.

Although the implementation of the new CWT is better and allows the possibility to invert the signal in any part, its representation is not time efficient, so it was necessary to revert to the previous representation because RailScan needs to be an agile application.

Since previous CWT representation does not provide a feature to invert the signal, this implementation was extended in order to apply that feature to the signal being analyzed. In this case, the inverse CWT becomes the marginal CWT, making it possible to measure the CWT power for any pair of chosen frequencies. With this extended feature we have another way to detect rail corrugation.

The Wavelet Packet function also suffered some innovations in RailScan V3.0. It can analyze both rails at the same time.

In RailScan V2.1 the one third octave spectrum used the norm DIN ISO 3095:2005, but the norm was updated in 2013 leaving RailScan outdated. The use of the renewed norm and the representation of both rails in that norm are innovations. RailScan V2.1 also assumed that the unit of measurement was micrometer (μm), and now all signals must be in the universal unit of measurement, meter (m).

RailScan V3.0 uses a new feature that can also detect if corrugation is present in the rail, the EN:13231-3:2012, a European norm that uses peak to peak values of the signal and if those values pass the max peak to peak value allowed for more than 5%, it is specified that corrugation is exceeding in the rail. This function did not exist in RailScan V2.1, so a comparison between both programs is not possible.

Corrugram was also implemented, this function is a new way to represent where and if corrugation is present in the rail and it was also implemented for the first time in RailScan V3.0.

The last main difference, is the capability of analyzing both rails at the same time. RailScan V2.1 could only analyze a rail and that was not practical, so the adjustment was necessary.

As stated before, this new version of RailScan no longer loads the displacement of the rail, it now loads a file with a structure that must be followed, or the program will not run correctly.

To choose what must be considered in the structure is important to know about the signal characteristics RailScan will analyze. The displacement of the rail is the most important part, so it is the first value to enter the structure. The name that should be in the structure is LeftRail_RightRail_m, and this variable must have data from both rails, otherwise it will not work.

The other variable that needs to be in the structure is the distance travelled by the train. With this distance, we can find the space between samples that are important to obtain the sampling frequency. The distance variable must be named distance_m and the space between measures ds_m.

The speed of the equipment to measure rail corrugation is also essential, because the sampling frequency is calculated using speed. The name of the variable is speed_m_s.

The sampling frequency variable name is fs_hz.

Some data acquired do not come in meter units, some of it are acquired in the form of acceleration (indirect measurement), so a variable that accounts for it must be created. If the data is already in meters, that variable is null.

To help the user with these specifications, it was created a help button that describes how RailScan variables must be, so it can work perfectly.

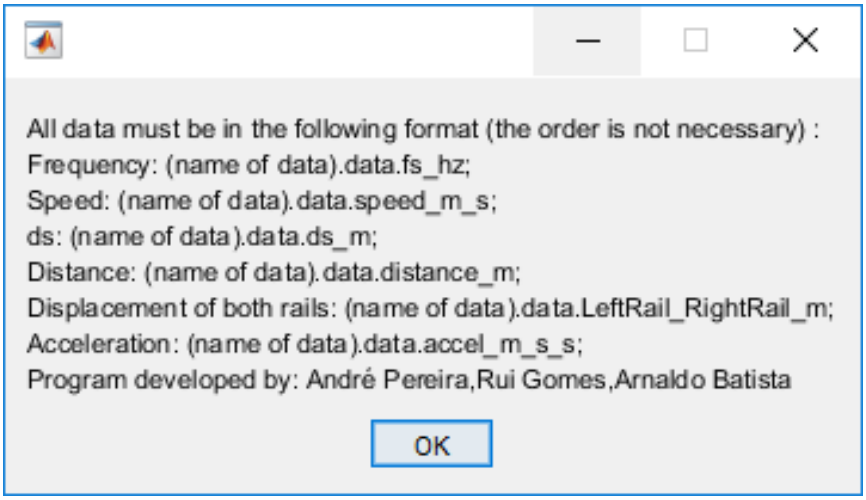

Figure 4.1 – Information shown in the help button

The loaded structure also comes with another part, the information about the signal. The information is provided by the data acquisition team. For example, it can have the name of the file, the distance travelled and how the data was acquired.

A button info was created, so the user can have a clear information about the signal.

4.2 Synthetic signal

As it was mention before, the CWT implementation was different in RailScan V3.0, so to verify if it was correctly implemented, a synthetic signal was created to simulate corrugation. To make the synthetic signal, it was used a chirp. A chirp is a signal in which the frequency increases

or decreases consistently. The chirp created was linear, with variable frequency from the highest wavelength to the lowest wavelength meaning that the frequency increases.

The highest wavelength a rail with corrugation can have is 1 m and the lowest is 0.003 m, so to use this values in the chirp signal, they must be passed to frequency, using equation (4.1).

$$f = \frac{\nu}{\lambda} \tag{4.1}$$

f is the frequency of the signal, ν is the velocity and λ the wavelength.

Assuming a velocity of 1 m/s, the frequency is easily calculated. So, the chirp will increase its frequency from 1 Hz to 333.3 Hz.

The next step is to define were in time, the frequency 333.3 Hz will be reached. The time defined was 125 s. With ν being 1 m/s, using the equation (4.2), it is possible to calculate the value of the distance travelled.

$$\delta = \nu * \tau \tag{4.2}$$

With these specifications, the chirp was implemented. The spectrogram plot (figure 4.2) will demonstrate the linear rate of change in frequency as a function of time, in this case from 1 to 333.3 Hz.

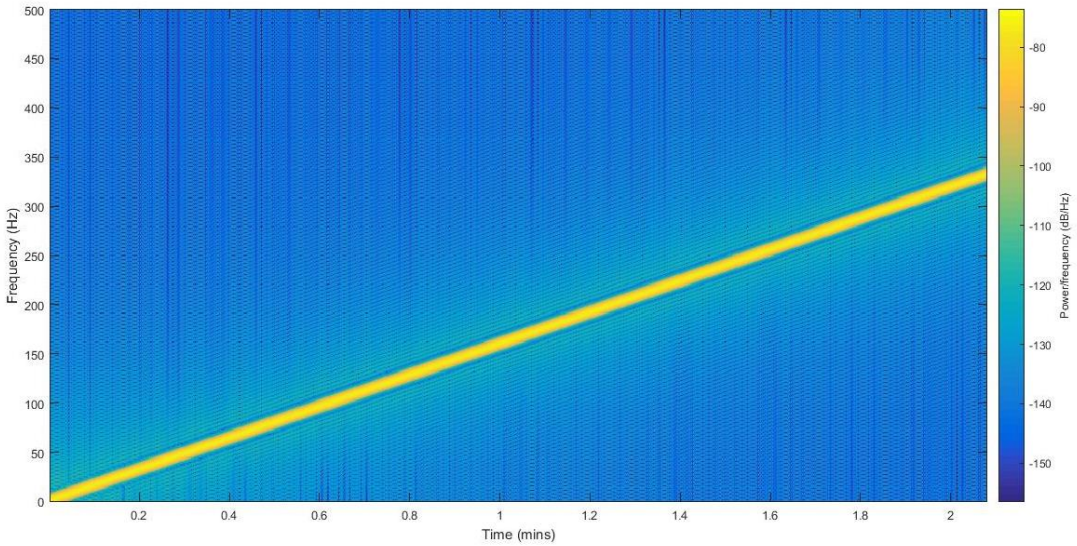

Figure 4.2 – Spectrogram of the synthetic signal

Using the new CWT, the graphic representation is expected to be very similar. CWT will construct a time-frequency representation of the synthetic signal. The synthetic signal is a linear signal that is increasing its frequency over time and that is why the CWT is expected to be equal to the spectrogram.

The CWT must have certain specifications to be implemented, the first one is to choose the mother wavelet, in this case the wavelet used was the Morlet Wavelet. The other spec is the number of voices per octave, this specification determines the resolution of the representation.

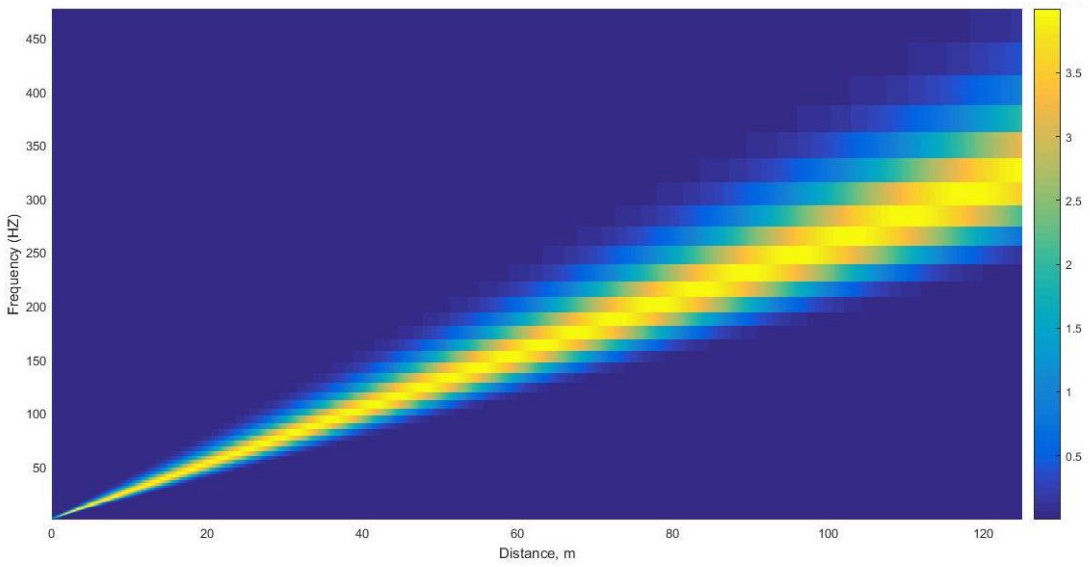

Figure 4.3 – CWT representation of the synthetic signal

As it is represented figure 4.3, the time-frequency representation is accurate. The representation is linear and varies from 1 Hz to 333.3 Hz. Other frequencies that are present in the signal are represented by colors that are less intensive than yellow.

With figures 4.2 and 4.3, it is possible to conclude that the implementation of the CWT was correct.

4.3 Inverse CWT

The new RailScan has an innovation, it can perform the inverse CWT in order to reconstruct the signal in a selected waveband.

Before using the inverse function, it was defined that the user could choose which part of the signal they would want to be reconstructed. Using ginput, a Matlab function that gives the x- and y-coordinates it is possible to determine exactly which parts of the CWT representation were selected.

After selecting the area, RailScan must reconstruct the new signal.

In the RailScan scalograms and spectograms, the x axis is the distance travelled and the y axis the frequency. With that values identified it is possible to invert the CWT to obtain the signal in a desired frequency band.

Obtaining the wavelet marginal (explained in the next section) was also possible in this representation.

4.4 Wavelet Marginal

The new version of RailScan grants the possibility to invert the CWT representation into the signal in user selected frequency band. It is also possible to obtain the CWT marginal.

It is computational efficient to obtain the wavelet marginal in the older CWT representation, not being however possible to reconstruct the signal in a desired waveband. This is due to the CWT representation being redundant. Redundancy has the advantage of improving the visualization of signal features in the scalogram.

The marginal will provide an analysis of the wavelet power in between any pair of frequencies selected by the user. This way, the corrugation power of the signal can be obtained in a shorter band and identify points on the rail where the rail is most corrugated. Basically, by selecting the frequencies the user could see where in the rail the corrugation is most critical.

4.5 Wavelet Selection

To implement the CWT, a mother wavelet, a bandwidth (Fb) and a center frequency (Fc) need to be selected. We have chosen the Morlet wavelet. Figure 4.4 is the representation of the Morlet Wavelet.

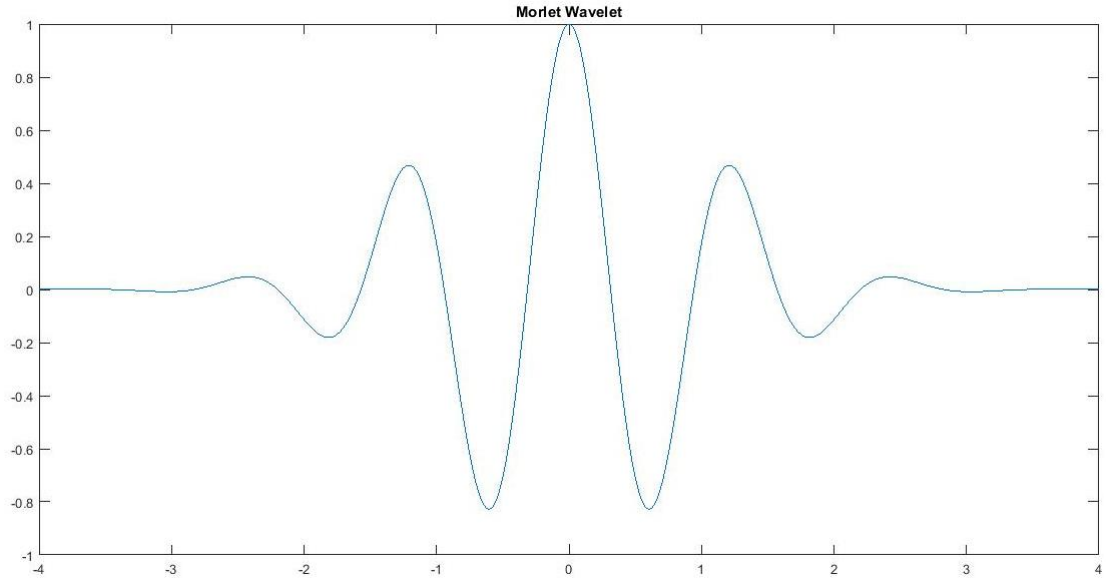

Figure 4.4 – Example of a Morlet Wavelet

The Morlet Wavelet was chosen due to its similarity to corrugation signals, because it has some features like the abrupt changes in small time that are similar to corrugation signals.

Fc must be selected near the frequency we want to examine, and the Fb must be calculated using equation 4.3 [25].

$$\sigma=\sqrt{\frac{T_p}{2}} \tag{4.3}$$

In 4.3 σ is the standard deviation and T_p is the period parameter.

Finding the value of T_p is important because it is directly related with the bandwidth desired. [25]

In all signals being analyzed, the Fc will be 1Hz given they all have a speed of 1 m/s. The velocity being 1 m/s represents a wavelength of 1 m, the maximum wavelength a corrugated rail can have. The Fb depends on what details of the signal are trying to be detected. Wavelets are zero-mean functions, so function 4.3 is used to calculate the standard deviation of the mother wavelet duration. In this case, for the signal analysis the standard deviation selected will be of 50, so to have a standard deviation of 50, the T_p must be 5000 and if T_p is directly linked with Fb, Fb assumes that value.

Results

5.1 Results

In this chapter, some signals will be analyzed using RailScan V3.0 to try to validate the functions implemented.

5.1.1 Metrosystem

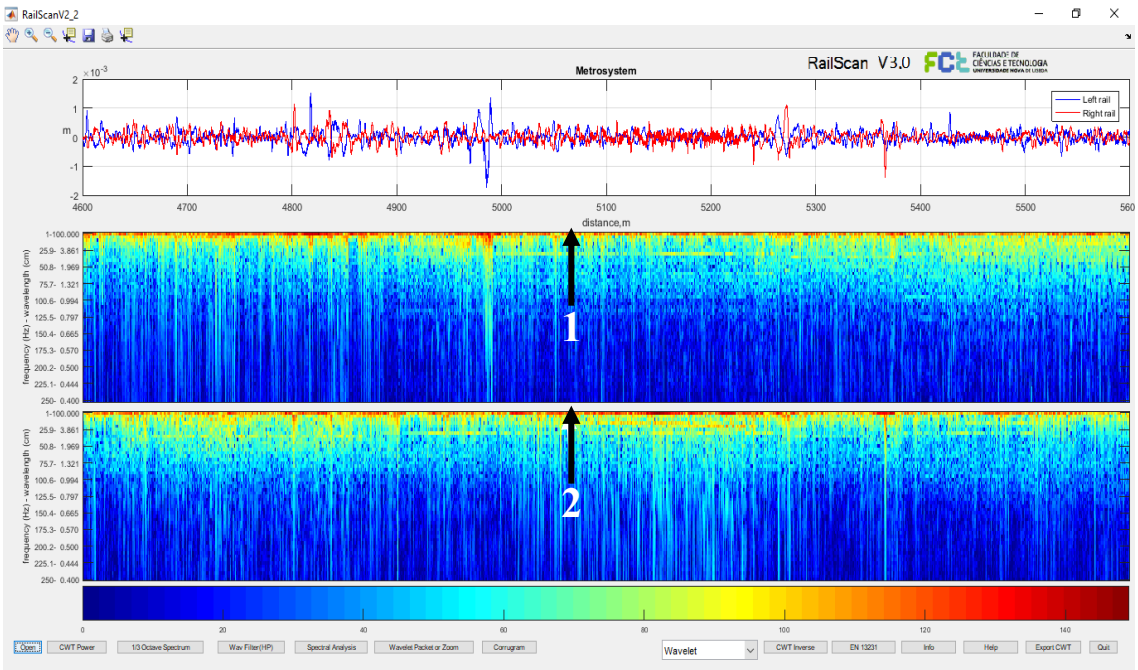

Figure 5.1 – Representation of the Metrosystem signal in RailScan. 1 and 2 represent the dominant level in the scalogram due to low frequency components, which are mainly due to terrain irregularities.

Figure 5.1 is the first image shown in RailScan. The first plot represents the original signal, in blue is the left rail and in red the right rail.

The CWT representation in the second and third plot is using the previous CWT representation (RailScan V2.1) and using Morlet wavelet (cmor5000-1).

The second plot represents the continuous wavelet transform (CWT) representation of the left rail. As displayed by number 1, the signal has higher energy bands in the lower frequencies, this is due mainly to terrain irregularities which are always present.

The third plot represents the CWT representation of the right rail. The right rail also has higher energy bands in lower frequencies as indicated by number 2. Figure 5.2 shows the spectral analysis of the original signal. With this analysis it is likely to observe that both rails have higher energy in frequencies around 0 Hz.

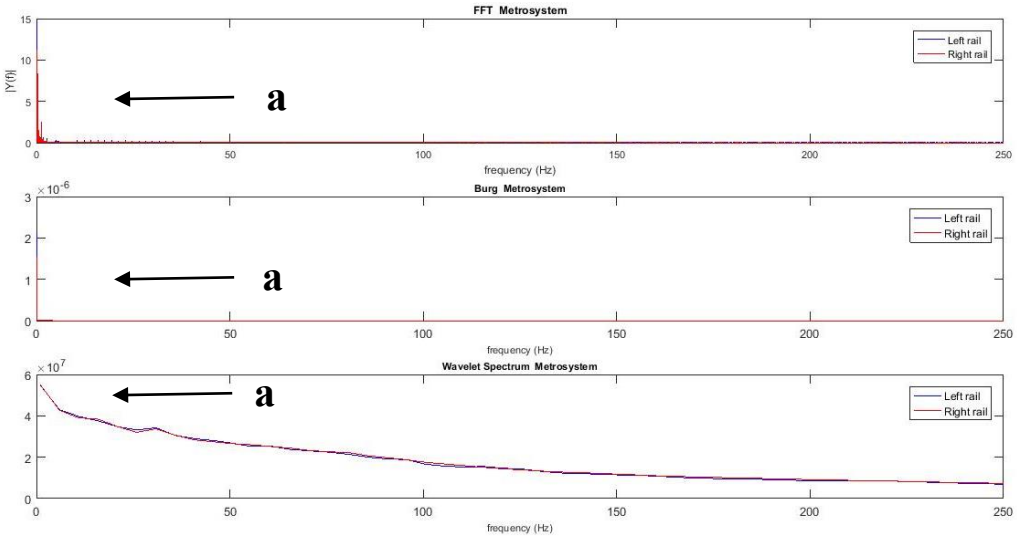

Figure 5.2 – Spectral analysis of the original Metrosystem signal. Identifications "a" show that both rails have significant power in lower frequencies.

The first plot of figure 5.2 (FFT Metrosystem) gives the FFT power of the signal and the results are what was expected, both signals have more power for frequencies near 0 Hz because they are not filtered (indicated by arrow "a"). With this information, it is necessary to filter the original signal for frequencies lower than 1 Hz, because corrugation is in frequencies higher than 1 Hz.

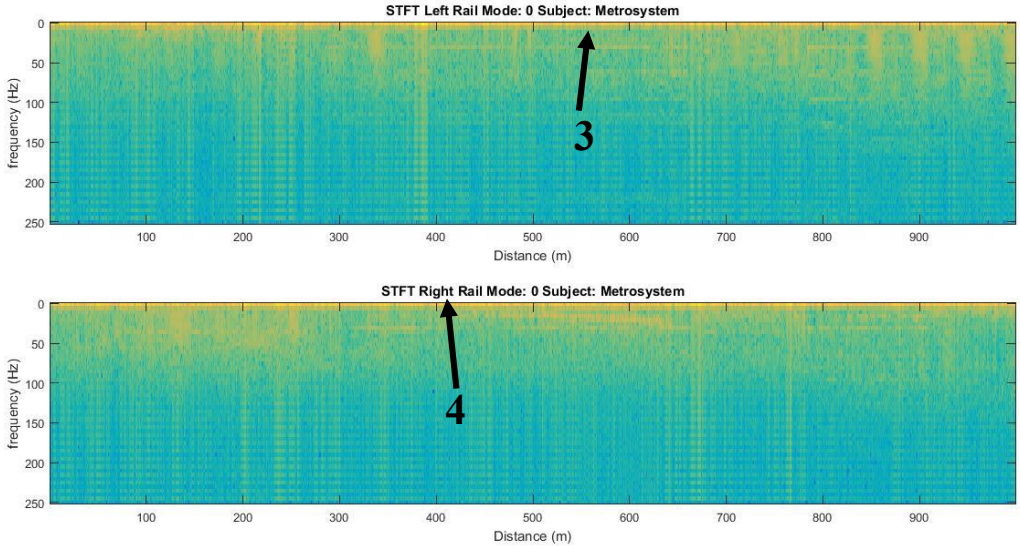

Figure 5.3 – STFT representation of Metrosystem rails. Numbers 3 and 4 indicate that in this representation both rails have greater power in lower frequencies

In figure 5.3 we can observe the difference between both CWT and STFT representations.

Likewise, the CWT case (figure 5.1), in figure 5.3 low frequency components are detected (arrows 3 and 4). In 1 and 2 of figure 5.1 both rails have substantial power for low frequencies and that power decreases if the frequency increases, however in 3 and 4 that simple visualization disappears. In chapter 3 it was explained the reason why STFT is not as effective to represent corrugation signals as the CWT and in figure 5.3 that is proved.

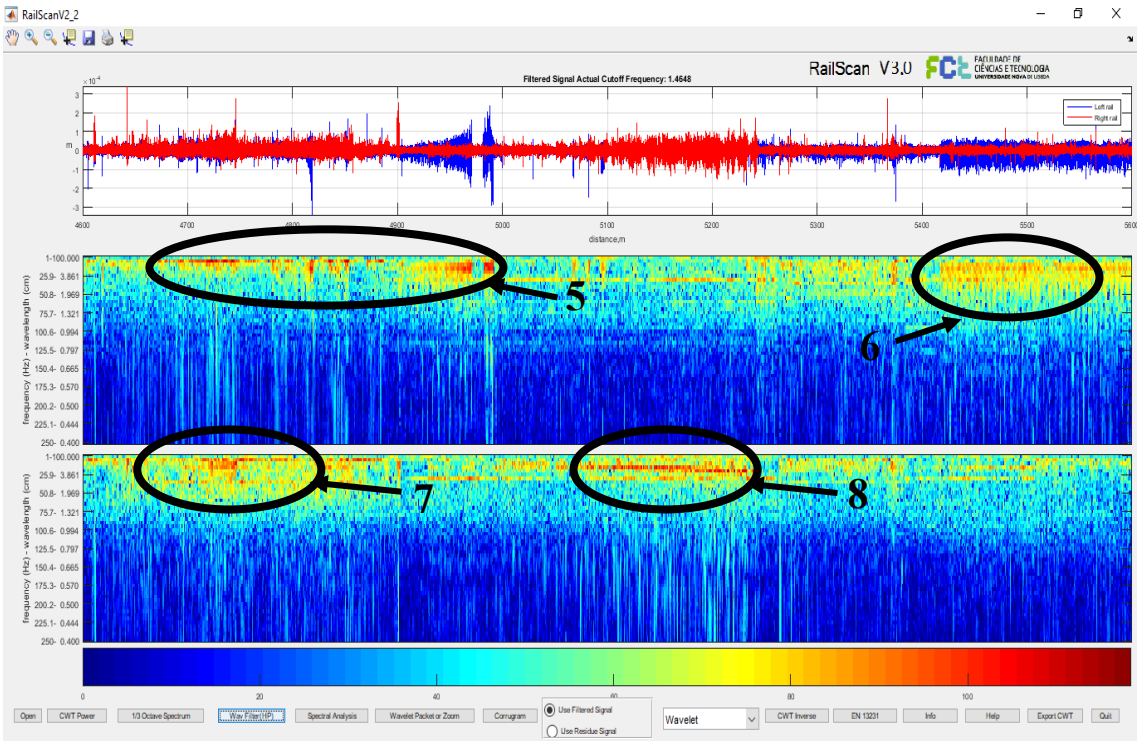

Figure 5.4 – Representation of the filtered Metrosystem signal in RailScan. 5 and 6 are the critical corrugation points identified in the left rail. 7 and 8 are the critical corrugation points identified in the right rail.

With the information obtained by the spectral analysis (Figure 5.2), a filter had to be applied to the original signal to remove frequencies that are not considered in corrugation analysis. In chapter 1, it was referred that the maximum rail corrugation wavelength was 100 cm. Using equation 5.1, it is possible to calculate the cut frequency of the filter. In the Metrosystem signal the equipment used to measure the signal had a speed of 1m/s and the maximum corrugation wavelength is 1 meter, so the cut frequency using expression 5.1 is 1 Hz [6].

$$f = \frac{v}{\lambda} \tag{5.1}$$

The CWT representation (figure 5.4) shows that for frequencies around 1 Hz and 25 Hz both signals have substantial power. Filtering the signal allowed a clear vision of where it is most

corrugated (numbers 5,6,7 and 8). The maximum power of the left rail appears to be between 4900 m and 5000 m (number 5) and between 5400 m and 5600 m (number 6). In the right rail the CWT the maximums appear between 4600 m and 4900 m (number 7) and between 5100 m and 5200 m (number 8). In both rails it is possible to see that various sets of wavelengths have corrugation in the same distance. Area number 8 appears to have more corrugation in lower wavelengths than areas 5 and 7. Area 6 is similar to area 8, but corrugation is higher in area 8. Later in this signal analysis these conclusions will be compared to the implementations of RailScan that are used to quantify and detect corrugation.

To verify if the filter was done correctly, a spectral analysis of the filtered signal was done (figure 5.5). The first plot of figure 5.5 shows that for frequencies near 0 Hz, there is not any power. With this observation, we can conclude that the filter was applied correctly.

In the first plot it is also possible to see that the left rail has more power in the lower frequencies than the right rail.

In the second plot of figure 5.5, an observation can be made about that higher value that the right rail had (identified as number 9). This value is consistent with the identifications made in figure 5.4 (number 7 and 8) where for a frequency around 5 Hz, the signal showed signals of corrugation. Number 10 is explained because of the identification made in figure 5.4 (number 8), for higher frequencies the right rail has more corrugation than the left rail.

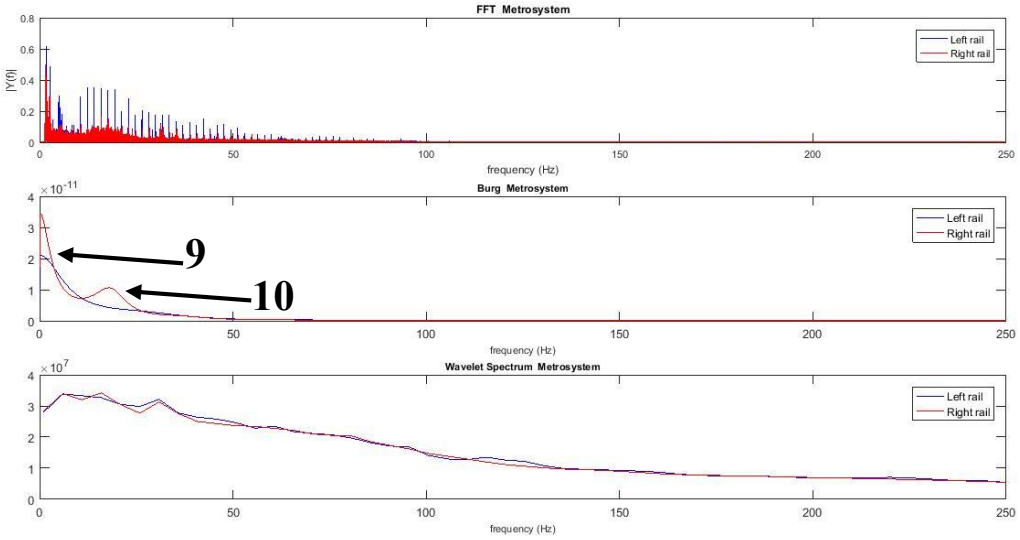

Figure 5.5 – Spectral analysis of the filtered Metrosystem signal. 9 and 10 are identifications of power in the frequency band for the right rail

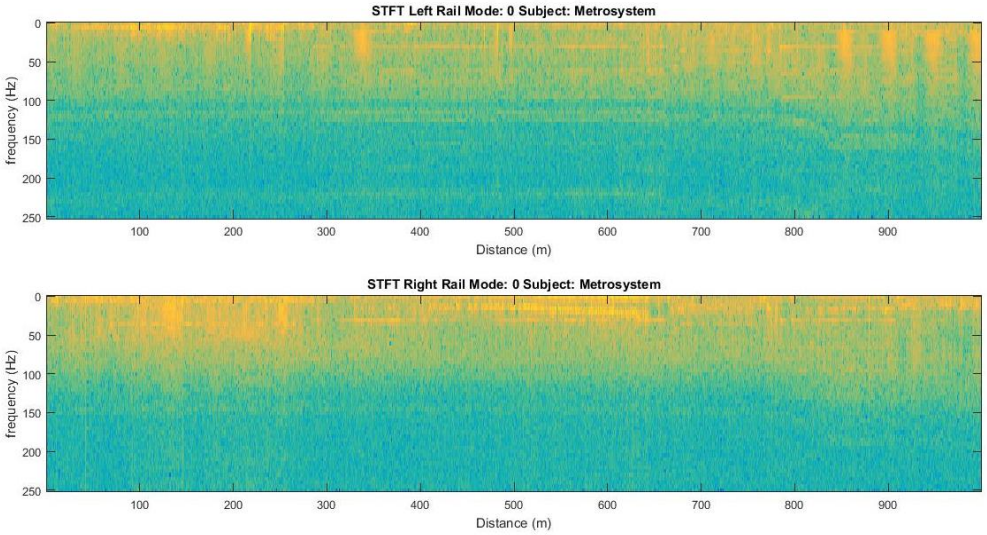

Figure 5.6 - STFT representation of the filtered Metrosystem signal

Figure 5.6 shows the STFT representation of the filtered signal. What was mention before in the STFT analysis of the original signal applies to this representation. This representation is not as illustrative as the CWT represention. The power differences in each frequency is not as visible as it is in the CWT representation. With the observations of figure 5.3 and figure 5.6 it is possible to conclude that the CWT is a better form of representing corrugation signals.

This analysis is visual, however is necessary to quantify how much corrugation is in the rail.

After this first analysis, it is necessary to use the pre-established norms to verify corrugation levels.

The first plot (figure 5.7) shows the one third octave spectrum of the signal.

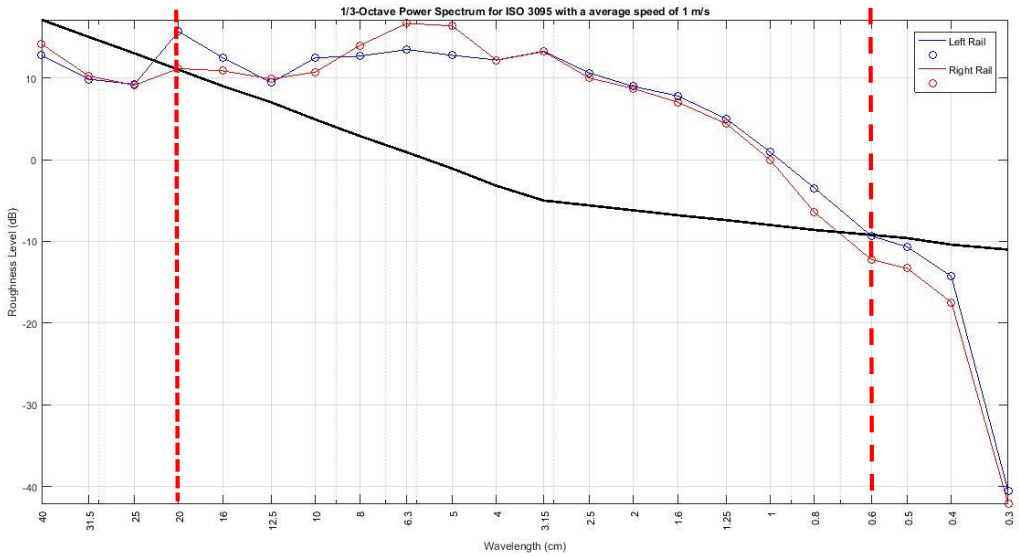

Figure 5.7 – One third octave spectrum using ISO 3095:2013 for the Metrosystem signal. The red dotted lines are the divisions into groups for a better analysis

The black line is the limit defined in the norm ISO 3095, which means that if any part of the signal passes that line the rail is corrugated.

To do a better analysis of the signal of where corrugation is present, the signal will be divided in 3 groups of wavelengths (0.3 cm to 0.6 cm; 0.8 cm to 20 cm; 25 cm to 40 cm) between the red lines.

In the first group, all wavelengths are below the black line, thus implying that the corrugation does not exceed the norm.

In the second group, all wavelengths are above the limit line. The acoustic roughness of the left rail reached 10 dB in wavelength 2.5 cm and it was higher than the right rail, but between 3.15 cm and 8 cm, the roughness level of the right rail is bigger than the left rail, with the right rail reaching a peak of 17 dB. In wavelength 10 cm, the acoustic roughness of the left rail passed the roughness of the right rail again. In wavelength 20 cm the left rail reaches a maximum peak of 15 dB.

In the third group all wavelengths are below the limit, meaning corrugation is below the limits in the rail for those wavelengths (25 cm to 40 cm).

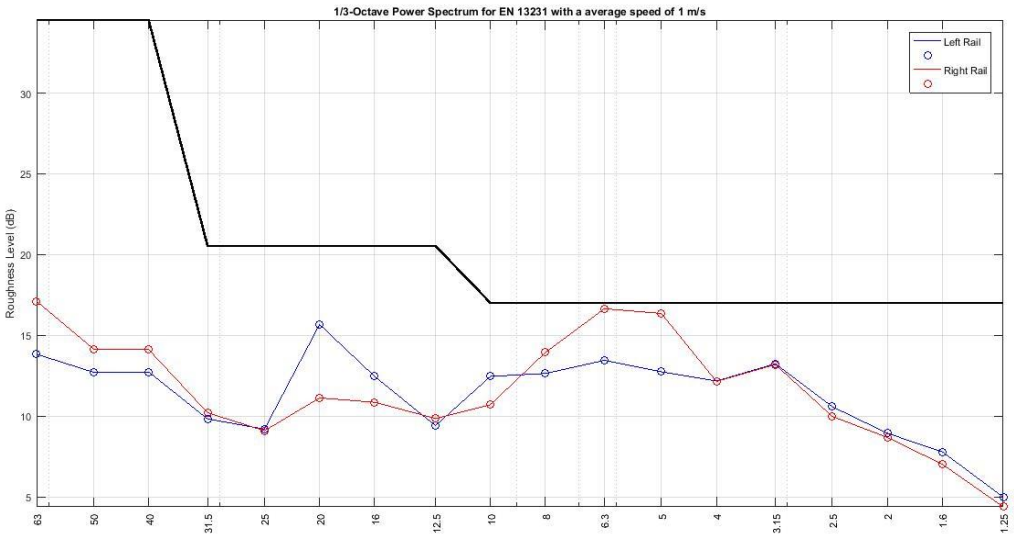

Figure 5.8 – One third octave spectrum using EN 13231:2012 for the Metrosystem signal

We proceed to compare the EN 13231 norm with ISO 3095 norm.

Figure 5.8 shows the one third octave spectrum as figure 5.7, but the difference is the values the black line assumes (figure 3.4).

By analyzing figure 5.8 it is possible to observe that none wavelength bypasses the black line, meaning corrugation levels are below using this norm. This conclusion makes sense with what was explained in chapter 4, the norm ISO 3095 is much more exigent.

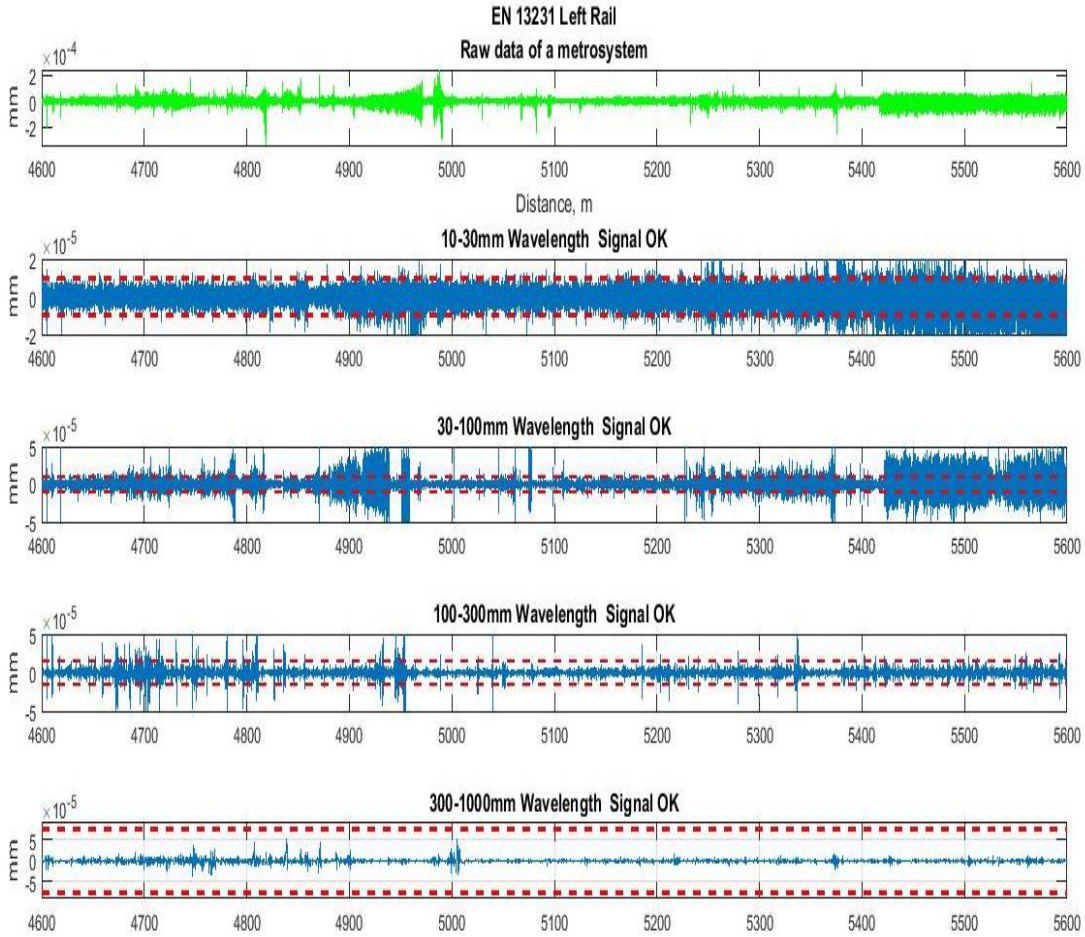

Figure 5.9 – EN 13231:2012 application in the left rail for the Metrosystem signal. The red dotted lines in the plots are the peak to peak limits.

In figure 5.9 the norm EN 13231 was applied using the rules explained in chapter 4 (tables 4.2 and 4.3). To be in accordance with the norm, the signal must be filtered into 4 different wavelengths as shown in the titles of the plots (figure 5.9). The first plot is the original signal. The second plot is the first filtered signal, it shows a signal with wavelengths between 10 mm and 30 mm. The peak to peak values (red dotted line) of this signal must not pass the 0.010 mm peak to peak limit. If we analyze the plot of the second plot we can see that almost none of the filtered signal is above the limit, so we can conclude that corrugation between these wavelengths is not concerning. An information output is also displayed, showing that for these wavelengths the signal is ok.

Signal ok means that corrugation is not exceeding the norms.

In the third plot, the information output says that the filtered signal is ok for wavelengths between 30 and 100 mm, which means that in those wavelengths the rail is not corrugated. Analyzing the plot, we can see that the signal passes the limit in some parts of the rail but that does not represent 5% of the total signal.

In the fourth plot, the information output says that the filtered signal is ok for the wavelengths of 100 and 300 mm, which means that in those wavelengths there is not corrugation in the rail.

In the fifth plot, there is the information output “Signal OK”, which means that the signal has no corrugation in those wavelengths. This bandwidth when compared to the others was the best in terms of not exceeding the limits.

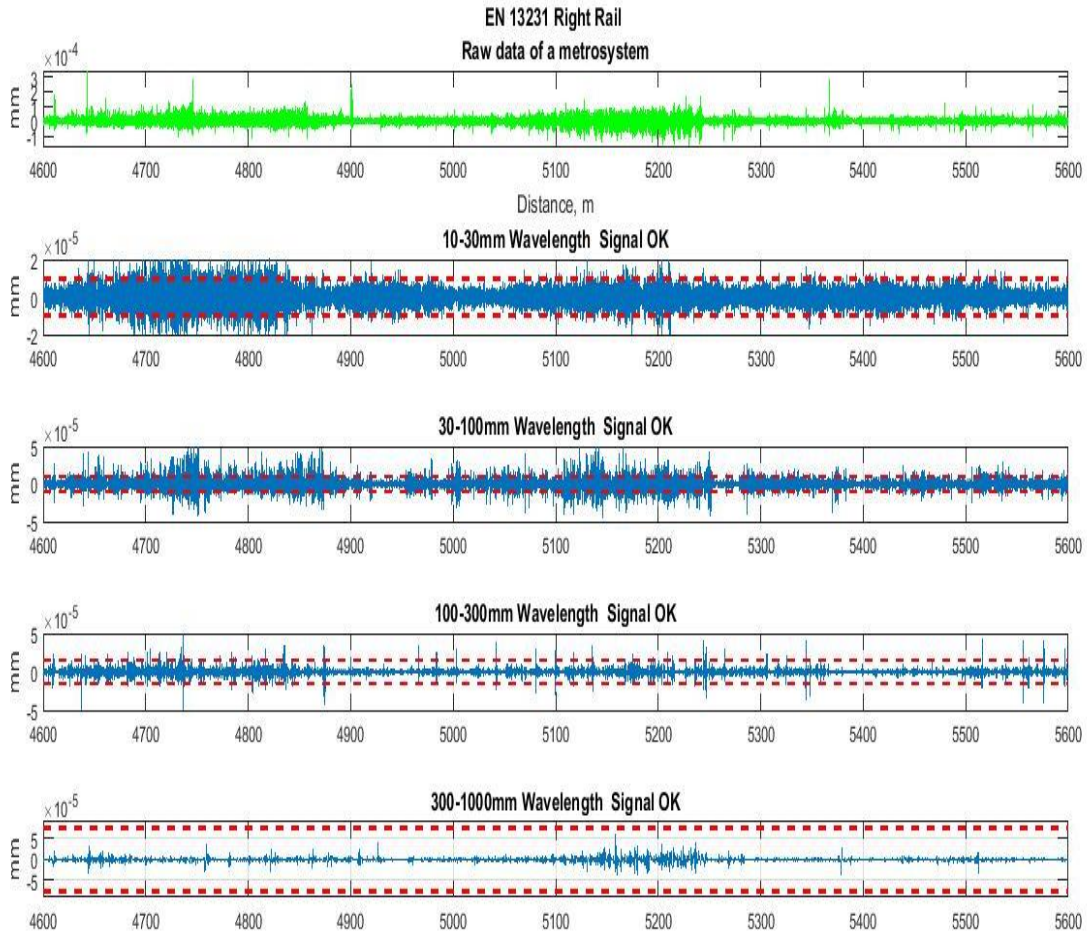

Figure 5.10 – EN 13231:2012 application in the right rail for the Metrosystem signal. The red dotted lines in the plots are the peak to peak limits.

The EN 13231:2013 representation of the right rail (figure 5.10) displays that none of the wavelengths are 5% above the limit, meaning they do not are considered corrugated. If an analysis is made in each plot, except the fifth plot, it is possible to observe that around 4750 m and 5100 m, the signal passes the limit, but that does not represent 5%, so the assumption is that there is not corrugation in the rail. The fifth plot when compared to the other plots was the best in terms of not exceeding the limits.

Comparing this information (figure 5.9 and 5.10) with the one third octave spectrum of the norm EN 13231 (figure 5.8) representation it is easy to confirm that they are in accordance, none wavelength has corrugation passing the limits.

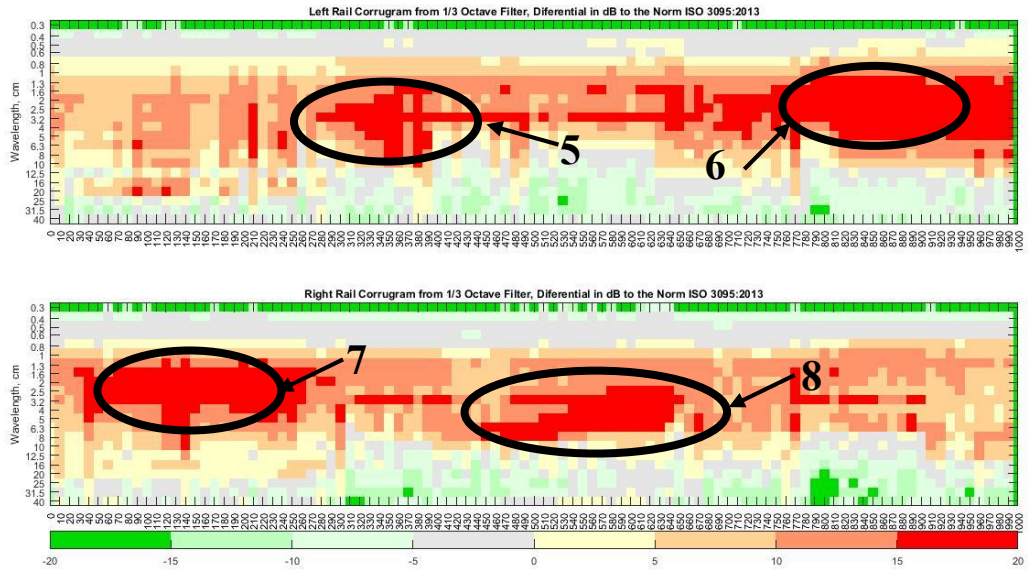

Figure 5.11 – Corrugram application using norm ISO 3095:2013 for the Metrosystem signal. 5,6,7 and 8 are identifications of spots in the rail that have a great amount of corrugation

Figure 5.11 displays the Corrugram representation of both rails. This representation brings the idea that the train began curving right and then began curving left. The signal is being divided in 10 m segments. The left rail in the beginning of the track shows little corrugation. As the distance covered by the train increases, the corrugation also increases. In the 260 m mark, there is a peak in corrugation between 1.3 cm and 8 cm wavelengths (area number 5). By analyzing the left rail using this new representation it is easy to see that the wavelengths between 1.3 cm and 12.5 cm are the most corrugated (area number 5 and 6) and if we compare this conclusion with the one third octave spectrum representation (figure 5.7), we can see that in these wavelengths the acoustic roughness is higher.

In the one third octave spectrum using ISO representation for the left rail (figure 5.7) wavelengths of 0.6 and 0.8 cm did not pass the black line but if we analyze the Corrugram representation it is possible to observe that those wavelengths have corrugation in some sections of the rail.

In the right rail, the representation is not very different. As it was said before, the signal gives the impression that the train is initially curving right and that is why the signal is more corrugated in the beginning. The peak corrugation comes between 40 m and 200 m (area number

7) for wavelengths around 1.6 cm and 10 cm. If we compare these values with the one third octave spectrum, we can see that the higher acoustic roughness values are between those wavelengths (figure 5.7).

The one third octave spectrum representation for the right rail (figure 5.7) also shows that for the 0.6 cm wavelength the right rail is not corrugated but analyzing the Corrugram representation for that rail it is possible to see that the 0.6 cm wavelength has corrugation in some parts of the rail.

This difference of information between the one third octave spectrum and the Corrugram, proves that the Corrugram presents a more detailed information.

The identifications made in figure 5.11 (numbers 5,6,7 and 8) when compared to figure 5.4 (numbers 5,6,7 and 8) are a perfect match, meaning that both CWT representation and Corrugram are correct and are identifying the same parts of the rail that have more corrugation. However, only in Corrugram as the possibility to quantify how much corrugation is in the rail.

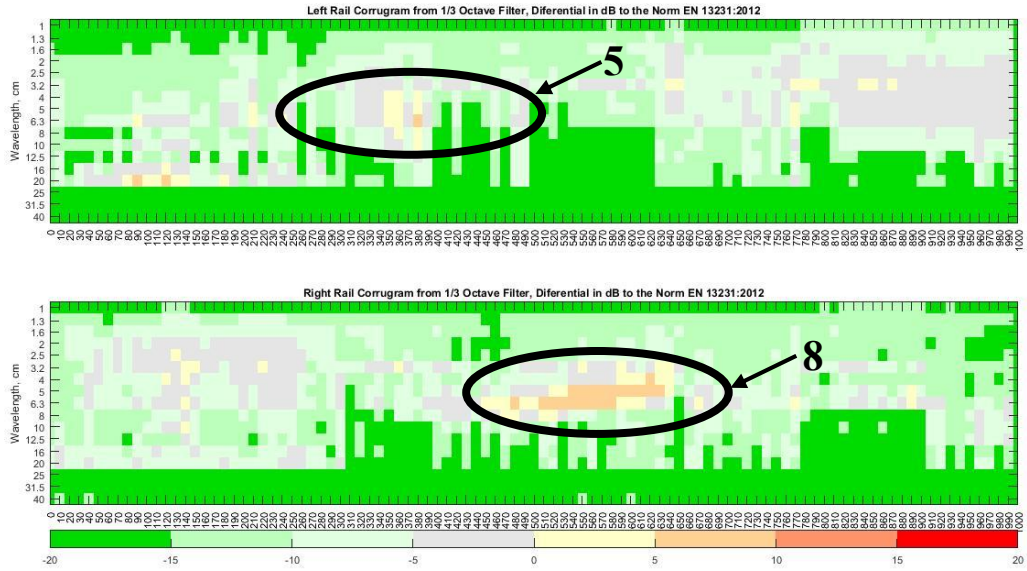

Figure 5.12 – Corrugram using the norm EN 13231:2012 for the Metrosystem signal. 5 and 8 are the places identified with corrugation

The Corrugram representation helps the user to better understand where and if there is corrugation in the rails. As expected using the norm EN 13231:2012 (figure 5.12) there are almost no spots with relevant corrugation levels. In the left rail representation, we can recognize that for the wavelengths of 3.2 cm to 6 cm there is corrugation in some parts the rail (area number 5). Comparing this results to the norm EN 13231 (figure 5.10) or even the one third octave spectrum for this norm (figure 5.8), we can determine that Corrugram is a much more detailed and effective way to detect corrugation, none of the other methods detected any corrugation, only Corrugram did.

In the Corrugram representation for the right rail we can observe that wavelengths between 3.2 cm and 8 cm have corrugation (identification number 8), but this corrugation is only for a small part of the rail. If we compare this information with what the EN 13231 displayed (figure 5.10), it is easy to understand why the EN 13231 display showed that there was not corrugation in the rail, only a very small part of rail has corrugation. For this reason it is possible to validate the Corrugram has a reliable and effective method in corrugation detection. The Corrugram identifies all the corrugated wavelengths the established norms identify and others that those norms could not identify.

In the beginning of this thesis, the idea was to represent the signals with the CWT function of Matlab to have the opportunity to use the CWT inverse. However, that option is not practical because it takes a great amount of computational power to represent the CWT of signal using the inverted version.

With the use of the older version of CWT, it made sense to obtain its power between any pair of frequencies chosen by the user. Figures 6.13 and 6.14 are the representation of the marginal (CWT power) of both rails. In the case of figures 6.13 and 6.14 the frequencies were chosen around 7 Hz and 45 Hz, that gives a wavelength of 13.6 cm and 2.2 cm respectively. Figures 6.13 and 6.14 are basically the same signal but in figure 5.14 the signal is filtered.

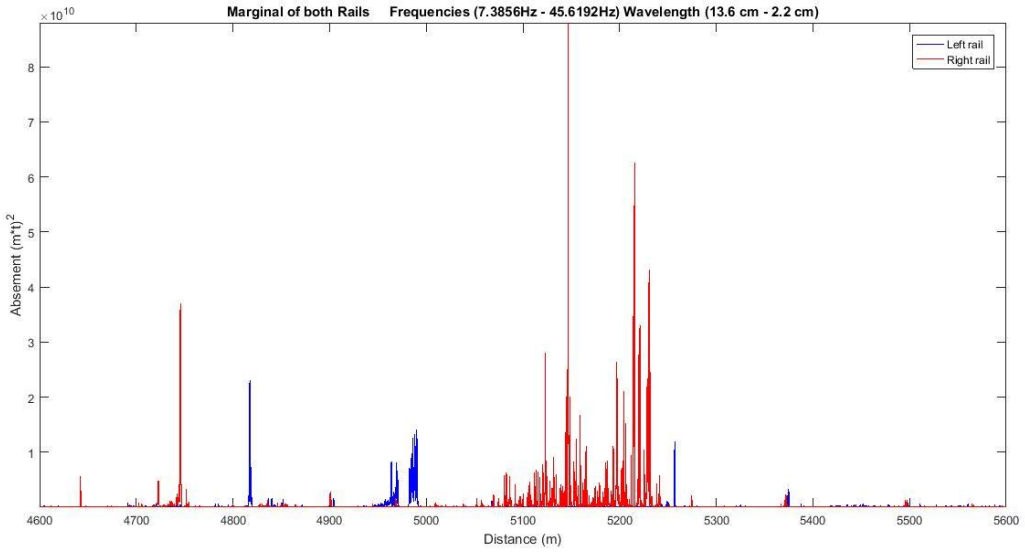

Figure 5.13 – CWT Marginal for both Rails in Metrosystem signal

The marginal gives plenty information about rail corrugation. For instance, the right rail has more power than the left rail, which is an expected resulted given the results of CWT representation (figure 5.1) or the one third octave spectrum (figure 5.7). The pair of frequencies were chosen by a visual observation of where is the most information in the CWT representation in both rails (figure 5.4). In figure 57 for the frequencies chosen the right rail had more acoustic

roughness, so the marginal results agree. The marginal also shows where in space the rails have more power and it can be compared with the Corrugram. For example, the right rail has a lot of power in the beginning of the rail and between the distances 5100 m and 5200 m and in Corrugram (figure 5.11) is possible to observe that around those distances the rail is most corrugated. The maximum acoustic roughness of the left rail in the one third octave representation (figure 5.7) was in wavelength 20 cm, a wavelength that is not represented in figure 5.13 because it does not belong in the group of frequencies chosen.

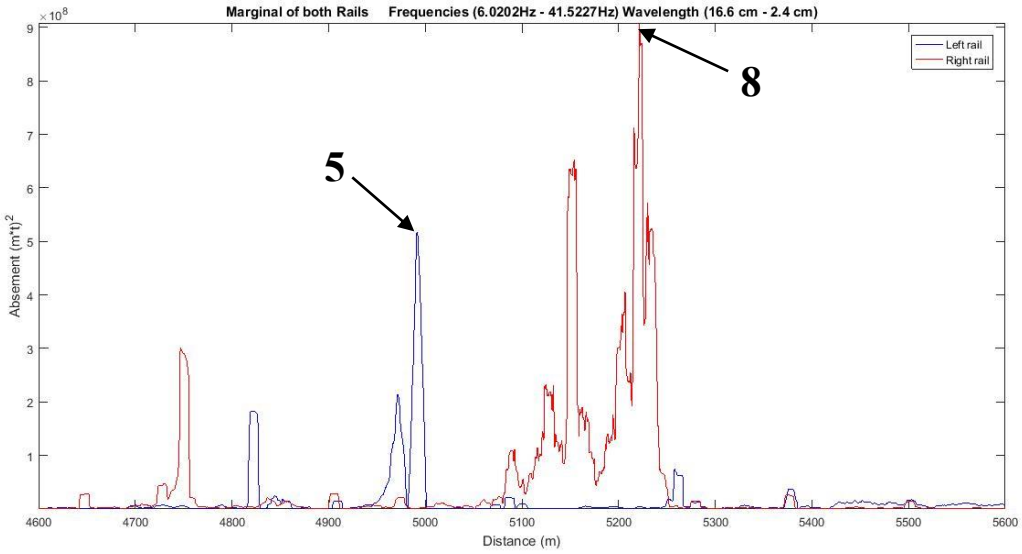

Figure 5.14 - Filtered Marginal of the CWT for both rails

Figure 5.14 shows a filtered representation of the marginal. The frequencies are different than the marginal of figure 5.13, in this case the frequencies are 6 Hz and 41 Hz. Having a smaller frequency than the previous representation helps understand how the signal works. The maximum power of the right rail remained the same (identified as 8) and that is in accordance with figure 5.1 and figure 5.7, because the maximum acoustic roughness value of the right rail is in wavelength 6.3 cm. According to figure 5.7 the maximum acoustic roughness value for the left rail was in wavelengths 16 cm and 20 cm, with the maximum being in wavelength 20 cm. In Figure 5.14 the wavelength 16 cm belongs to the group of inputs that will be used to calculate the marginal of the signal. Even though the maximum value of the marginal still belongs to the right rail, the maximum of the left was higher when compared to the maximum of figure 5.13, because of wavelength 16 cm. With the marginal a conclusion can be made that around 5000 m the left rail is highly corrugated (identified as 5).

5.1.2 Curva Pragal

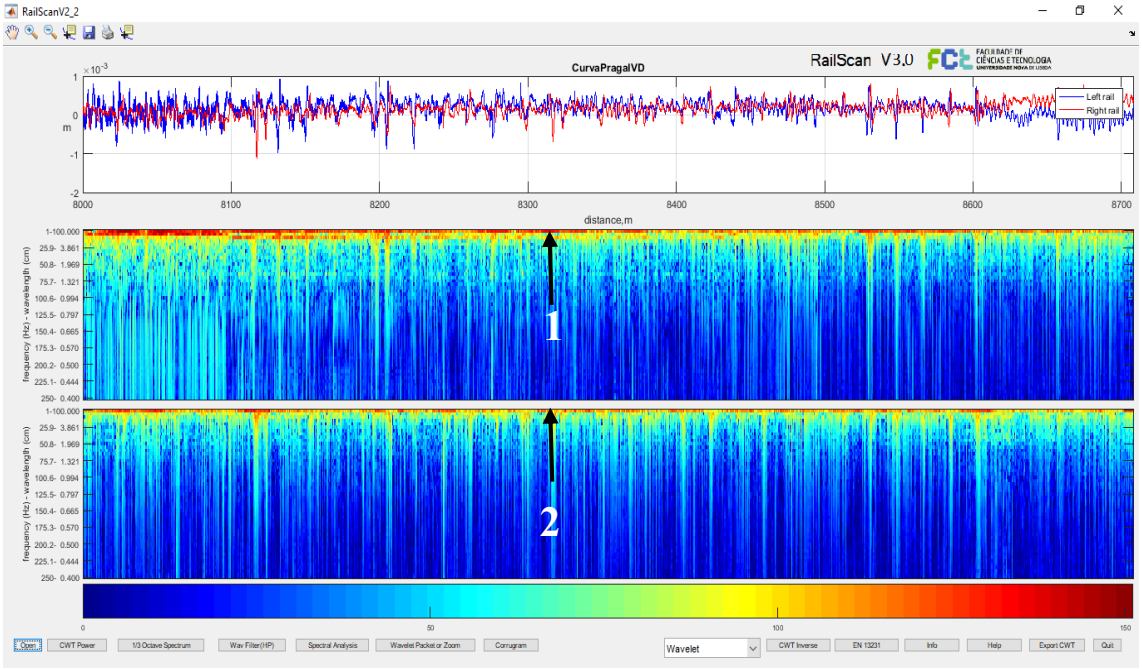

Figure 5.15 – Representation of the signal Curva Pragal in RailScan. 1 and 2 represent the dominant level in the scalogram due to low frequency components, which are mainly due to terrain irregularities.

Figure 5.15 is the representation of the signal Curva Pragal. The first plot is the original signal, in blue is represented the left rail and in red the right rail.

The second plot represents the continuous wavelet transform (CWT) representation of the left rail. As it is shown by number 1, the signal has higher energy bands in the lower frequencies.

The third plot represents the CWT representation of the right rail. The right rail has also higher energy bands in the lower frequencies (identification made by number 2).

This representation of the CWT appears to show the train curving left in the beginning of the rail, because there is a lot of energy in the lower frequencies for the left rail when compared to the right rail. This hypothesis will be confirmed later in this chapter. In figure 5.16 it will be shown the spectral analysis of the original signal. With this spectral analysis it is expected to see a lot of energy in frequencies around 0 Hz.

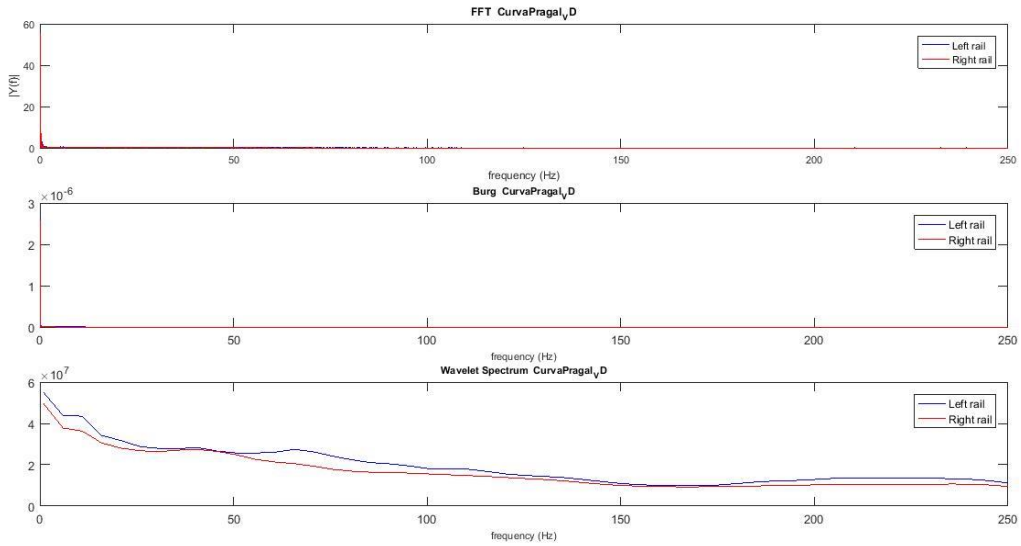

Figure 5.16 – Spectral analysis of Curva Pragal signal

The first plot of figure 5.16 (FFT Metrosystem) gives the FFT power of the signal and the result is what was expected, the signal has more power for frequencies near 0 Hz and it is not possible to analyze where corrugation is located. With this information, it is necessary to filter the original signal for frequencies lower than 1 Hz, because the information that is being analyzed is all in frequencies higher than 1 Hz.

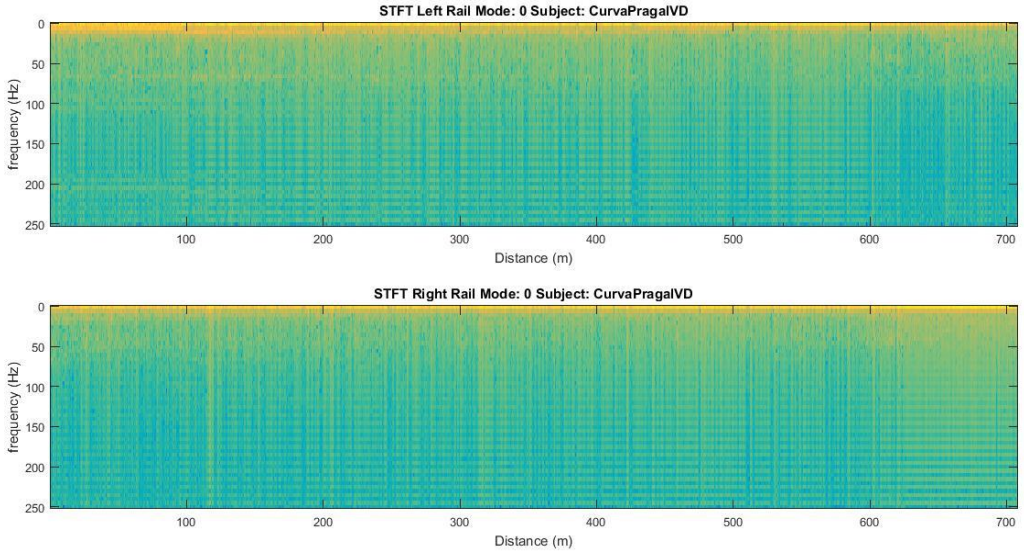

Figure 5.17 – STFT representation of Curva Pragal signal

In figure 5.17 we can see the difference between the CWT and the STFT representations, even tough for this specific signal there is not a big difference because the signal for both rails does not change abruptly.

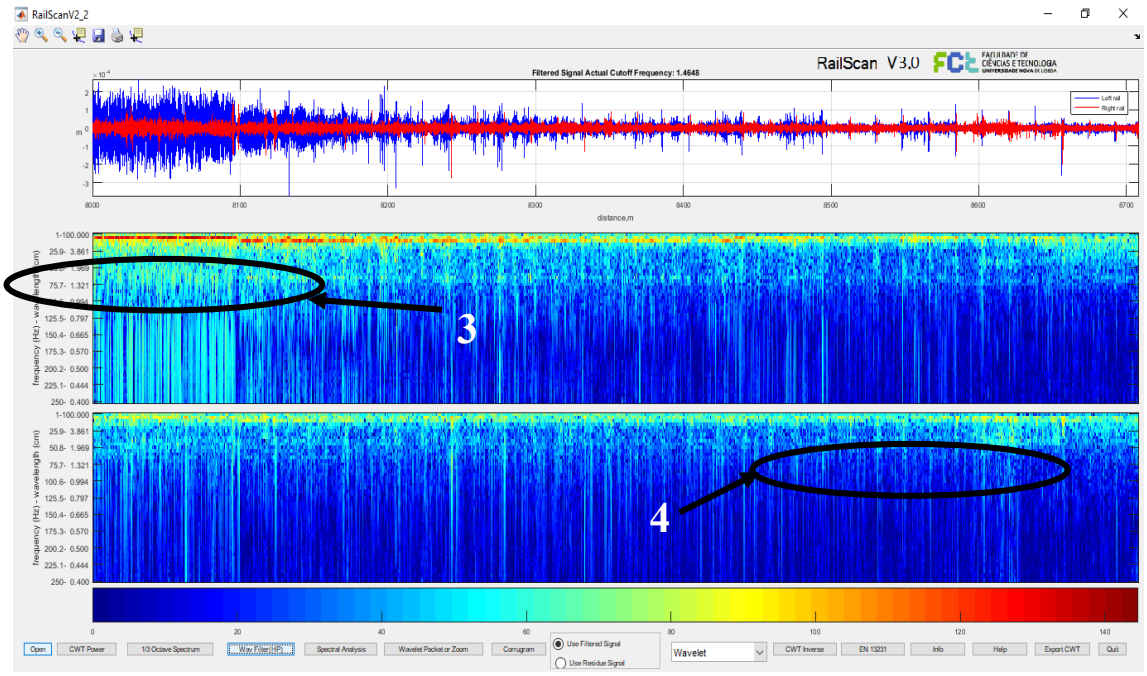

Figure 5.18 – Representation of the filtered Curva Pragal signal in RailScan

With the information obtained by the spectral analysis (Figure 5.16), a filter had to be applied to the original signal to remove the frequencies that are not used to measure corrugation. The CWT representation shows that for frequencies around 1 Hz the left rail has a lot of power (indicated by number 3). The maximum power of the left rail appears to be between 8000 m and 8200 m (area selected by number 3). In the right rail the CWT representation is more linear and with no apparent maximum, which should mean that that the right rail is not as much corrugated (area selected by number 4). With area number 3 the signal appears to be curving left in that area.

Both signals have different wavelengths with corrugation for the same distance in the rail.

To verify if the filter was done correctly, a spectral analysis of the filtered signal was done (figure 5.19). The first plot of figure 5.19 shows that for frequencies near 0 Hz, there is not any power. With this observation, we can conclude that the filter was applied correctly. In the first plot it is also possible to see that the right rail surprisingly has more power than the left rail for frequencies near 0 Hz.

The second plot (identification number 5 and 6) is correctly assuming that for low frequencies the left rail has a greater power than the right rail.

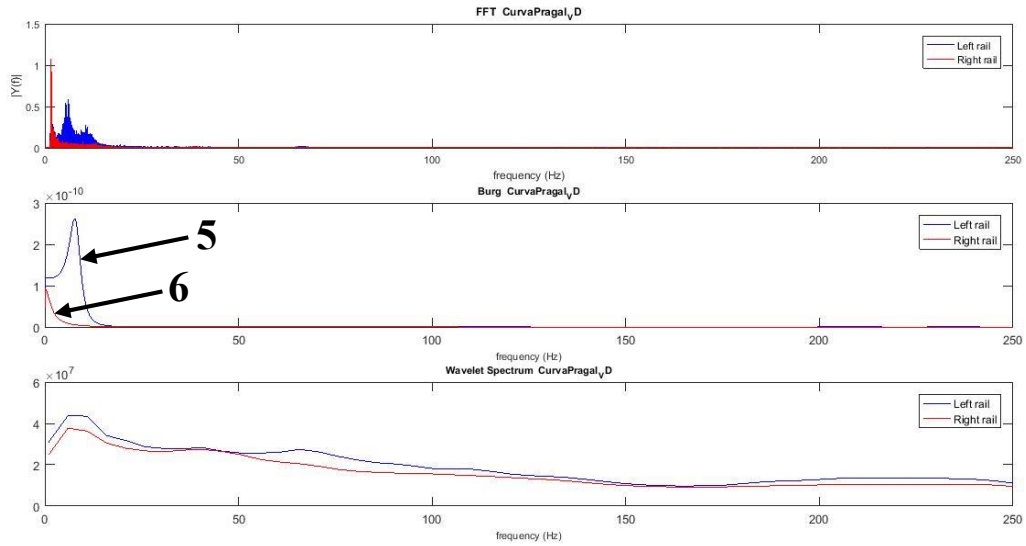

Figure 5.19 – Spectral analysis of the filtered Curva Pragal signal

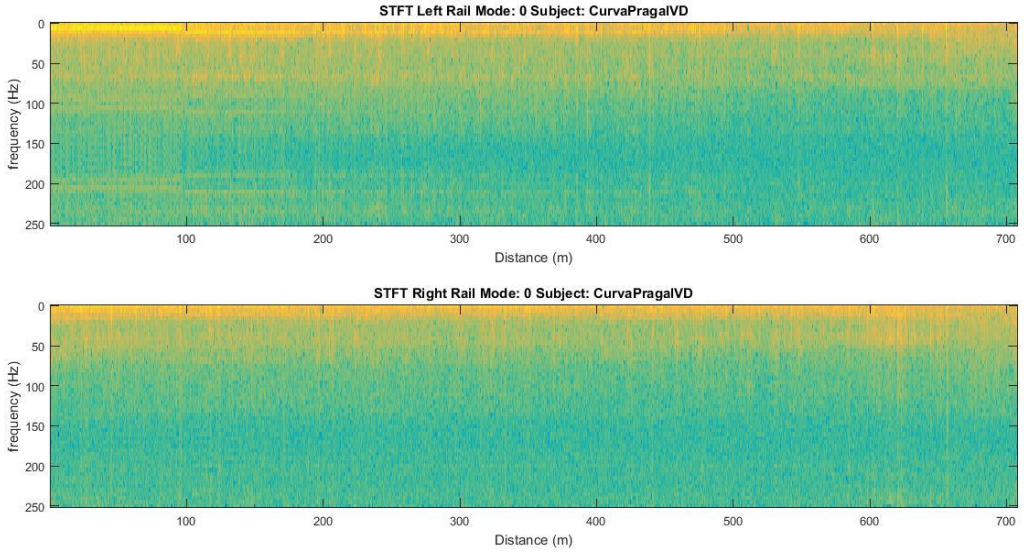

Figure 5.20 – STFT representation of the filtered Curva Pragal signal

Figure 5.20 shows the STFT representation of the filtered signal and what was mention before in the analysis of the original signal applies to this representation, this signal does not vary that much so the representation even though not as much informative, does not miss any information but represents badly power changes in different frequency bands.

After this first analysis, it is necessary to use the pre-established norms to quantify rail corrugation.

The first plot (figure 5.21) shows the one third octave spectrum of the signal.

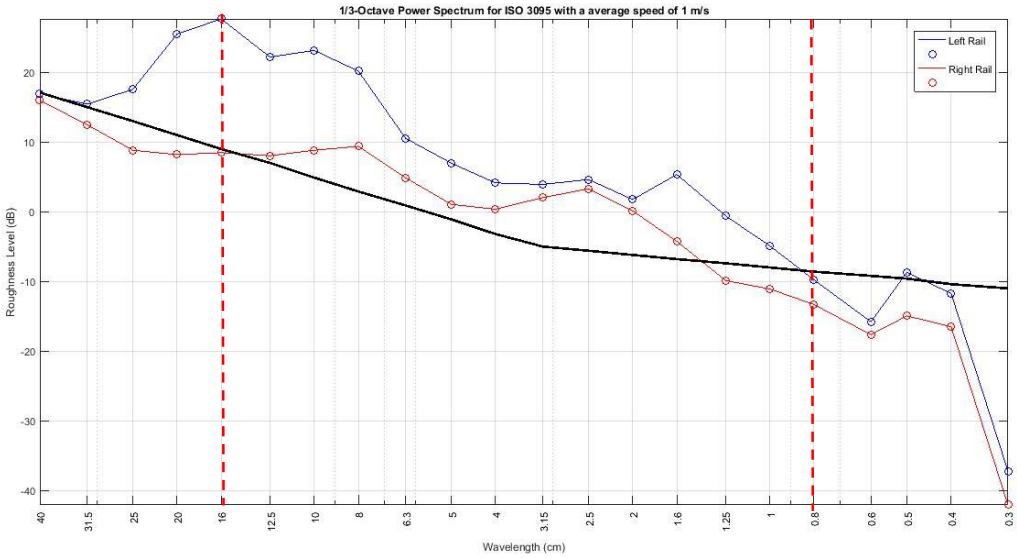

Figure 5.21 – One third octave spectrum using ISO 3095:2013 for the signal Curva Pragal. The red dotted lines are the divisions into groups for a better analysis

The black line is the limit defined in the norm ISO 3095, which means that if any part of the signal passes that line the rail is corrugated.

To do a better analysis of the signal, and where corrugation is present, the signal will be divided in 3 groups of wavelengths (0.3 cm to 0.8 cm; 1 cm to 16 cm;20 cm to 40 cm) between the red lines.

In the first group, almost all wavelengths that are below the black line, 0.6 cm for instance in both signals. There are also wavelengths that are above the black line, 0.5 cm for instance but only for the left rail. By analyzing both signals it is possible to see that the roughness level (dB) in the left rail is higher and that none wavelength passes the limit for the right rail.

In the second group, the acoustic roughness of the left rail began to increase reaching a maximum of 22 dB in the wavelength 10 cm. Both rails passed the limit in all wavelengths, meaning that for wavelengths between 1 cm and 16 cm all rail is corrugated. In the third group, the acoustic roughness of the left rail continued to increase, reaching a max of around 30 dB in the wavelength 16 cm. The right rail does not have any wavelength passing the limit.

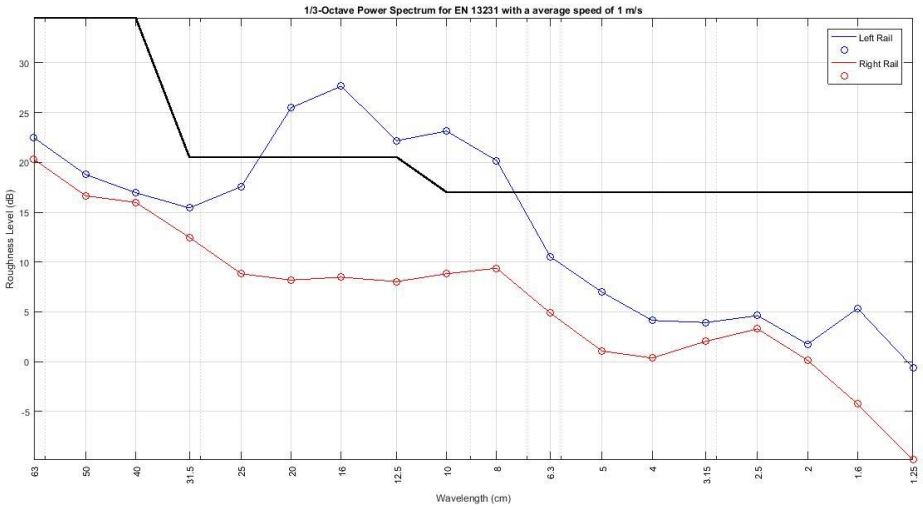

Figure 5.22 – One third octave spectrum using EN 13231:2012 for the signal Curva Pragal

Figure 5.22 shows the one third octave spectrum as figure 5.21, but the difference is the values the black line assumes. By analyzing figure 5.22 it is possible to see that none wavelength of the right rail passes the black line, meaning that none wavelength has surpassing corrugation. The left rail only has exceeding corrugation in wavelengths between 8 cm to 20 cm. This conclusion makes sense with what was said in chapter 4, the norm ISO 3095 is much more exigent.

It is expected when applying the norm EN 13231 to the left rail that it will detect corrugation in at least one group of wavelengths.

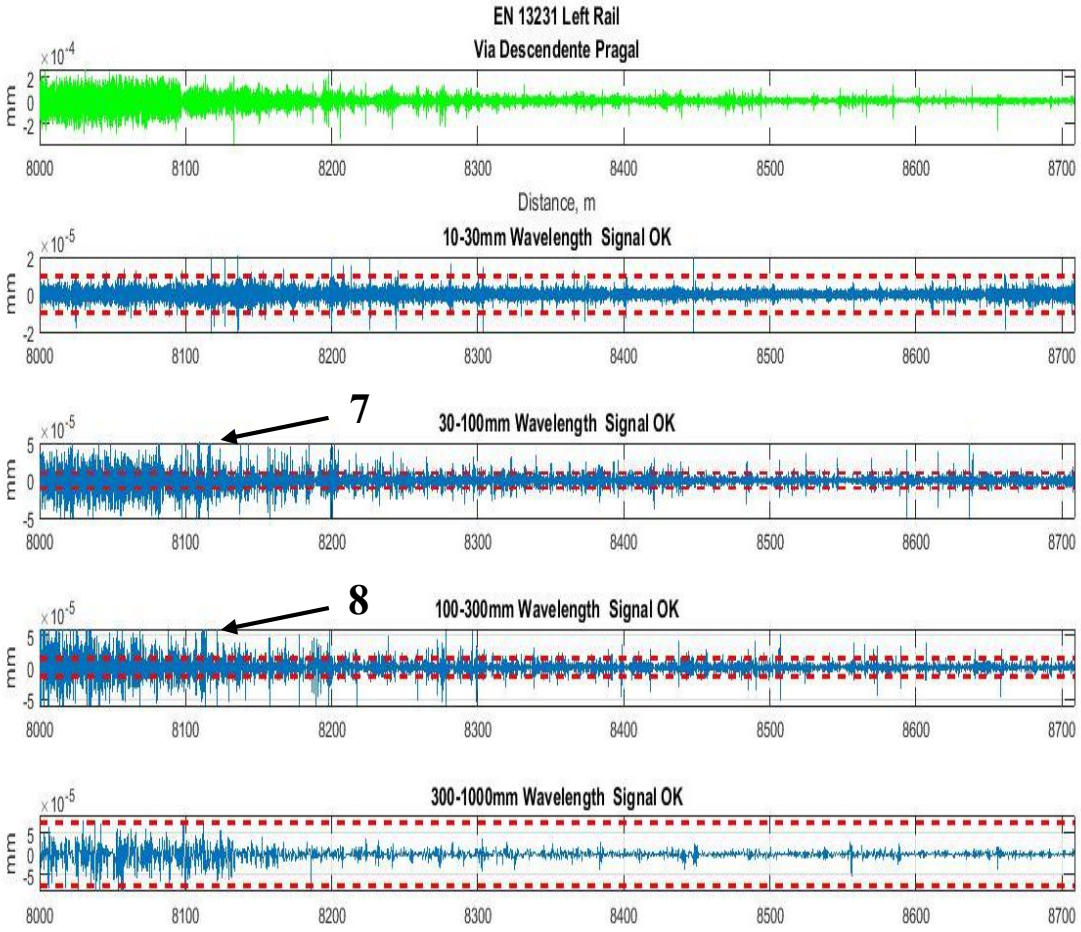

Figure 5.23 – EN 13231:2012 application to the left rail for Curva Pragal signal. 7 and 8 are indicating parts of the signal that pass the limit. The red dotted lines in the plots are the peak to peak limits.

In figure 5.23 the norm EN 13231 was applied using the rules explained in chapter 4 (tables 4.2 and 4.3). To be in accordance with the norm, the signal must be filtered into 4 different wavelengths as shown in the titles of the plots (figure 5.23). If we analyze the information output of the second plot we can determine that almost none of the filtered signal is above the limit, so we can conclude that there is not exceeding corrugation between these wavelengths.

In the third plot, the information output says that the filtered signal is ok for wavelengths between 30 and 100 mm, which means that in those wavelengths there is not overpassing corrugation in the rail. Analyzing the plot, we can see that the signal passes the limit in some parts of the rail but that does not correspond with 5% of the total signal. In this case it only surpasses around 4% of the limit. This comes to show how ineffective in detecting corrugation the norm EN 13231 is.

In the fourth plot, the information output says that the filtered signal is ok for the wavelengths of 100 and 300 mm, which means that in those wavelengths there is not exceeding corrugation in the rail. The justification here is the same as it was in the third plot. Wavelengths

between 8 cm to 20 cm have corrugation in both representations of the one third octave spectrum, so it was expected that at least of group of wavelengths had been identified by the norm EN13231, but they were not, which confirms that this norm is not as effective as the ISO 3095.

In the fifth plot, there is the information output “Signal OK”, which means that the signal has no corrugation in those wavelengths.

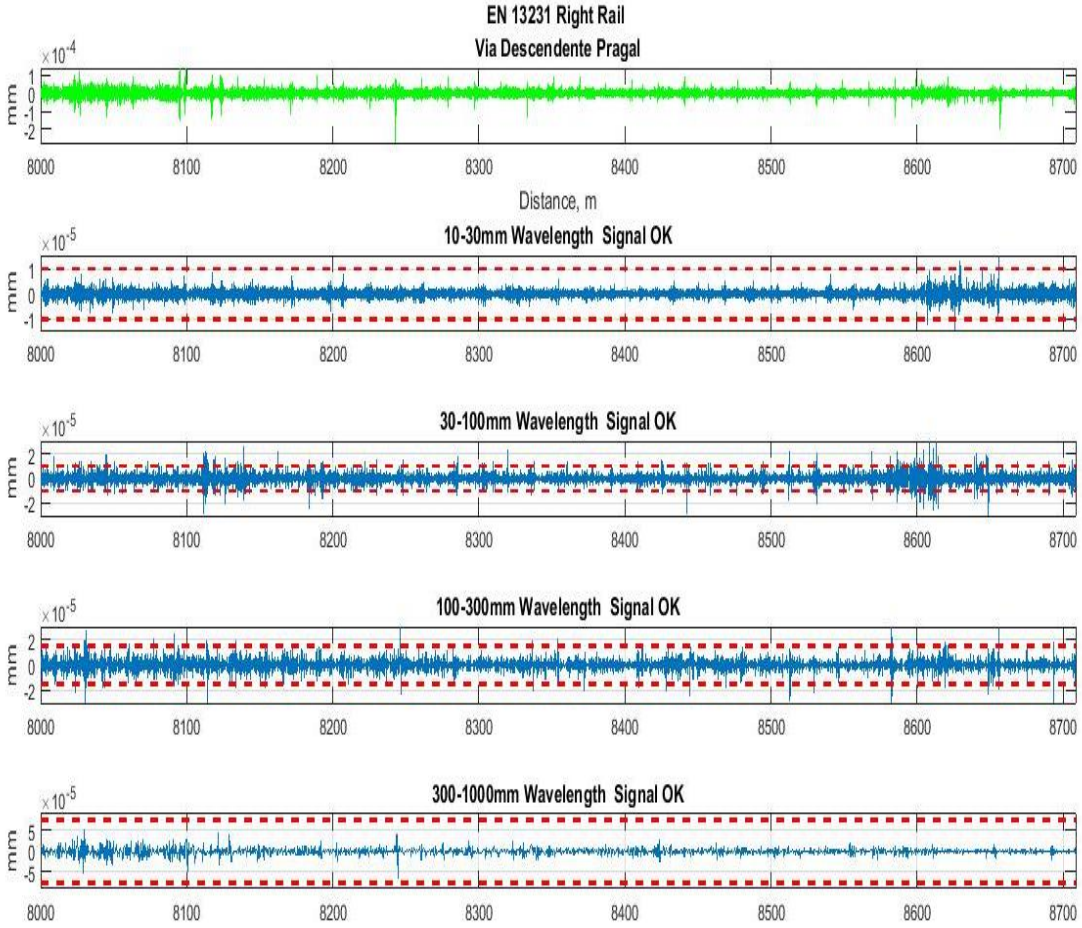

Figure 5.24 - EN 13231:2012 application to the right rail for Curva Pragal signal. The red dotted lines in the plots are the peak to peak limits.

The EN 13231:2013 representation of the right rail (figure 5.24) displays that for that rail none of the wavelengths are 5% above the limit. If we analyze the plot in each wavelength we can determine that the signal does not pass the limit in any part of the rail so there is not corrugation in the rail.

Comparing this information with the one third octave spectrum of the norm EN 13231 (figure 5.22) representation it is easy to verify that they are in accordance, none wavelength is considered corrugated.

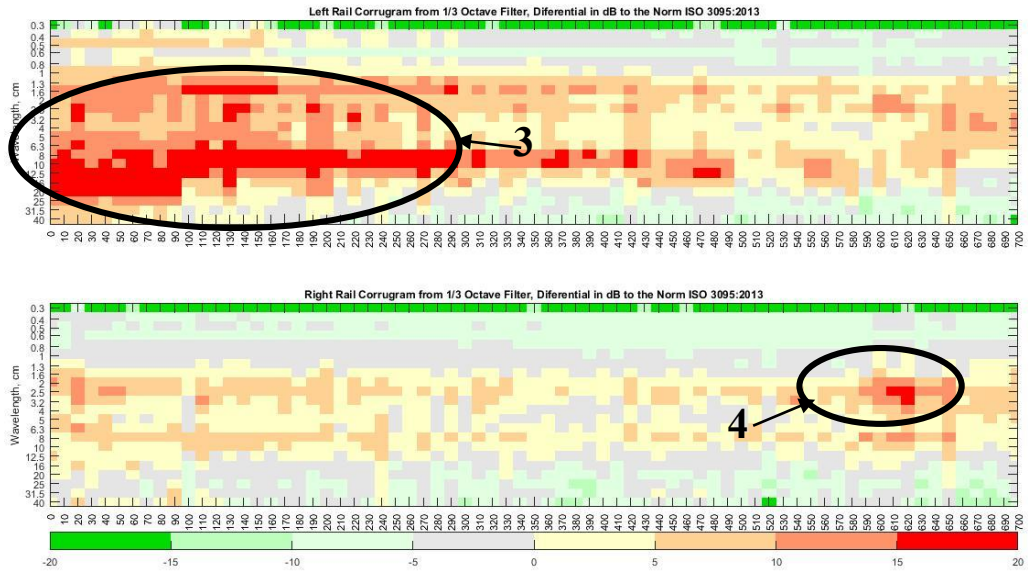

Figure 5.25 – Corrugram using the norm ISO 3095:2013 for Curva Pragal signal. 3 and 4 are the spots Corrugram identified as most corrugated

In figure 5.25 it is shown the Corrugram representation of both rails. This representation of the Corrugram confirms the idea that the train began curving left. The signal is being divided into parts of 10 m each. The left rail in the beginning of the track shows a lot corrugation, this confirms the theory that the rail is curving left in the beginning of the rail. By analyzing the left rail using this new representation it is easy to determine that the left rail is highly corrugated in wavelengths between 1.3 cm and 20 cm and if we compare this conclusion with the one third octave spectrum representation, we can see that in these wavelengths the acoustic roughness is higher. In Corrugram it is not possible to know which wavelength is most corrugated, but that is the least important thing, if the wavelength has an acoustic roughness that is not in accordance with the norms it should be identified and that is what Corrugram does.

In the identification made by number 3, the left rail appears to be in pressure, so the ideia that the train might be turning left is correct. This identification (area number 3) was also made by the CWT representation (figure 5.15), meaning these identifications are an exact match.

In the one third octave spectrum representation for the left rail (figure 5.21) the wavelengths of 0.6 and 0.8 cm did not pass the limit line but by analyzing the Corrugram representation for the left rail it is possible to observe that those wavelengths have corrugation in some sections of the rail.

In the right rail, the representation is very different. There are some wavelengths that have corrugation along the rail (number 4 is the critical point), but this rail compared to the left rail has almost no corrugation. The identification made with number 4 is the same as the number 4 of figure 5.15, meaning that the CWT can be used to detect parts in the rail that are corrugated.

The one third octave spectrum representation for the right rail (figure 5.21) also shows that for the 40 cm wavelength the rail is not considered corrugated but analyzing the Corrugram representation for that rail it is possible to see that the 40 cm wavelength has corrugation.

This difference of information between the one third octave spectrum and the Corrugram, proves once again that this method presents a more detailed information

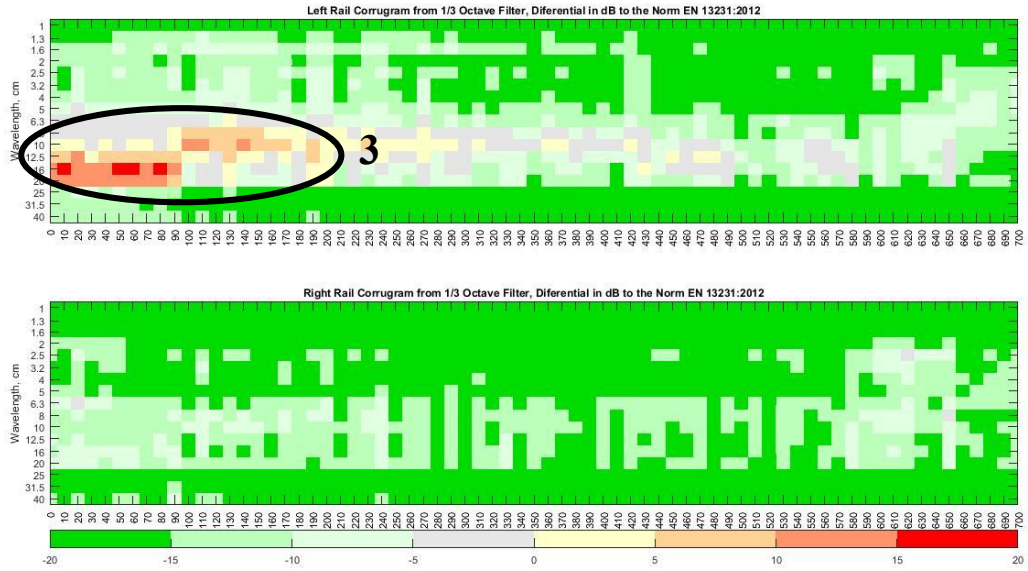

Figure 5.26 – Corrugram using the norm EN 13231:2012

The Corrugram representations help the user to better understand where and if there is corrugation present in the rails. As it was expected using the norm EN 13231:2012 (figure 5.26) there are almost no spots with corrugation, which is an expected result because this norm is less exigent. In the left rail representation, we can see that for the wavelengths of 8 cm to 20 cm (indicated by number 3) there is corrugation present in the beginning of the rail, comparing this results to the norm EN 13231 or even the one third octave spectrum for this norm (figure 5.22), we can see that Corrugram is a much more detailed and effective way to detect corrugation, for instance the 6 cm wavelength was only detected with corrugation by Corrugram.

The Corrugram representation for the right rail is perfect according to the norm EN13231. None of the wavelengths that are considered in this norm have corrugation.

Figure 5.27 is the representation of the marginal (CWT power) of both rails. In the case of figures 6.27 the pair of frequencies chosen were around 3 Hz and 42 Hz, that gives a wavelength of 52 cm and 2.5 cm respectively. With this pair of frequencies chosen it is expected to see a lot of power in the left rail and a small power of the right rail when compared to the left rail.

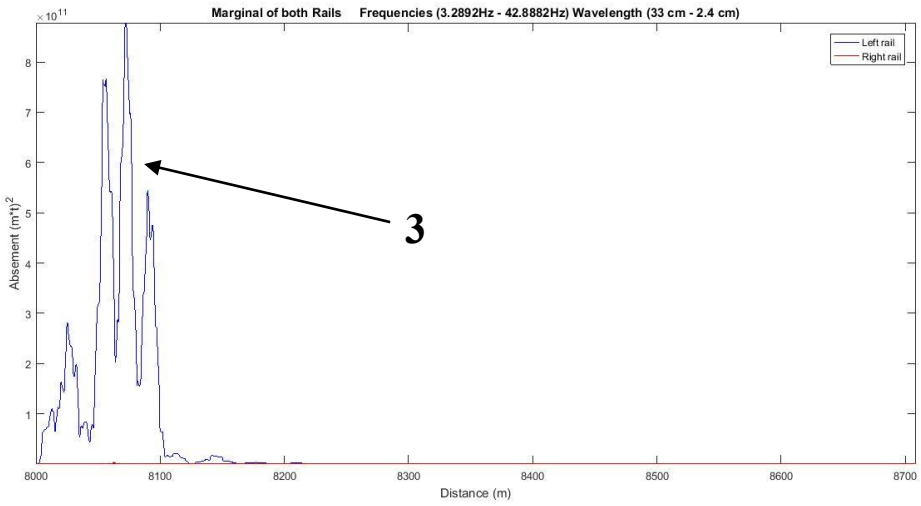

Figure 5.27 – Marginal of the CWT for both Rails. 3 is the demosntration that the power in the left rail is much higher than the right rail

The marginal can give a lot of information about the corrugation of the signal but it this case it cannot. The power of the CWT of the left rail for the frequencies chosen is so much higher than the CWT power of the right rail that is not possible to examine both signals. Figure 5.27 shows that in the beginning of the track the left rail has superior power, meaning that is heavily corrugated. This information when compared to the one third octave spectrum (figure 5.21) or the Corrugram (figure 5.25) is correct. With this correct comparison the marginal became another method to visually analyze a signal for signs of corrugation.

5.1.3 CinturaVAS

Given that all signals must pass through a filter, the next analysis will only bring the filtered signal.

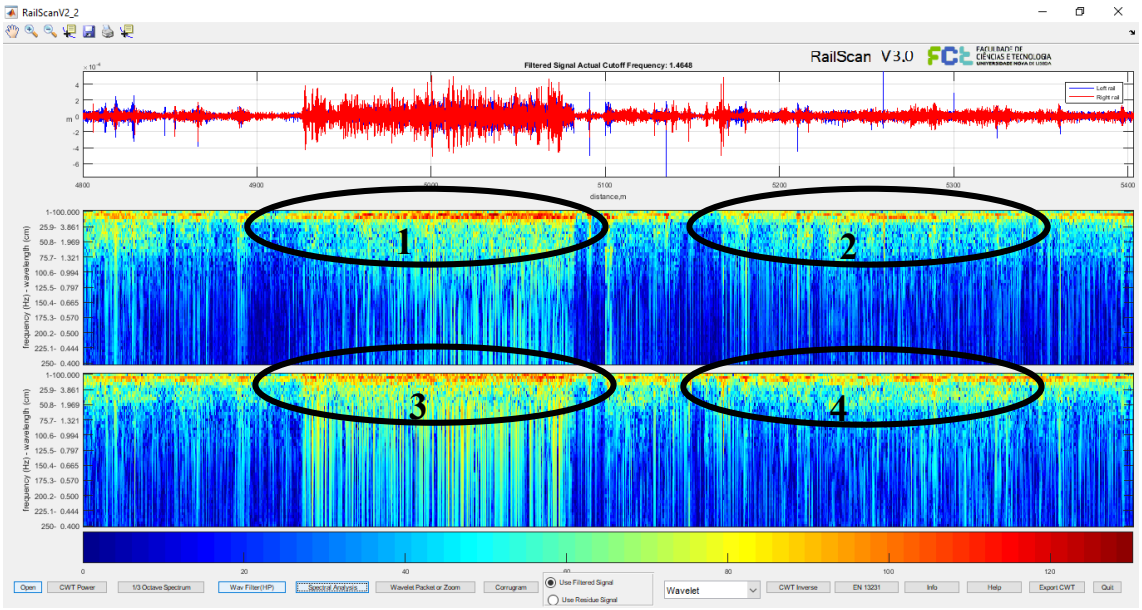

Figure 5.28 – Representation of the filtered CinturaVAS signal in RailScan. Identifications 1 and 2 are the critical corrugation poins of the left rail. Identifications 3 and 4 are the critical points of the rigt rail

The CWT representation shows that for frequencies around 1 Hz and 25 Hz both signals have a lot of power. The maximum corrugation power of the left rail appears to be between 4900 me and 5000 m (area number 1) and around 5200 m (area number 2). In the right rail the CWT representation displays maximums between 4900 m and 5000 m (area number 3) and around 5200 m (area number 4). Both signals appear to have maximums in the same distance, with a higher level of corrugation in the right rail (identified by number 3).

To verify if the filter was done correctly, a spectral analysis of the filtered signal was done (figure 5.29). The first plot of figure 5.29 shows that for frequencies near 0 Hz, there is not any power. With this observation, we can conclude that the filter was applied correctly. In the first plot it is also possible to see that the right rail has a lot of more power in the lower frequencies than the left rail.

In the first and second plot it is possible to see that the right rail has more power than the left rail in the lower frequencies (area 5 and 6), which is an expected result because of the interpretation made in the CWT representation (areas 3 and 4 of figure 5.28).

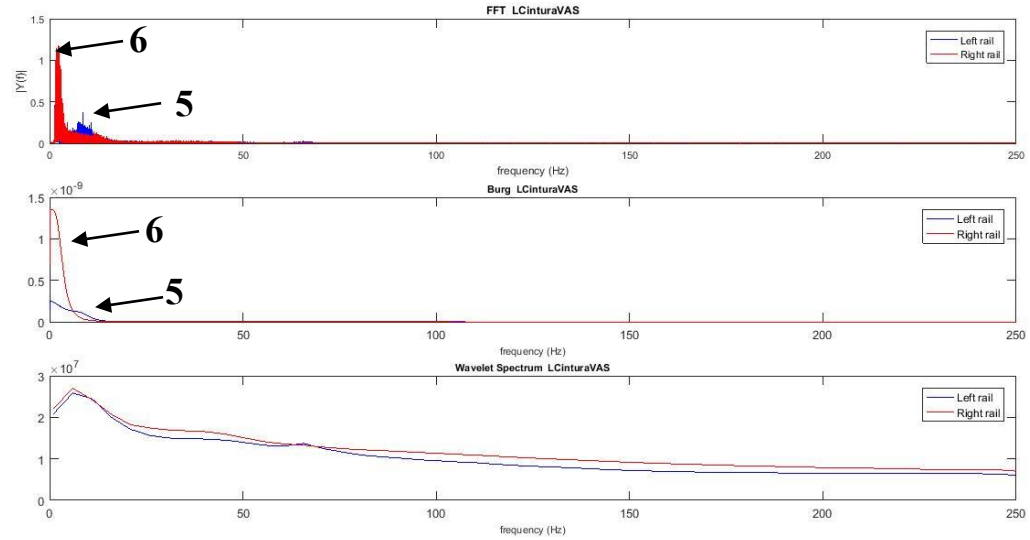

Figure 5.29 – Spectral analysis of the filtered Cintura VAS signal. 5 and 6 in both plots are the identification of the higher power frequencies in both rails.

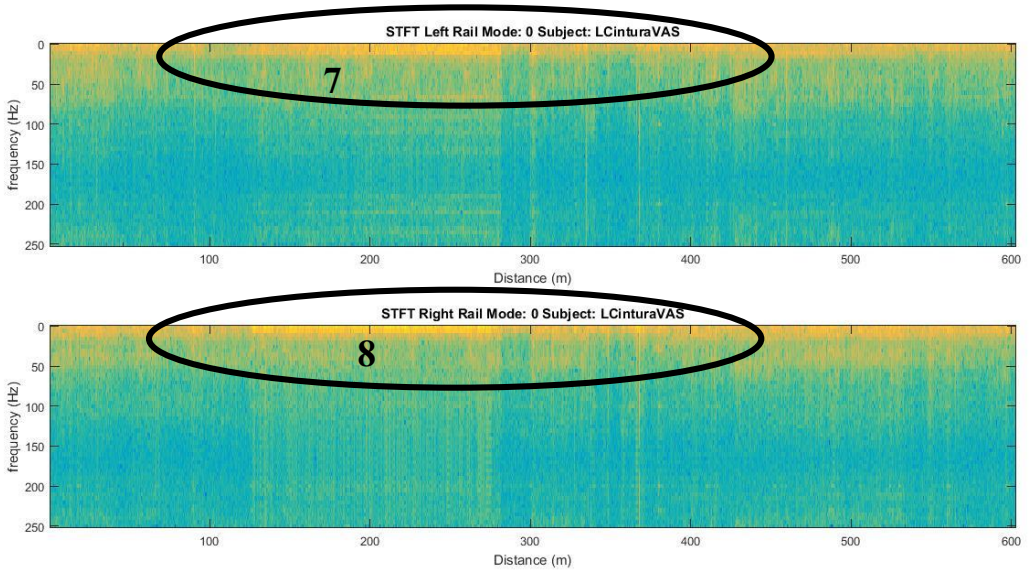

Figure 5.30 –STFT representation of the filtered Cintura VAS signal. Numbers 7 and 8 represent the areas where the identification of the higher power frequencies was possible.

Figure 5.30 shows the STFT representation of the filtered signal and what was said before in the analysis of the original signal applies to this representation. The STFT can identify points on the rail that have corrugation but the difference between the highest corrugation value and the lowest value is not easily detected.

After this first analysis, it is necessary to use the pre-established norms to verify if there is corrugation present in the rail and to quantify it.

The first plot (figure 5.31) shows the one third octave spectrum of the signal.

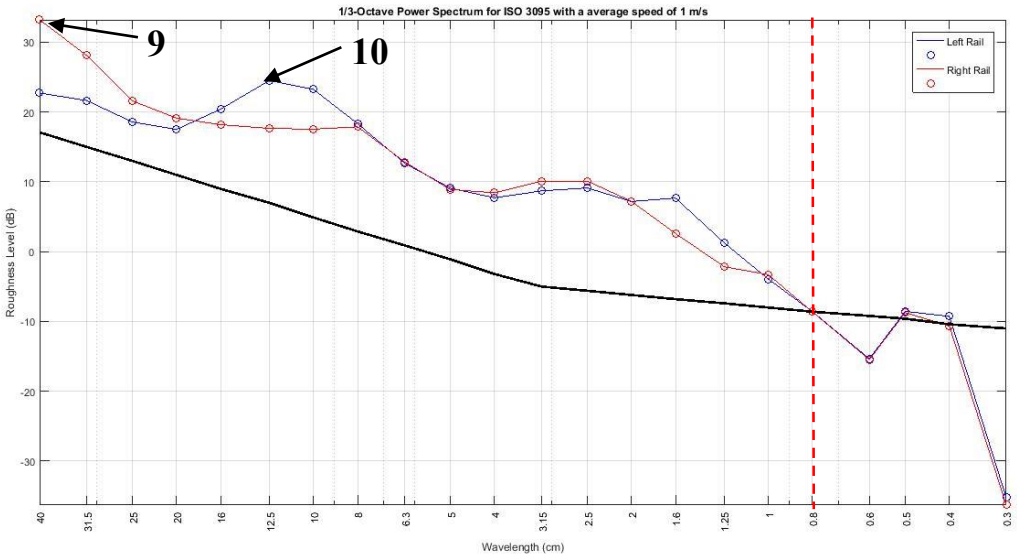

Figure 5.31 – One third octave spectrum using ISO 3095:2013 for signal Cintura VAS. 9 and 10 identify the highest acoustic roughness values for both rails. The red dotted line is the divisions into groups for a better analysis

The black line is the limit defined in the norm ISO 3095, which means that if any part of the signal passes that line the rail is corrugated.

To do a better analysis of the signal, and where corrugation is present, the signal will be divided in 2 groups of wavelengths (0.3 cm to 0.8 cm; 1 cm to 40 cm) between the red dotted line.

In the first group all wavelengths that are below the black line, 0.6 cm for instance in both signals. By analyzing both signals it is possible to see that the roughness level (dB) in the left rail is almost the same as the right rail for the all wavelengths that belong in this group.

In the second group, the roughness level for both rails remains almost the same, with the left rail reaching its maximum in wavelength 12.5 cm with a roughness level of 22 dB. Both rails have all wavelengths passing the limit defined in the norm, meaning for this group the rail is all corrugated.

The right rail reached a maximum of 30 dB in wavelength 40 cm.

Comparing this analysis with the CWT representation (figure 5.28), it is possible to see that in area 3 of figure 5.28 the right rail has more power than the left rail in higher frequencies and that is represented in figure 5.31.

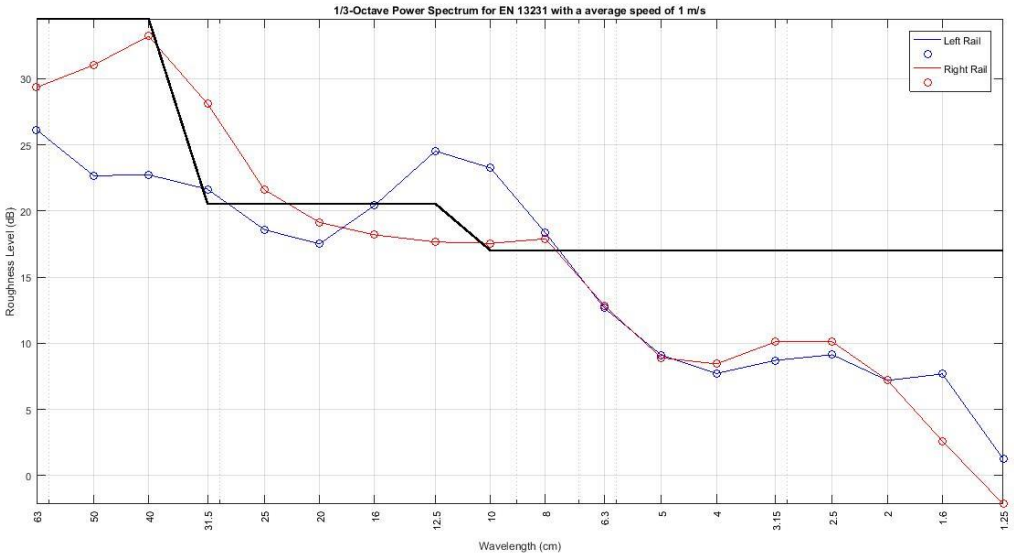

Figure 5.32 – One third octave spectrum using EN 13231:2012 for signal Cintura VAS

Figure 5.32 shows the one third octave spectrum as figure 5.31, the only difference is the values the black line assumes. By analyzing figure 5.32 it is possible to see that only some wavelengths pass the limit for the norm EN 13231. The left rail only has wavelengths 8, 10 and 12.5 cm passing the limit, a great difference when compared to the one third octave spectrum for ISO 3095 (figure 5.31).

The right rail has only two wavelengths passing the limit, wavelengths 20 cm and 31.5 cm, it is expected that the norm EN 13231 will detect corrugation in this group of wavelengths.

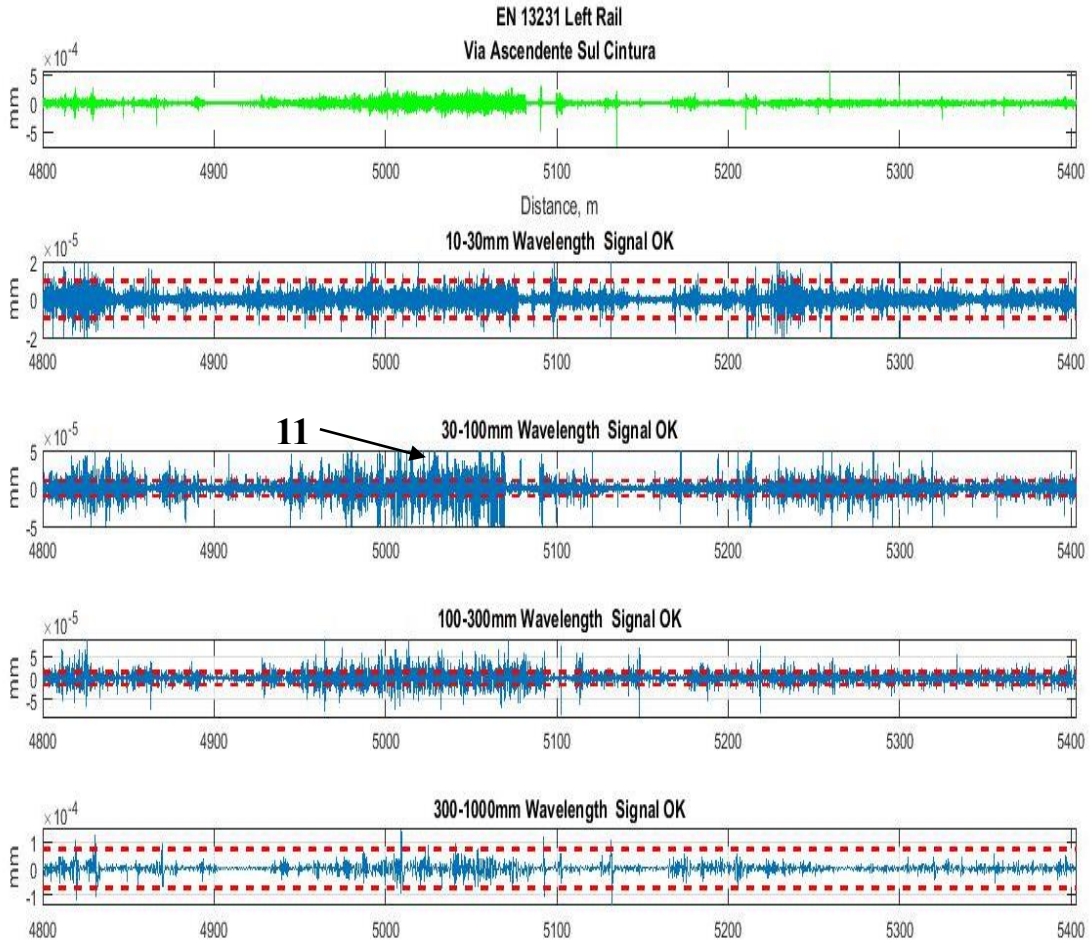

Figure 5.33 – EN 13231:2012 application to the left rail of signal Cintura VAS. 11 is identifying parts of the signal that are passing the estableshid limit. The red dotted lines in the plots are the peak to peak limits.

In figure 5.33 the norm EN 13231 was applied using the rules explained in chapter 4 (tables 4.2 and 4.3). To be in accordance with the norm, the signal must be filtered into 4 different wavelengths as shown in the titles of the plots (figure 5.33).The first plot is the original signal. If we analyze the information output of the second plot we can verify that almost none of the filtered signal is above the limit, so we can conclude that there is not exceeding corrugation present between these wavelengths.

In the third plot, the information output says that the filtered signal is ok for the wavelengths between 30 and 100 mm, which means that in those wavelengths there is not corrugation present in the rail. Analyzing the plot, we can see that the signal passes the limit in some parts of the rail but that does not correspond with 5% of the total signal (identified with number 11).

In the fourth plot, the information output says that the filtered signal is ok for the wavelengths of 100 and 300 mm, which means that in those wavelengths there is not corrugation present in the rail.

In the fifth plot, there is the information output “Signal OK”, which means that the signal has no corrugation in those wavelengths.

The norm EN 13231 it is not very precise. In figures 6.31 (one third octave spectrum using ISO 3095) and 6.32 (one third octave spectrum using EN 13231) or even the CWT representation (figure 5.28) it was possible to conclude that the left rail had plenty corrugation, but if that is not 5% of the all signal, the rail is not considered corrugated.

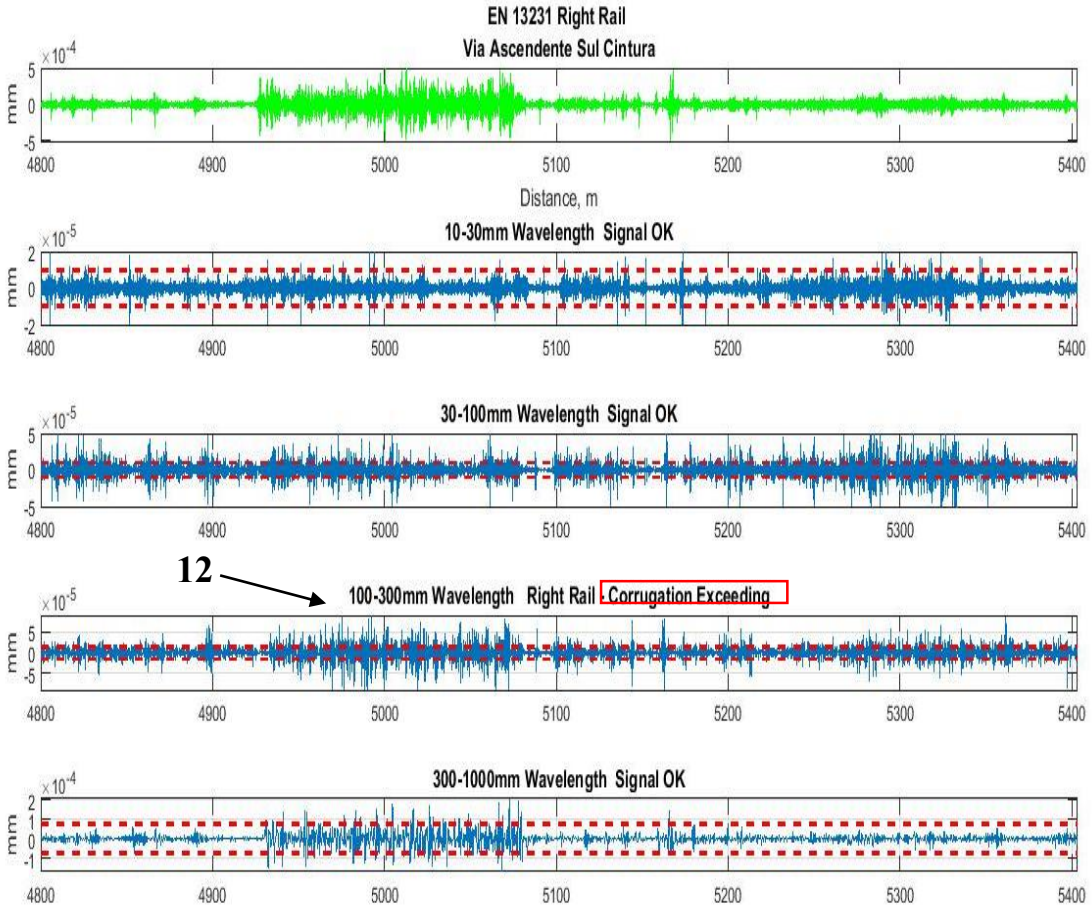

Figure 5.34 – EN 13231:2012 application to the right rail for the signal Cintura VAS. 12 is the identification of parts of the signal that is passing the established limit. The red rectangle is used to display the information output of the third plot.

The EN 13231:2012 representation of the right rail (figure 5.34) displays that for that rail only one group of wavelengths is 5% above the limit. Using the information output the norm gives, it is easy to confirm that the rail has corrugation between wavelength 10 cm and 30 cm (indicated by number 12).

Comparing this information with the one third octave spectrum of the norm EN 13231 (figure 5.32) representation it is easy to verify that they are in accordance, for those wavelengths the signal is considered corrugated.

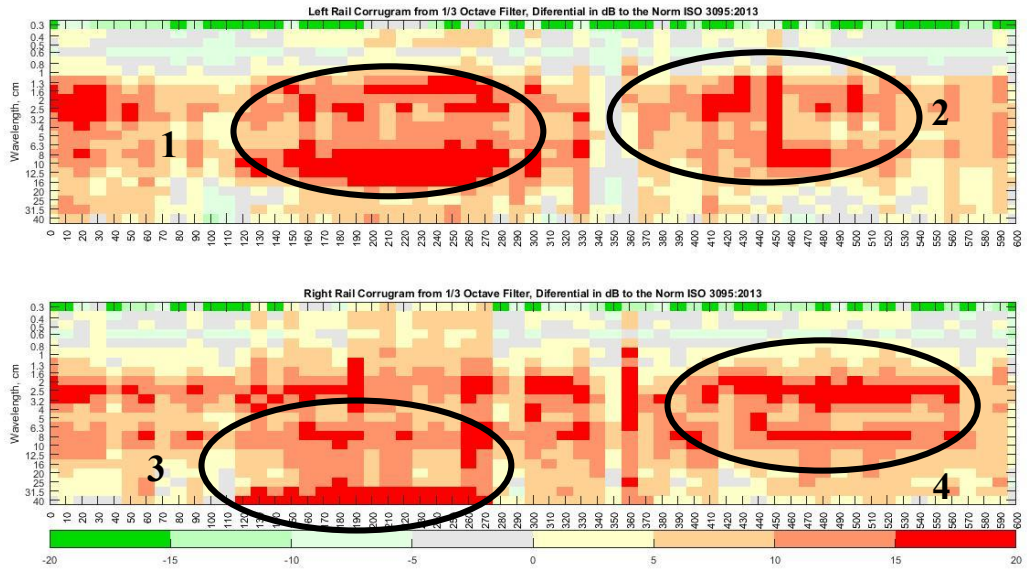

Figure 5.35 – Corrugram using norm ISO 3095:2013 for the signal Cintura VAS. Numbers 1 and 12 are identifications of critical corrugation parts in the left rail. Numbers 3 and 4 are the identification of critical corrugation parts in the right rail.

In figure 5.35 it is shown the Corrugram representation of both rails using ISO 3095. This representation of the Corrugram confirms the idea that the train is moving in a linear track.

If numbers 1 and 2 are compared to numbers 1 and 2 of figure 5.28 (CWT Representation of the filtered signal) they are an exact match, the maximum corrugation points detected in figure 5.28 are in the exact same place in the Corrugram. The same applies for the right rail, numbers 3 and 4 are an exact image of numbers 3 and 4.

The left rail in the beginning of the track shows a little corrugation. As the distance covered by the rail increases, the corrugation also increases. In the 200 m mark, there is a peak in corrugation between 1 cm and 16 cm wavelengths. By analyzing the left rail using this new representation it is easy to see that the wavelengths between 1 cm and 16 cm are the most corrugated and if we compare this conclusion with the one third octave spectrum representation (figure 5.31), we can see that in these wavelengths the acoustic roughness is higher.

In the one third octave spectrum representation for the left rail (figure 5.31), wavelength 0.6 cm did not pass the limit line, meaning that there is not corrugation present in the rail, but if analyze the Corrugram representation for the left rail it is possible to observe that this wavelength has corrugation in some sections of the rail.

In the right rail, the representation is not very different. As it was said before, the signal gives the impression that the train is moving in a linear track. The peak of the corrugation comes between 100 m and 200 m for wavelengths between 25 cm and 40 cm. If we compare this with the one third octave spectrum (figure 5.31), we can see that the higher values of acoustic roughness are between those wavelengths.

The one third octave spectrum representation for the right rail (figure 5.31) also shows that for the 0.6 cm wavelength the rail is not corrugated but analyzing the Corrugram representation it is possible to verify that the 0.6 cm wavelength has corrugation in some sections of the rail.

This difference of information between the one third octave spectrum and the Corrugram, proves that the Corrugram presents a more detailed information.

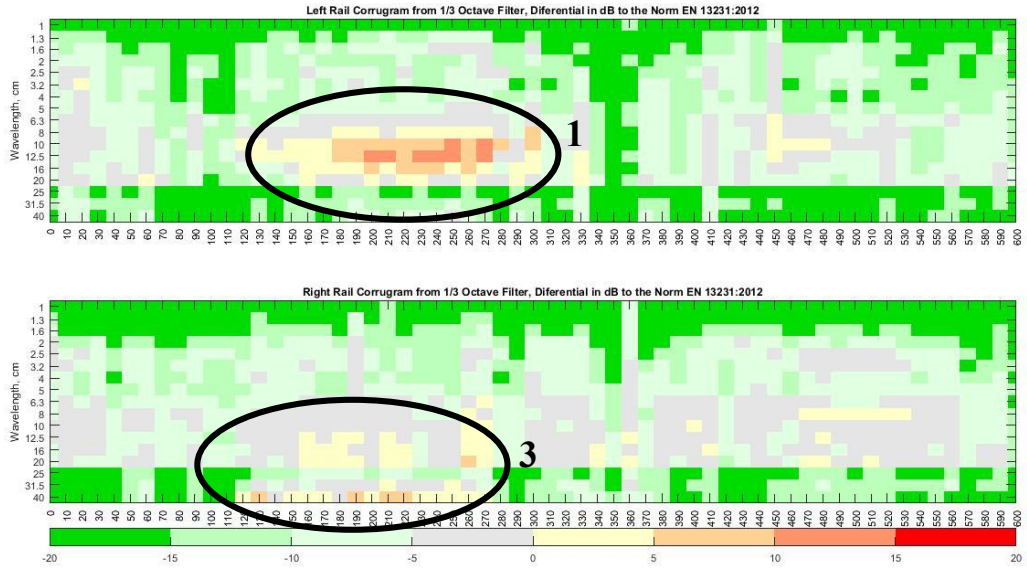

Figure 5.36 – Corrugram using the norm EN 13231:2012 for the signal Cintura VAS. 1 and 3 are the corrugation points in both rails.

As it was expected by using the norm EN 13231:2012 (figure 5.32) there are almost no spots that have corrugation. In the left rail representation, we can observe that for wavelengths 8 cm to 12.5 cm (number 1) there is corrugation present in some parts the rail, comparing this results to EN 13231 (figure 5.33) or even the one third octave spectrum for this norm (figure 5.32), we can verify that Corrugram is a much more detailed and effective way to detect corrugation, none of the other norms detected any corrugation, only Corrugram did.

In the Corrugram representation for the right rail we can determine that in wavelengths between 16 cm and 40 cm there is corrugation present (number 3), but this corrugation is only for a small part of the rail. If we compare this information with what the EN 13231 displayed (figure 5.34), it is easy to understand why the EN 13231 display showed that there was not corrugation present, only a very small part of rail has corrugation and for this reason it is possible to validate the Corrugram has a reliable and effective method. The Corrugram identifies all the corrugated wavelengths the established norms identify and others that those norms could not identify.

Figure 5.37 is the representation of the marginal (power of the CWT) of both rails. In case of figure 5.37 the pair of frequencies chosen were around 7 Hz and 42 Hz, that gives a wavelength of 14.5 cm and 2.3 cm respectively.

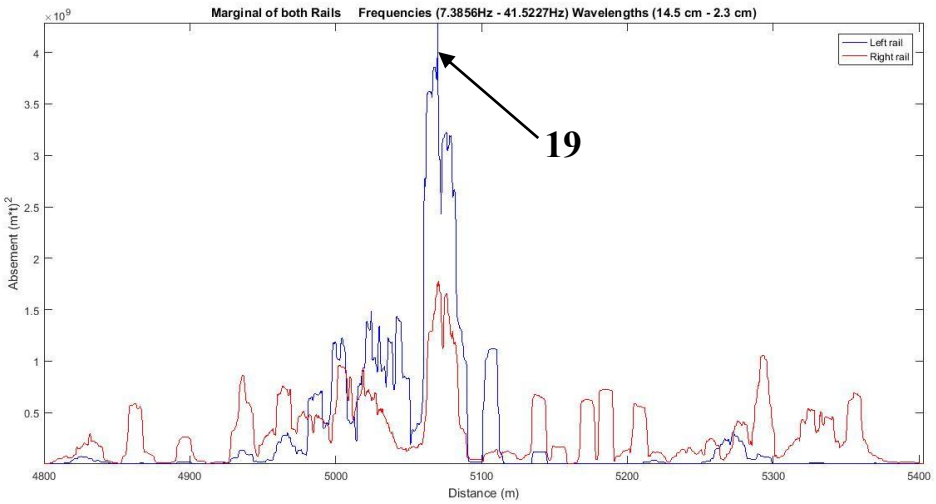

Figure 5.37 – Marginal of the CWT for both Rails. 19 displays the highest power of the CWT for the frequencies chosen

The marginal gives a lot of information about the corrugation of the signal, for instance the right rail has a lot more power than the left rail which is an expected resulted if we analyze the results of the CWT representation (figure 5.28). The pair of frequencies were chosen by a visual observation of where is the most information in the CWT representation of both rails. In the one third octave spectrum (figure 5.31) for the frequencies chosen the left rail had more acoustic roughness, so the result of figure 5.37 is in accordance. The marginal also shows where in space the rails have more power and with that it can be compared with the Corrugram. For example, both rails have meaningful power in the beginning of the rail and between the distances 5000 m and 5100 m. In figure 5.35 it is possible to observe that around those distances is where the rail is most corrugated. Using the marginal to analyze the signal also is a way to detect if and where the rail is corrugated even though lower detail and precision when compared to the Corrugram.

5.1.4 SintraVDE

Given that all signals pass through a filter, this analysis will only be about the filtered signal.

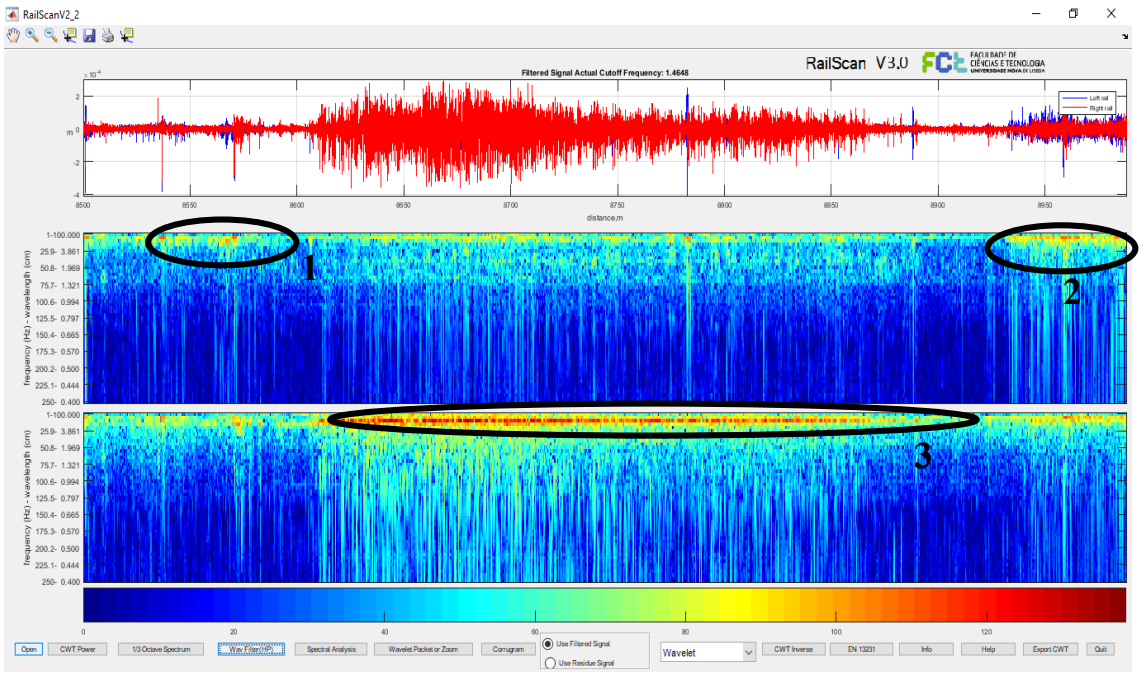

Figure 5.38 – Representation of the filtered signal SintraVDE in RailScan. 1 and 2 are the corrugation identified in the left rail. 3 is the corrugation identified in the right rail.

The CWT representation shows that for frequencies around 1 Hz and 25 Hz both signals have a lot of power, but the right rail has much more power than the left rail in distances 8600 m to 8800 m (area number 3). With this representation (figure 5.38), the train appears to be curving right around 8600 m.

To verify if the filter was done correctly, a spectral analysis of the filtered signal was done (figure 5.39). The first plot of figure 5.39 shows that for frequencies near 0 Hz, there is not any power. With this observation, we can conclude that the filter was applied correctly. In the first plot it is also possible to see that the right rail has a lot of more power in the lower frequencies than the left rail, which was expected because of the CWT representation.

Numbers 3 and 4 are pointing to the maximum frequency power in each rail. In the first plot, the right rail (number 4) has so much power that the identification of the left rail (number 3) is difficult.

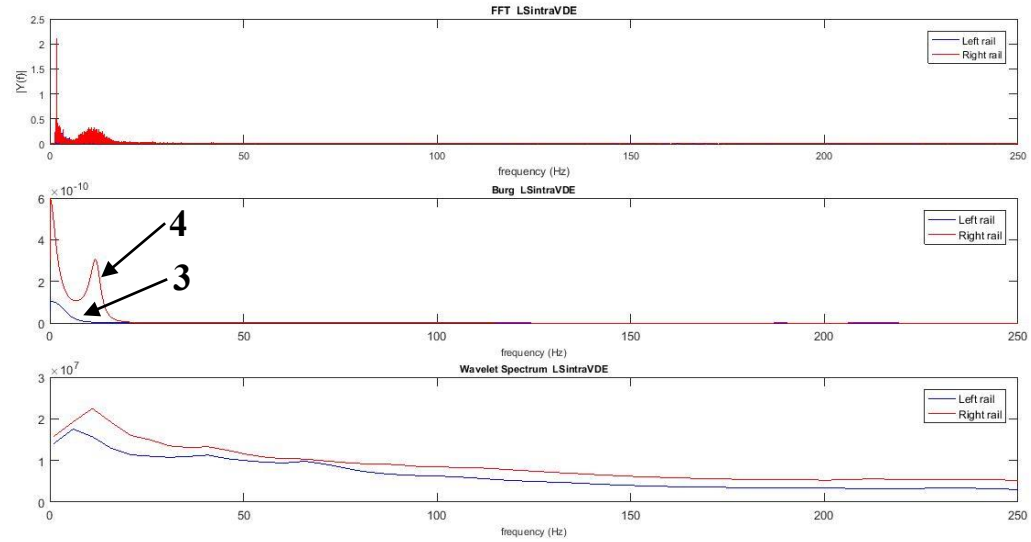

Figure 5.39 – Spectral analysis of the filtered Sintra VDE signal. 3 and 4 are the maximum frequency power for each rail.

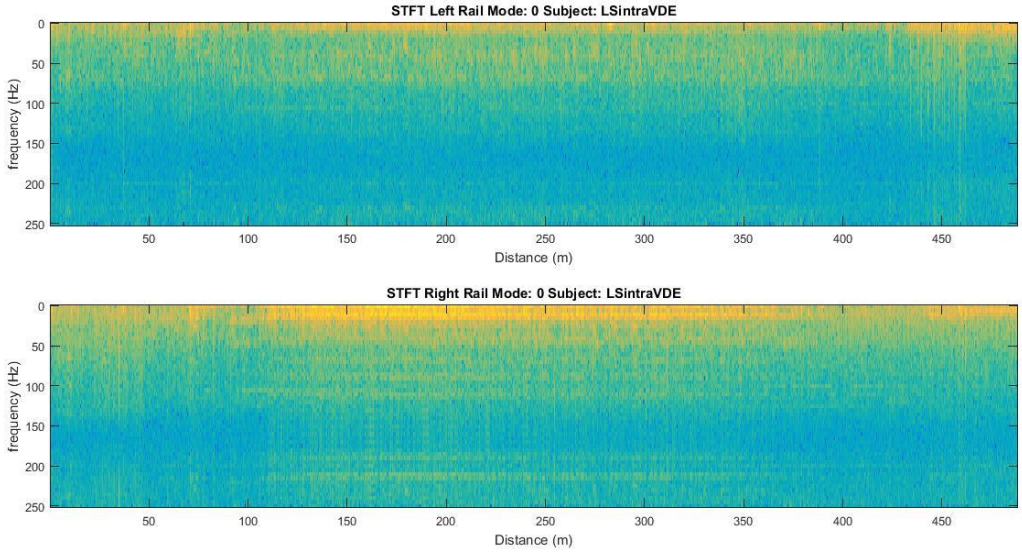

Figure 5.40 – STFT representation of the filtered Sintra VDE signal

Figure 5.40 shows the STFT representation of the filtered signal. In this plot, is possible to identify the massive power in the lower frequencies of the right rail, but this plot gives the idea that other frequencies might also have a significant amount of corrugation and that is not correct. After this first analysis, it is necessary to use the pre-established norms to verify if there is corrugation present in the rail.

The first plot (figure 5.41) shows the one third octave spectrum of the signal.

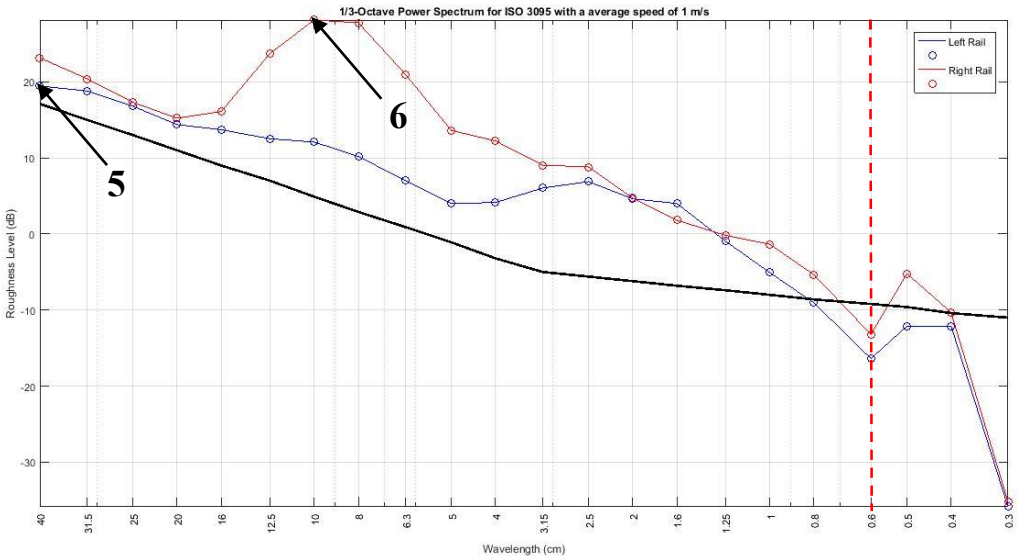

Figure 5.41 – One third octave spectrum using EN ISO 3095:2013 for the signal SintraVDE. Numbers 5 and 6 identify the highest acoustic roughness values for both rails. The red dotted line is the divisions into groups for a better analysis

The black line is the limit defined in the norm ISO 3095, which means that if any part of the signal passes that line the rail is corrugated.

To do a better analysis of the signal, and where corrugation is present, the signal will be divided in 2 groups of wavelengths (0.3 cm to 0.6 cm; 0.8 cm to 40 cm).

In the first group, there are wavelengths that are below the black line, 0.6 cm for instance in both signals. There are also wavelengths that are above the black line, 0.5 cm for instance. By analyzing both signals it is possible to verify that the roughness level (dB) in the right rail is higher. In the second group, all wavelengths pass the limit meaning they are all corrugated. The roughness level in both rails increased and in the right rail it was reached a maximum of 25 dB (number 6) in wavelength 10 cm. The difference between the roughness level of both rails is large and this difference is in accordance with the CWT representation (area 3 of figure 5.38).

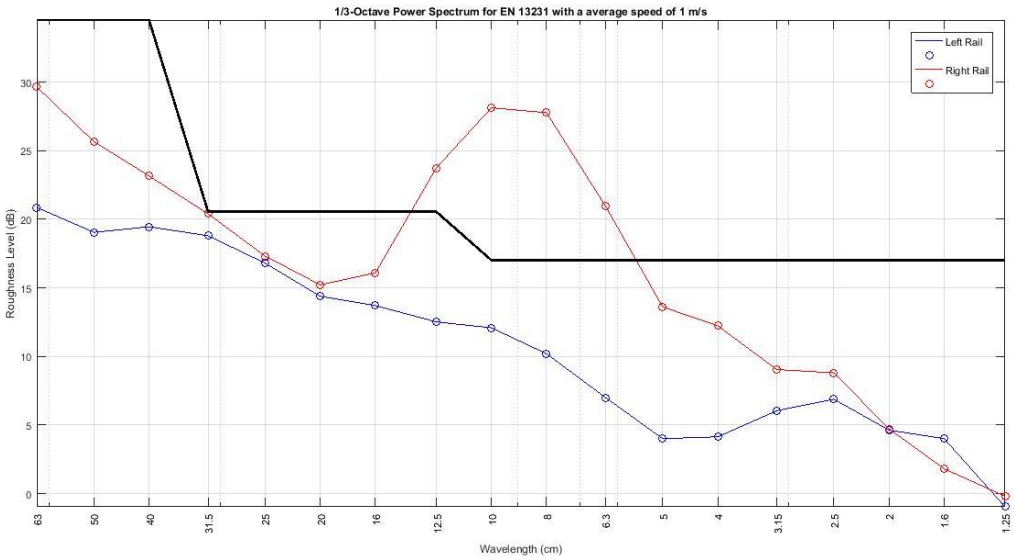

Figure 5.42 – One third octave spectrum using EN 13231:2012 for SintraVDE signal

By analyzing figure 5.42 it is possible to observe was what expected, only wavelengths between 6.3 cm and 12.5 cm are corrugated because these wavelengths presented an acoustic roughness level much greater than the others in figure 5.41. The left rail does not have any wavelength passing the limit, which was expected because using the norm EN 13231 the limit is much higher than the norm ISO 3095.

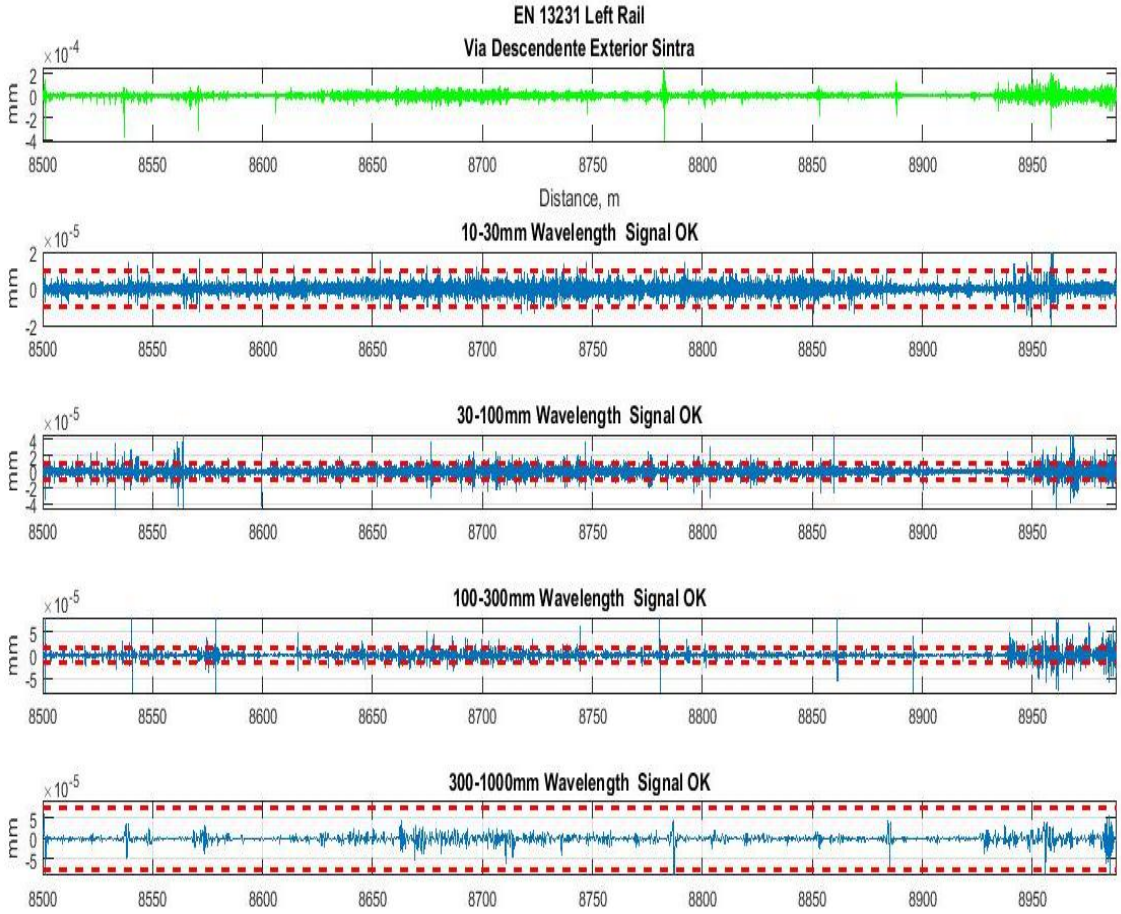

Figure 5.43 – EN 13231:2012 application to the left rail of the SintraVDE signal. The red dotted lines in the plots are the peak to peak limits.

Using the EN 13231 to represent the rails, we can also conclude if there is corrugation present in the rails. To be in accordance with the norm, the signal must be filtered into 4 different signals (figure 5.43). If we analyze the information output of the second plot we can determine that almost none of the filtered signal is above the limit, so we can conclude that there is not corrugation present between these wavelengths.

In the third plot, the information output says that the filtered signal is ok for the wavelengths between 30 and 100 mm, which means that in those wavelengths there is not corrugation present in the rail.

In the fourth plot, the information output says that the filtered signal is ok for the wavelengths of 100 and 300 mm, which means that in those wavelengths there is not exceeding corrugation present in the rail.

In the fifth plot, there is the information output “Signal OK”, which means that the signal has no surpassing corrugation in those wavelengths.

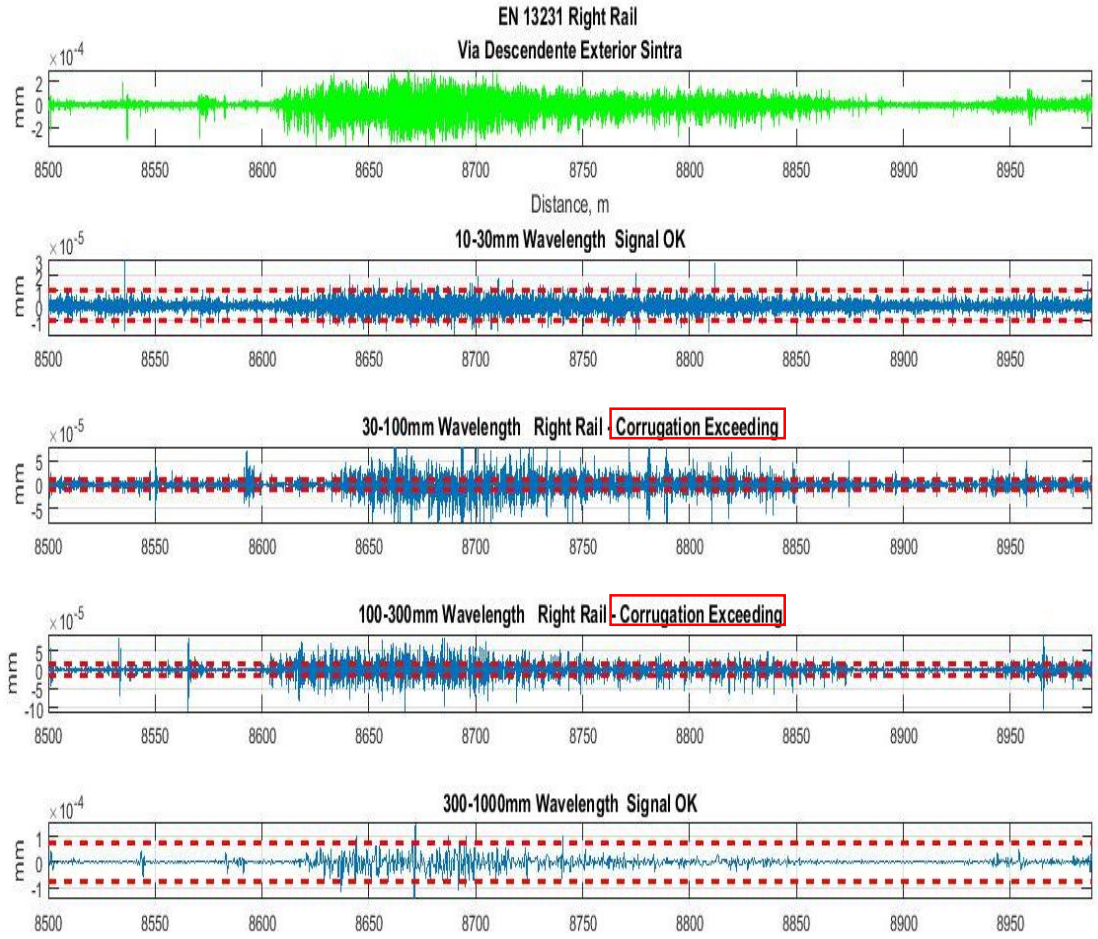

Figure 5.44 – EN 13231:2012 application to the right rail for the SintraVDE signal. The third and fourth plot have a red rectangle indicating that the rails is corrugated.

The EN 13231:2013 representation of the right rail (figure 5.44) displays that for wavelengths between 3 cm and 30 cm there is corrugation in the rail. Comparing this information with the one third octave spectrum of the norm EN 13231 (figure 5.42) representation it is easy to verify that they are in accordance, in wavelengths that belong to those groups, some wavelengths were identified with corrugation, for example 8 cm or 10 cm wavelength.

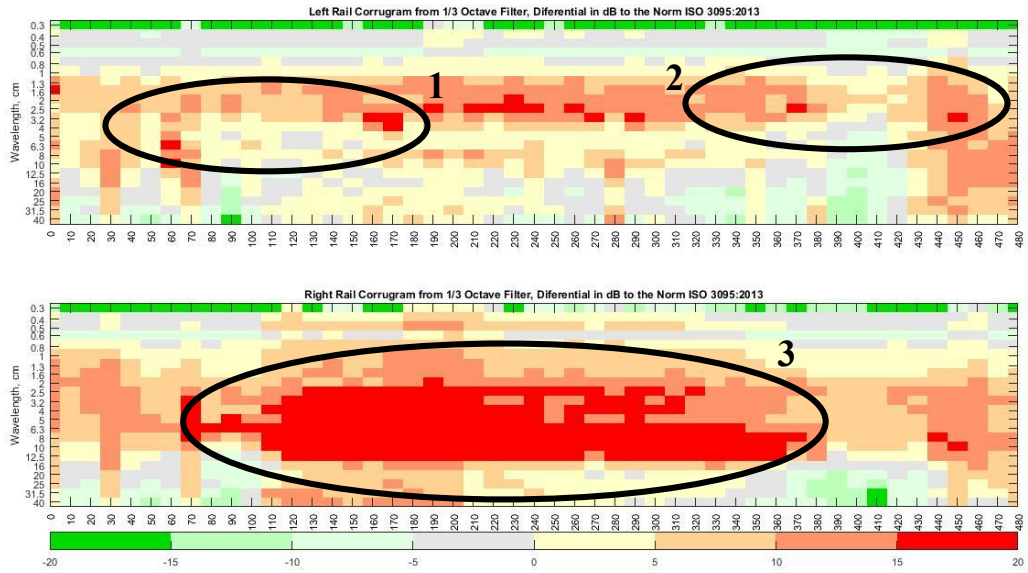

Figure 5.45 – Corrugram using the norm ISO 3095:2013 for the signal SintraVDE. 1and 2 are the critical corrugation points of the left rail. 3 is the critical corrugation point of the right rail

In figure 5.45 it is shown the Corrugram representation of both rails. This representation of the Corrugram confirms the theory that around 8600 m the train began curving right (number 3). By analyzing figure 5.45 we can see that the right rail has corrugation in more places than the left rail.

Numbers 1, 2 and 3 are perfectly matched with numbers 1,2 and 3 of the CWT representation (figure 5.38). This means that both implementations are correct and are identifying the same corrugations points.

In the one third octave spectrum representation for the left rail (figure 5.41) the 0.8 cm wavelength did not pass the limit line, meaning that there is not corrugation present in the rail, but if we analyze the Corrugram representation for the left rail it is possible to observe that in those the rail has some sections with corrugation.

The one third octave spectrum representation for the right rail (figure 5.42) also shows that for the 0.8 cm wavelength the rail is not corrugated but analyzing the Corrugram representation for that rail it is possible to see that the 0.8 cm wavelength has corrugation in some sections of the rail.

This difference of information between the one third octave spectrum and the Corrugram, proves that the Corrugram presents a more detailed information.

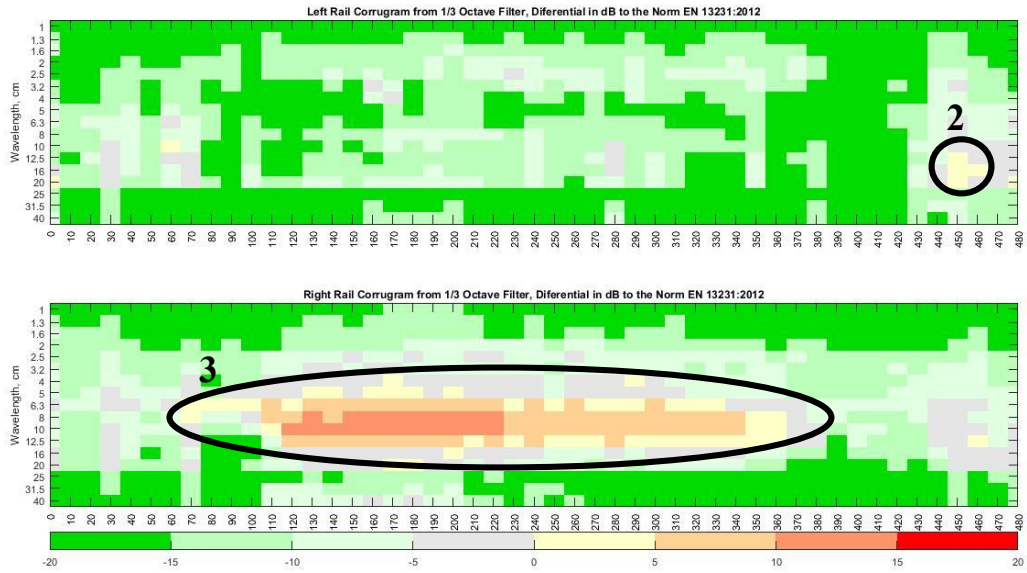

Figure 5.46 – Corrugram using the norm EN 13231:2012 for the signal SintraVDE. 2 and 3 are the only parts identified with corrugation in both rails.

The Corrugram representations help the user to better understand where and if there is corrugation present in the rails. As it was expected using the norm EN 13231:2012 (figure 5.46) there are almost no spots that have corrugation. In the left rail representation, we can see that for only one part of the rail is corrugated in 8850 m for wavelengths 16 cm and 20 cm (number 2). If we compare this information with what the EN 13231 displayed, it is easy to understand why the EN 13231 display showed that there was not corrugation in the rail, only a very small part of rail has corrugation and for this reason it is possible to validate the Corrugram has a reliable and effective method. The Corrugram identifies all the corrugated wavelengths the established norms identify and others that those norms could not identify.

In the Corrugram representation for the right rail we can verify that for the wavelengths between 6.3 cm and 20 cm there is corrugation present (number 3). If we compare this information with what the EN 13231 displayed, it can be verified that they agree. Figure 5.47 is the representation of the marginal (CWT power) of both rails. In case of figure 5.47 the pair of frequencies chosen were around 3 Hz and 40 Hz, that gives a wavelength of 30.4 cm and 2.5 cm respectively.

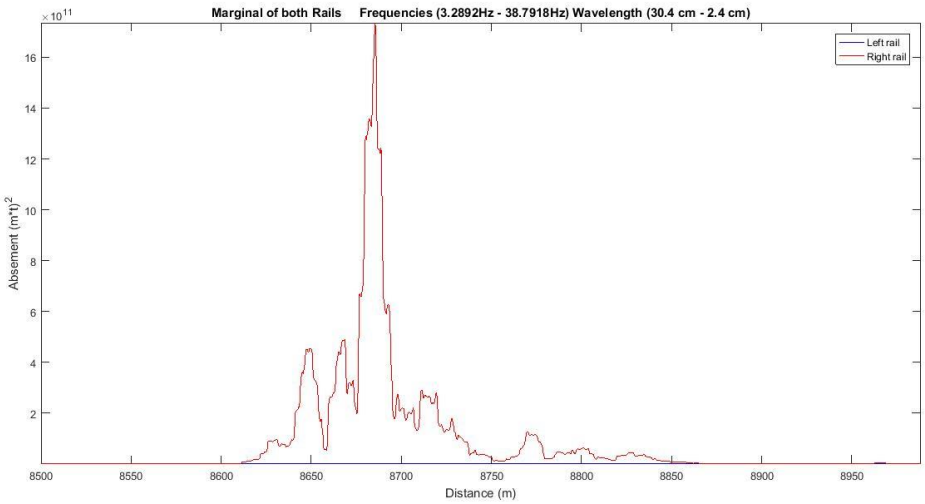

Figure 5.47 – Marginal of the CWT for both Rails. The power of the right rail is so much higher than the left rail that the left rail becomes almost invisible.

The marginal gives a lot of information about the corrugation of the signal, but in this case, it does not. The pair of frequencies chosen is where the right rail has more power and in the beginning of this signal analysis (figure 5.38) with was observed that the right rail had more power than the left rail, so when using the marginal the only thing it is possible to see is the right rail power. With this representation it is easy to confirm that in between 8600 m and 8800 m the right rail has more corrugation, confirmation that was also verified in the Corrugram. Even though in this case the power of the right rail was so much higher than the left rail, the marginal still identified the critical corrugation point of the rail.

5.1.5 Inverse CWT

Even though, this implementation is not being used right now by RailScan some tests were made to validate it. The following figures 6.48 and 6.49 show the inverse CWT at full display.

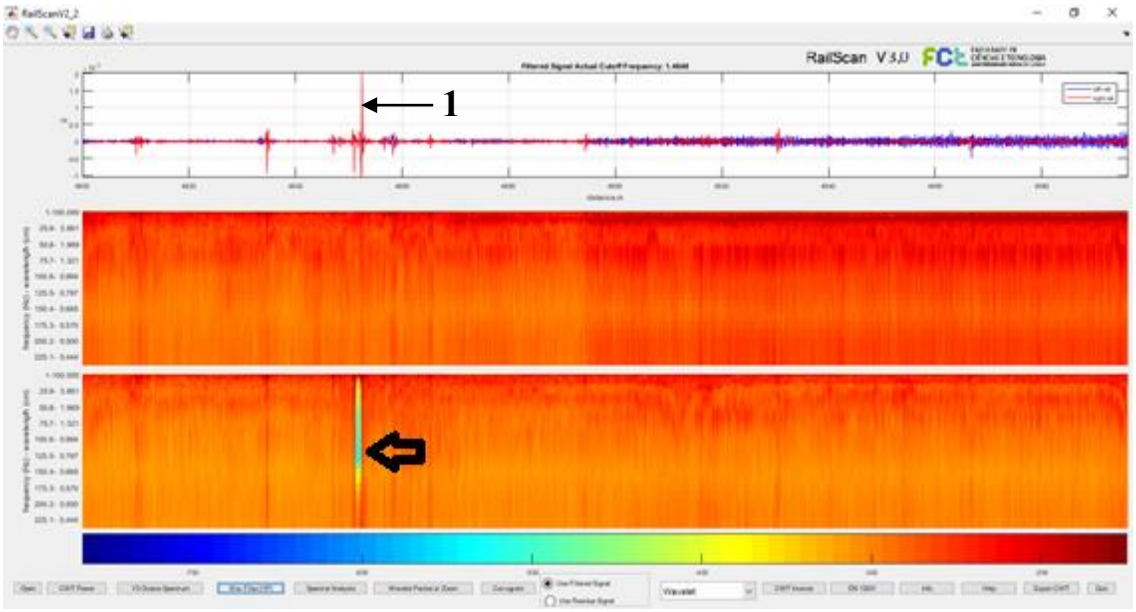

Figure 5.48 – Representation of a signal with the new CWT. A black arrow is pointing to the part of the signal that will be inverted. 1 is the part of the signal being analyzed.

The inverse CWT will only be applied to one rail and in the part that is being pointed by the black arrow.

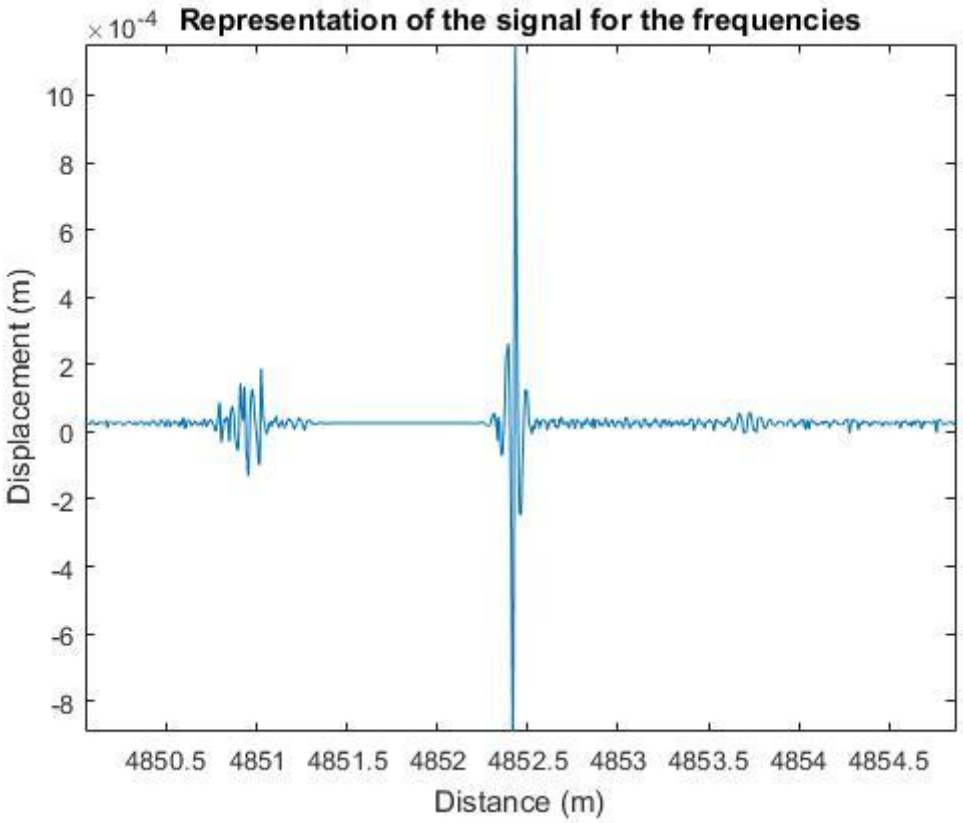

Figure 5.49 – Representation of the original signal in the frequencies and distances selected by the user

Comparing figure 5.49 with number 1 of figure 5.48 it is possible to analyze that the inverse was done correctly.

Conclusion and Future Work

Conclusion

The main objective of the thesis was to implement new methods to detect and quantify rail corrugation levels using Wavelets, European and International norms.

Although there was a previous application developed in FCT-UNL, RailScan V2.1, the program needed some modifications. The first was to implement the capability of analyzing both rails at the same time, which was a necessary feature to be included in this application.

This new addition in RailScan allows both signals to be displayed and processed simultaneously. A feature for CWT inversion to the signal reconstruction was added, however could not be consistently used since is computationally heavy.

The method using International norms was already implemented in the previous version of RailScan. This norm was revised in 2013 so an adjustment was necessary.

A new norm was included the EN 13231:2012. This European norm divides the signal into groups of wavelengths and measures if those groups are above an established limit.

The Corrugram, was also integrated into RailScan. The Corrugram is a patent developed in FCT-UNL and it is a different way to represent the signal and to help the user analyze where corrugation is located.

A robust database of real signals was also achieved. Having this database helped to understand if the implementation of RailScan was being done correctly.

The main objective of this thesis was achieved, new methods to detect and analyze rail corrugation were implemented and it can now be concluded that the Corrugram is a reliable form to quantify corrugation. It was implemented for both norms (DIN ISO 3095 and EN 13231:2012) and it can achieve better results than both.

The CWT has identified with a very good precision the parts in the rail that are most corrugated and respective wavelengths. The CWT is a power visual tool to illustrate corrugation location and levels. The only problem regarding CWT is not being adopted as a normative analysis method. At least at this state.

The STFT proved to be not as ineffective as the CWT to analyze corrugation signals. It can identify the higher power in the very low frequency band, but if the frequency increases the representation becomes unclear. This is due to the fact that the STFT projects signals in sine waves and corrugation signals are not sines waves.

Corrugram is a software tool that can be used by anybody, it does not require expertise in signal processing to analyze it, whereas in the CWT representation it is necessary to have knowledge in that area.

The Corrugram when compared to the simple use of norms ISO 3095 or EN 13231 showed substantially more information, because it segments the rail into sections, becoming more detailed and informative. The norm EN 13231 when compared to Corrugram, ISO 3095 or even the CWT showed very little detail and missed important parts of the rail that have critical corrugation situations.

The CWT marginal was a new implementation since the inverse CWT could not be extensively used because it is computational demanding. The reason for using the marginal was to compare it with the norms implemented regarding corrugation detection. The wavelet marginal performed very well. It produces a detailed representation of corrugation but is not as global as the Corrugram.

RailScan with these innovations became a powerful tool in rail corrugation analysis, it uses all the norms that are being used in nowadays and also a function that is at the moment only being used by it (Corrugram).

RailScan has proved to be a powerful application to process long distance railways and it has been designed with that feature in mind.

Future work

The future work for RailScan can be divided into 3 parts.

The first part is to develop methods to have RailScan use less graphic memory, perhaps parallel processing could be considered. RailScan should integrate big data processing. This would make the corrugation analysis of high distances railways more effective.

The second part and probably the most important is to increase the database with data from around the world and increase the validation process. Having data acquired from direct and indirect measurements is also helpful.

The third part of the future work is to always be aware if some norm changes or if a different one is introduced. Being aware of this is a very important process to not leave RailScan outdated.

References

[1] C. Hory, L. Bouillaut, and P. Aknin, “Time – frequency characterization of rail corrugation under a combined auto-regressive and matched filter scheme,” *Mech. Syst. Signal Process.*, vol. 29, pp. 174–186, 2012.

[2] “CORRUGATION.EU - RESEARCH & FACTS.” [Online]. Available: http://www.corrugation.eu/research/. [Accessed: 02-Mar-2017].

[3] M. Hecht and H. Zhang, “Monitoring Railway Noise , Rail and Wheel Roughness,” pp. 4843–4850, 2016.

[4] X. Zhao, Z. Wen, H. Wang, X. Jin, and M. Zhu, “Modeling of high-speed wheel-rail rolling contact on a corrugated rail and corrugation development *,” vol. 15, no. 12, pp. 946–963, 2014.

[5] N. Correa, O. Oyarzabal, E. G. Vadillo, J. Santamaria, and J. Gomez, “Rail corrugation development in high speed lines,” *Wear*, vol. 271, no. 9–10, pp. 2438–2447, 2011.

[6] S. L. Grassie, “Measurement of railhead longitudinal profiles: a comparison of different techniques,” *Wear*, vol. 191, no. 1–2, pp. 245–251, 1996.

[7] A. Bracciali and P. Folgarait, “<050 Techrail (2002) Corrugation Meas for Noise.pdf>.”

[8] “V & P / RMF 2.3E.” [Online]. Available: http://www.vogelundploetscher.de/e/rmf/. [Accessed: 06-Jan-2018].

[9] S. L. Grassie, “Rail irregularities, corrugation and acoustic roughness: characteristics, significance and effects of reprofiling,” *Proc. Inst. Mech. Eng. Part F J. Rail Rapid Transit*, vol. 226, no. 5, pp. 542–557, 2012

[10] “Rail corrugation analysis trolley - CAT | Rail Measurement.” [Online]. Available: http://railmeasurement.com/corrugation-analysis-trolley-cat/. [Accessed: 02-Mar-2017].

[11] “Measure rail corrugation and acoustic roughness on two rails.” [Online]. Available: http://railmeasurement.com/bi-cat/. [Accessed: 02-Mar-2017].

[12] “Rail corrugation and acoustic roughness analyser vehicle.” [Online]. Available: http://railmeasurement.com/rail-corrugation-analyser-rca/. [Accessed: 02-Mar-2017].

[13] “High Speed Rail Corrugation Analyser - HSRCA | Rail Measurement.” [Online]. Available: http://railmeasurement.com/hsrca/. [Accessed: 02-Mar-2017].

[14] “TriTops | Railway wheel circumferential irregularities measurement.” [Online]. Available: http://railmeasurement.com/tritops/. [Accessed: 02-Mar-2017].

[15] R. Pedro and D. A. Gomes, “RailScan – Desenvolvimento de Software para a Detecção e Caracterização de Desgaste Ondulatório em Ferrovias Por,” 2010.

[16] R. Gomes, A. Batista, M. Ortigueira, R. Rato, M. Baldeiras, and U. N . De Lisboa, “Railscan : A Tool for the Detection and Quantification of,” pp. 401–408, 2010.

[17] R. X. Gao and R. Yan, “Wavelets: Theory and applications for manufacturing,” *Wavelets Theory Appl. Manuf.*, pp. 1–224, 2011.

[18] “Understanding Wavelets, Part 1: What Are Wavelets Video - MATLAB.” [Online]. Available: https://www.mathworks.com/videos/understanding-wavelets-part-1-what-are-wavelets-121279.html. [Accessed: 03-Jul-2017].

[19] “Music and Computers.” [Online]. Available: http://cmc.music.columbia.edu/MusicAndComputers/chapter3/03_06.php. [Accessed: 03-Jul-2017].

[20] N. Peleg, “Introduction to Wavelets Lets start with … Fourier Analysis,” 2000.

[21] “Continuous and Discrete Wavelet Transforms - MATLAB & Simulink.” [Online]. Available: https://www.mathworks.com/help/wavelet/gs/continuous-and-discrete-wavelet-transforms.html. [Accessed: 03-Jul-2017].

[22] https://www.mathworks.com/help/wavelet/gs/discrete-wavelet-transform.html. [Accessed: 03-Jul-2017].

[23] http://eur-lex.europa.eu/legal-content/EN/TXT/?uri=CELEX%3A32006D0066. [Accessed: 10-Mar-2018].

[24] E. C. for Standardization, "Railway applications — Track — Acceptance of works," Part 3 Accept. reprofiling rails track, vol. EN 13231-3, 2012.

[25] "matlab - what is proper setting for Fb,Fc in Complex morlet wavelet (cmor)? - Signal Processing Stack Exchange." [Online]. Available: https://dsp.stackexchange.com/questions/10196/what-is-proper-setting-for-fb-fc-in-complex-morlet-wavelet-cmor. [Accessed: 17-Mar-2018].

[26] N. Barrento, A. Batista, M. Ortigueira, F. Coito, and U. N . De Lisboa, "PPP_Corrugrama" .

[27] M. Corrugation, "RailMeasurement," pp. 2–3, 2012.

[28] P. D. Welch, "of for of," no. 2, pp. 70–73, 1967.

[29] L. Li, C. Cheng, D. Han, Q. Sun, and G. Shi, "Phase Retrieval from Multiple-Window Short-Time Fourier Measurements," IEEE Signal Process. Lett., vol. 24, no. 4, pp. 372–376, 2017.

[30] S. Sinha, P. S. Routh, P. D. Anno, and J. P. Castagna, "Spectral decomposition of seismic data with continuous-wavelet transform," Geophysics, vol. 70, no. 6, p. P19, 2005.

[31] J. Chen, J. Rostami, P. W. Tse, and X. Wan, "The design of a novel mother wavelet that is tailor-made for continuous wavelet transform in extracting defect-related features from reflected guided wave signals," Meas. J. Int. Meas. Confed., vol. 110, no. October, pp. 176–191, 2017.

[32] Daubechies, I.:. Ten Lectures on Wavelets. Society for Industrial and AppliedMathematics.

[33] Z. Hong-tu and Y. Jing, "The Wavelet Decomposition And Reconstruction Based on The Matlab," Proc. Third Int. Symp. Electron. Commer. Secur. Work., no. July, pp. 143–145, 2010.

[34] J. N. Varandas, R. Silva, M. A. G. Silva, N. Lopes, and P. Hölscher, "The Impact of Rail Corrugation on the Degradation of Ballast," pp. 1–20, 2012.